BuMines OFR 103-81

A minerals research contract report
November 1980

DEVELOPMENT OF TESTS AND CRITERIA TO EVALUATE GROUNDING SYSTEMS

Bureau of Mines Open File Report 103-81

Contract J0199116
West Virginia University

BUREAU OF MINES ★ UNITED STATES DEPARTMENT OF THE INTERIOR
Minerals Health and Safety Technology

The views and conclusions contained in this document are those of the authors and should not be interpreted as necessarily representing the official policies or recommendations of the Interior Department's Bureau of Mines or of the United States Government.

FOREWORD

This report was prepared by West Virginia University Engineering Experiment Station, Morgantown, West Virginia under USBM Contract No. J0199116. The contract was initiated under the Coal Mine Health and Safety Research Program. It was administered under the technical direction of the Pittsburgh Research Center with Mr. Roger L. King acting as Technical Project Officer. Mr. Doyne W. Teets was the Contracting Officer for the Bureau of Mines.

This report covers work performed on this contract from 1 July 1979 to 31 October 1980. This report was submitted by the authors in November 1980.

TABLE OF CONTENTS

Table of Contents - Continued

Table of Contents - Continued

EXECUTIVE SUMMARY

Several loosely related tasks were executed under research contract J0199116. All areas of work were related to coal mine electrical grounding, and essentially all of the objectives of the studies were realized. One of the tasks represents a continuation (and culmination) of effort begun under USBM G0188087.

Chapter I describes the work accomplished on an integrated ground fault-ground check monitor. At the present time detection of ground faults on the mine resistance-grounded power system is accomplished by equipment which is totally independent of equipment used to monitor the continuity of the safety ground wire. A survey is presented of characteristics and failure modes of present ground fault and ground check techniques. The chapter ends with a detailed design description of a combined ground fault-ground check monitor system. Implementation of the design has been carried to the point of demonstrating its proper operation under laboratory conditions.

Chapter II is a study of grounding methods for dc vehicles powered through trailing cables. Six presently-used grounding methods are investigated, with special consideration given to their relative advantages and disadvantages. To aid in this comparison, a computer simulation was made of four of the systems. This is used to estimate the voltage which appears on a machine frame during various phases of normal and abnormal operation, as well as the voltage transients which appear on grounding diodes. The chapter ends with a table showing the important characteristics and potential dangers of each type of grounding. It is concluded that no system is clearly superior to all the others.

Chapter III describes the completion of an evaluation of Xit ground rods begun under grant G0188087. Eleven rods were monitored at field installations in West Virginia, Ohio, and Pennsylvania. After having them in place for at least one year, as many rods were recovered as possible. The rods were examined for corrosion and for evidence of the effectiveness of the self-salting feature. The resistance measurements and inspections of recovered rods raises serious questions about the effectiveness of these rods in the environment of the Appalachian coal fields. The rods appear to be only slightly more effective than solid metal rods of similar dimensions.

Chapter IV covers an extensive study of composite material ground beds. Mining operations are often carried out in regions of high soil resistivity, where the establishment of a low-resistance ground bed can be extremely difficult. Rather than bury a very large metal electrode, the composite technique can make it possible to obtain adequately low resistance by burying a great quantity of an inexpensive semi-conducting material in contact with a relatively small metal electrode. The chapter begins with an evaluation of a few semiconducting fill materials. The bulk of the chapter is a development of relationships to express the theoretical resistance and estimated construction cost of several configurations of composite ground beds. The chapter ends with an analysis of voltage gradients near a composite bed. The overall conclusion is that composite ground beds are cheaper and safer than conventional construction in many high resistivity areas.

Chapter V deals with construction of a borehole-type safety ground bed

extending through the coal seam. A theoretical analysis of the situation and a field measurment of the electrical characteristics of the stratified overburden and coal seam indicate that it is desirable to extend a borehole safety ground through the coal seam.

Chapter VI describes a workshop on Mine Substation Grounding and Bonding that was developed for the mining industry. Extensive audio-visual material was developed around a rubber-sheet analog and photographs of actual mine installations. The workshop was very popular, being oversubscribed by more than 30%. Attendees gave it very high ratings, which data is given in the chapter.

Chapter VII reviews accomplishments relative to the testing of shuttle car grounding diodes. Undetected failures of these devices (especially a loss of continuity) can cause a severe shock hazard under some conditions, which are outlined in the chapter. Present methods of testing diodes are discussed, showing how they can damage the device or create a shock hazard during the test. Finally, a safe and automatic method of testing the diodes without removing the shuttle car from operation is presented.

CHAPTER I

INTEGRATED GROUND FAULT - GROUND CHECK MONITOR

1.1 ABSTRACT

Currently mine monitoring for phase-to-ground faults and ground wire-pilot wire continuity is done using two separate systems, termed ground fault and ground check monitoring, respectively. This report presents a survey of current ground check-ground fault practices and the design of an integrated monitoring system. The integrated approach combines the two types of monitors into a single device, thereby centralizing fault detection.

1.2 SURVEY OF CURRENT GROUND CHECK-GROUND FAULT MONITORING PRACTICES

The schematic of a mine substation is shown in figure 1.1. In this circuit it is desired that certain safety conditions be met. Monitoring this circuit requires assessing continuity of the ground-pilot loop (A&B, figure 1.1) and fault detection. The safety conditions are as follows:

1.2.1 Continuity

1) The pilot wire (A, figure 1.1) if used, should be continuous and connected at the substation to a monitor and at the machine frame to the frame.

2) The ground wire (B, figure 1.1) should be continuous and grounded at one end in a low-resistance ground bed and connected to the machine frame at the other end.

3) The ground wire impedance shall not exceed a nominal value, usually designated as 4 Ω.

If any of the preceeding conditions (especially 2) and 3)) are violated, a ground fault occurring on the system would produce dangerous potentials on the equipment.

1.2.2 Faults

Line to ground or frame faults can cause dangerous potentials to appear on machine frames. Because the current is limited by the grounding resistor, the over-current protection will not trip at the circuit breaker. Line to line faults will be controlled by the overcurrent protection. In addition, a pilot wire to ground wire fault can cause the ground check monitor to ignore part of the ground wire, and thus pilot to ground short detection should be included in the ground check monitor circuitry. Figure 1.2 shows the various faults that can occur.

If any of the conditions 1) through 3) in section 1.2.1 or any of the faults described in this section occur, a breaker should be activated that removes power from the affected area of the mine until the problem is corrected. Various methods are used in monitoring for hazardous situations.

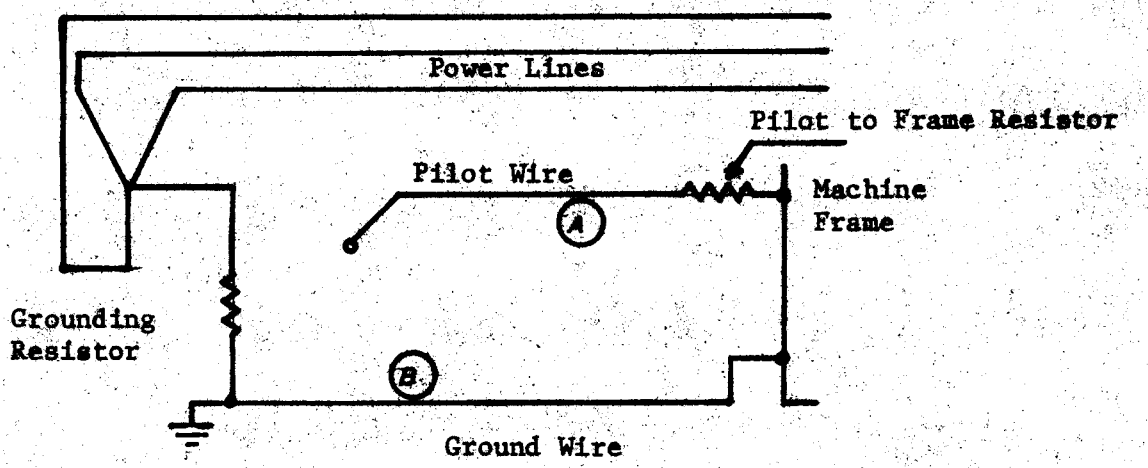

FIGURE 1.1. - Mine substation schematic.

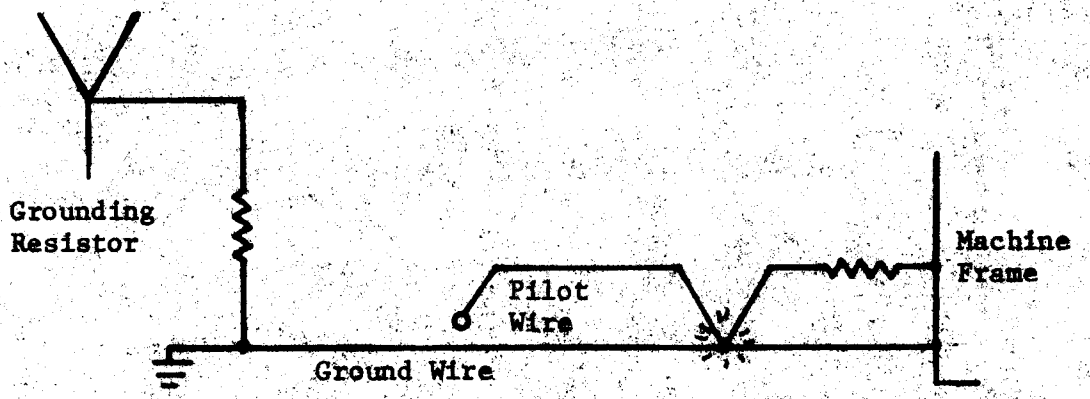

FIGURE 1.2a. - Pilot to ground fault.

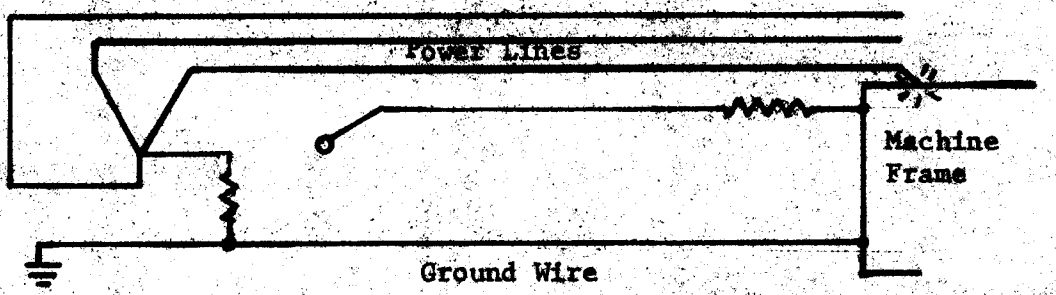

FIGURE 1.2b. - Line to frame fault.

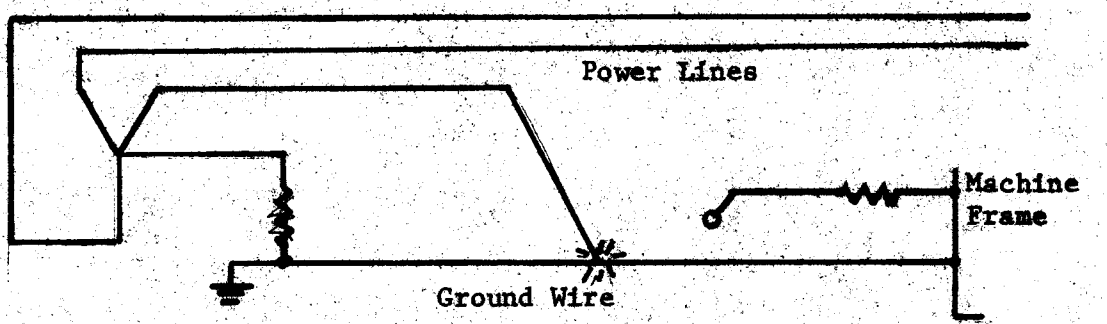

FIGURE1.2c. - Line to ground fault.

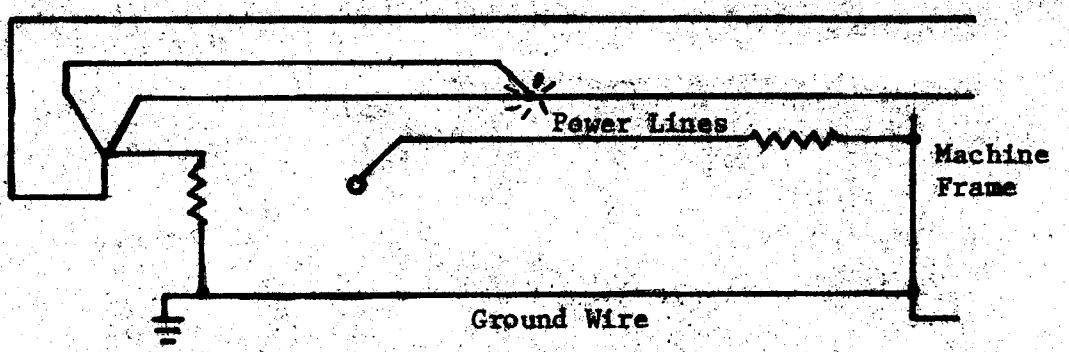

FIGURE 1.2d. - Line to line fault.

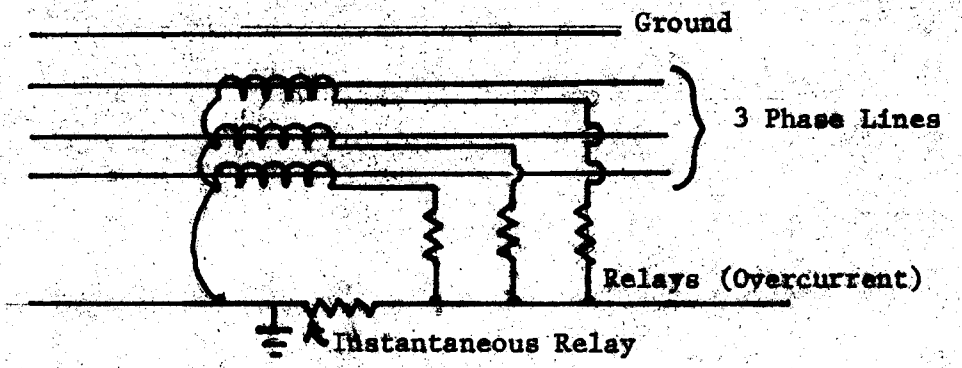

FIGURE 1.3a. - Residual trip relaying.

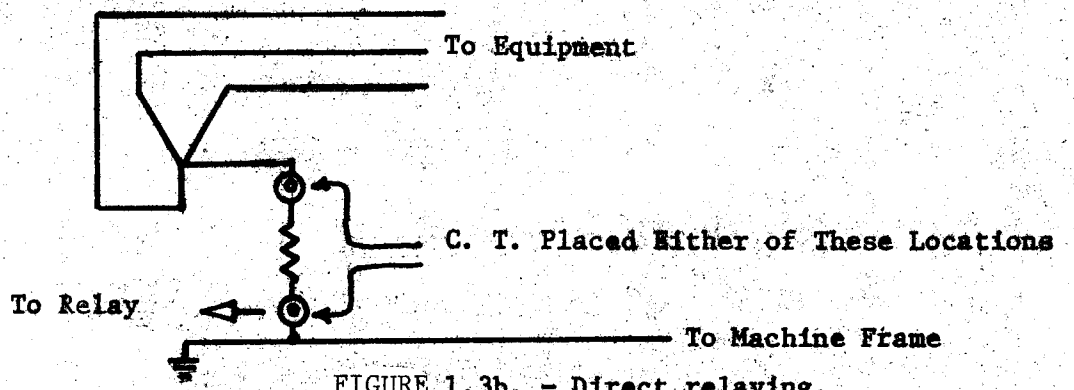

FIGURE 1.3b. - Direct relaying.

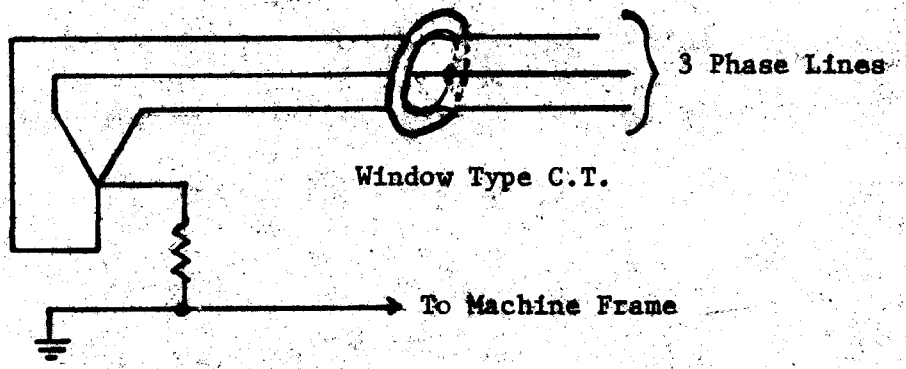

FIGURE 1.3c. - Balanced flux relaying.

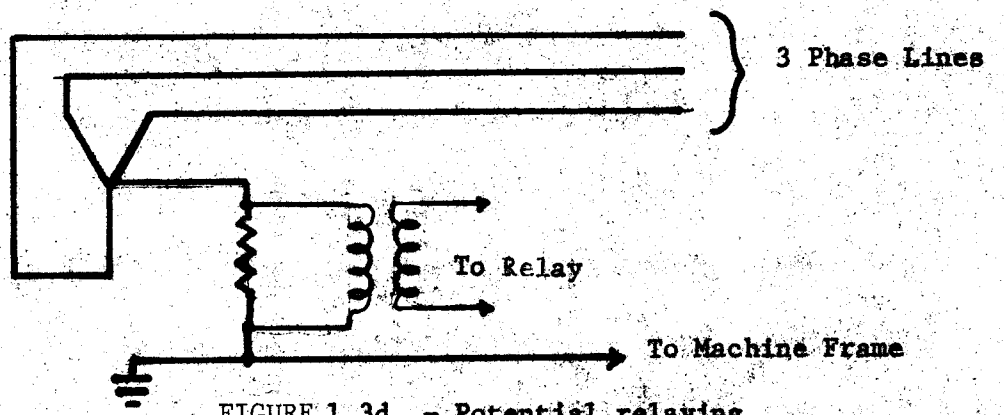

FIGURE 1.3d. - Potential relaying.

Monitors that check the integrity of the ground wire-pilot wire circuit (conditions 1) through 3)) are ground check monitors, and those that detect line-to-ground or line to frame faults are termed ground fault monitors.

1.2.3 Ground Check Monitor Types

The ground-check monitor itself can be one of several types as outlined in Chapter 4 of the 1975-76 Annual Report by West Virginia University for the USBM Grant No. G0144138 [1].

1.2.4 Ground Fault Monitors

Four common methods are used in ground fault detection [2]

1) Residual trip relaying

2) Direct relaying

3) Balanced flux relaying

4) Potential relaying

An important factor when considering fault protection is selectivity (i.e. the ability of a detection system to shut down a small section of the mine during local fault conditions, leaving the rest of the mine up). This is accomplished using time dial relays and coordination (the relay nearest the fault drops out first). Some of the ground-fault detection schemes are not inherently selective. Below, each of these methods is described with respect to whether or not it is selective.

1) Residual trip relaying

This method detects ground faults as an imbalance in line currents. Three bar-type current transformers (C.T.'s) are used to detect any imbalance and trip out the relay (figure 1.3a)). This method is expensive and is not currently a popular method of ground fault detection. It is selective because only the affected circuit need be tripped.

2) Direct Relaying

This is the most popular technique for substation circuitry. A window-type C.T. is placed directly in the resistance-grounded neutral line of the transformer (figure 1.3b)). This method is not selective because it cannot determine which circuit fed by the transformer contains the fault.

3) Balanced Flux Relaying

This is the most used detection system for underground power centers, as it is selective as well as inexpensive. An imbalance in the 3ϕ circuit is detected with a window-type C.T. around all three phase lines (figure 1.3c)).

4) Potential Relaying

This type of relaying is the most popular backup system. It is accomplished

by placing a potential transformer across the grounding resistor (figure 1.3d)). The voltage impressed across the resistor during the fault is used to trip the relay. It is not selective.

The following section describes an integrated monitor which was designed to do the job of both of the previously mentioned monitors, but in a single system as opposed to two separate systems. The inherent advantages of an integrated system, rather than having the two separated systems, are enhanced reliability, less equipment to install, and more rapid identification of the source of system outages.

1.3 INTEGRATED GROUND FAULT-GROUND CHECK MONITOR

1.3.1 Selection

The circuit selected as having the most promise as an integrated ground-check-ground fault system was a bridge circuit (figure 1.4)) comprised of the pilot wire (A), ground wire (B), grounding resistor (C), pilot-to-frame resistor (D), and the switching resistor (E). From point (F) to ground is an audio oscillator which drives the bridge. At (G) and (H) are two bridge balance resistors.

To facilitate the following explanation, the circuit is redrawn in the basic bridge configuration of figure 1.5. The bridge is balanced at nodes 1 and 2 in these two figures by selecting resistor RA_2 to balance the grounding resistor (R_G), and by selecting RA_1 to balance the sum of the ground wire resistance (R_{WE}) and the pilot-to-frame resistor (R_P). This relationship is in accordance with the bridge balance equation $Z_1 Z_4 = Z_2 Z_3$ where $RA_1 = Z_1$, $RA_2 = Z_2$, $R_G = Z_3$ and $Z_4 = R_P + R_{WE}$, and is the standard Wheatstone bridge. The detector (located between points 1 and 2 in figures 1.4 and 1.5) is designed to detect the potential difference between these two nodes.

By switching R_{SW} in and out of the ground wire leg, the bridge voltage is made to vary between a balanced (when R_{SW} is shorted) and an unbalanced (when R_{SW} is in the circuit) condition. A capacitor at the output of the detector is charged by this varying balance voltage and is used to hold in a relay. Thus, if the ground wire changes impedance by several ohms, the bridge design causes this to be seen as a constant imbalance between the nodes. The relay trips the circuit breaker, thereby insuring a low impedance ground wire. Similarly, an opening of a wire anywhere in the bridge or any component failure will cause the breaker to trip.

If a fault occurs, zener diodes on the node inputs conduct, which make the balance voltages disappear, causing a trip. In addition, high-voltage (HV) detectors located at nodes 1 and 2 detect any faults or high 60 Hz voltages and likewise trip the system. If during a fault condition one of the HV detectors fails, an LED indicates that a detector failed to detect the fault. It also indicates which one it is, so repairs can be made if necessary. All three (balance and two high voltage) detectors are separately

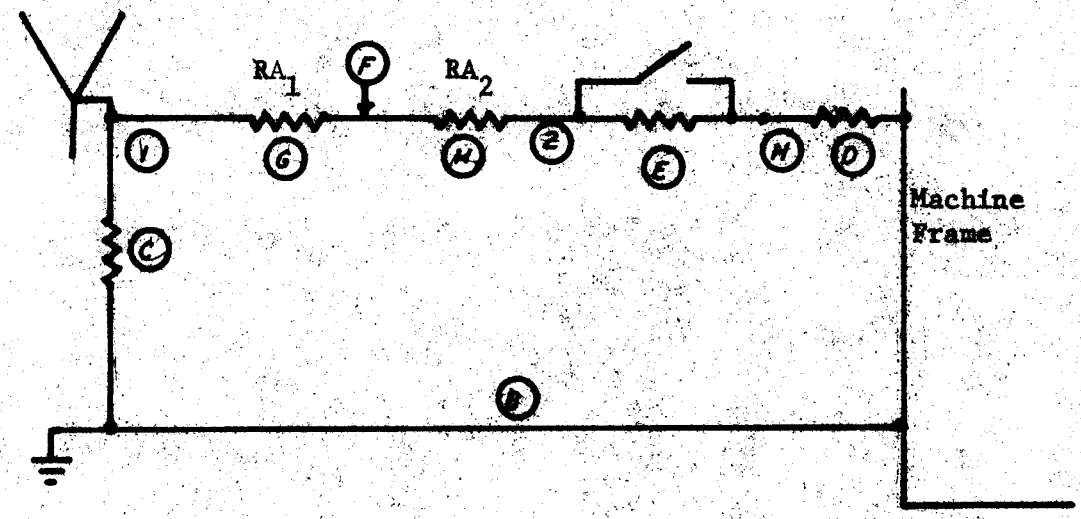

FIGURE 1.4. - Bridge circuit.

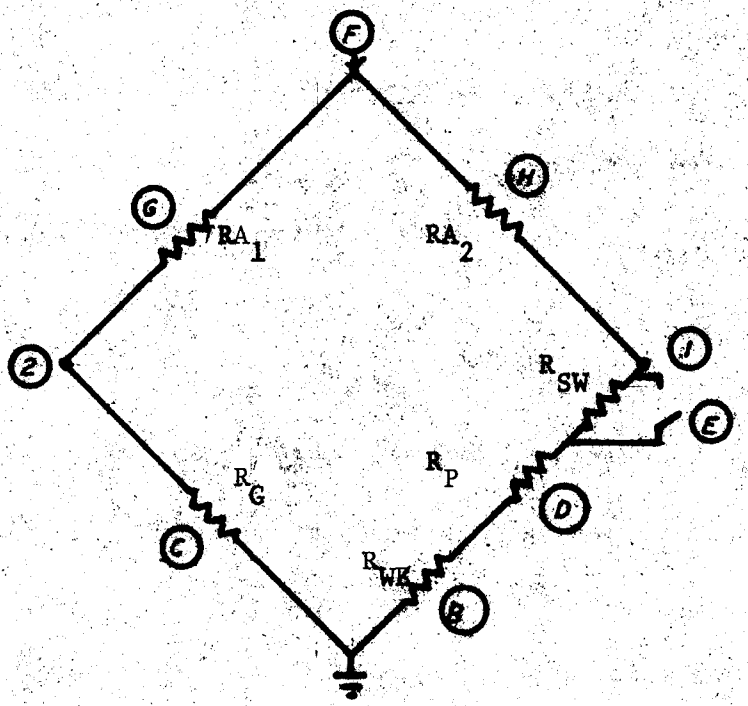

FIGURE 1.5. - Standard bridge circuit.

capable of tripping the relays. A detailed account of the monitor's reaction to fault is given in section 1.4.

A block diagram of the circuitry is shown in figure 1.6. The detector is protected with overvoltage circuitry, and the bridge components are rated to withstand fault currents and voltages for short periods of time. This is discussed in Appendix A.1, and further recommendations are in section 1.5.

The audio oscillator located at point F in figures 1.4 and 1.5 sources a 1 kHz sine wave that is used to drive the bridge.

1.3.2 Description of Operation

The monitor consists of two separate parts; the bridge (figures 1.4 and 1.5) and the detector (figure 1.6).

1.3.3 Bridge

Figures 1.4 and 1.5 show a bridge circuit built into the mine power circuitry at the substation. If continuity conditions 1), 2), and 3) in section 1.2 are met, and there is no ground fault on the system, the bridge will be balanced when R_{SW} is shorted and unbalanced when this resistor is in the circuit. This switching is performed at a 10 Hz rate by an oscillator-driven relay. It is this continuous balancing and unbalancing of the bridge that holds in the relay. This method was chosen because it acts to check the detector circuitry. When R_{SW} is switched out of the bridge (shorted), the bridge is balanced if the ground wire impedance is at the right level and the capacitor holding in the relay is "pumped" through another capacitor. R_{SW} is then switched in the system and the bridge is unbalanced enough to slightly drop the voltage off the capacitor before R_{SW} is switched out, again pumping the capacitor. If the bridge becomes continuously unbalanced, then the pumping voltage remains either high or low and the pumping action ceases. The monitor sensitivity is determined by the switched resistor in figures 1.4 and 1.5 (R_{SW}), which is sized for the percentage of ground wire impedance change to be allowed. For example, if a maximum ground wire impedance of 4 Ω is desired and the ground wire nominal impedance is 2 Ω, R_{WE} should be ≈ 2 Ω. In this way, if the ground wire's impedance exceeds 4 Ω, the relay is tripped (this is discussed in detail later). Also, a failure or impedance change of other elements of the bridge will cause a continuous bridge imbalance which will trip the relay. The power rating of the bridge resistors is determined largely by fault conditions and is discussed in the mathematical monitor description in Appendix A.1.

A small value of bridge balance voltage was chosen because the larger RA_1 and RA_2 (the top bridge legs) are, the less power they must dissipate under fault conditions. Therefore, it is desired to let them be as large as possible and still give sufficient sensitivity. Therefore only ≈ 1 V of the 12.8 V rms driving voltage is used for balance voltage, the rest being

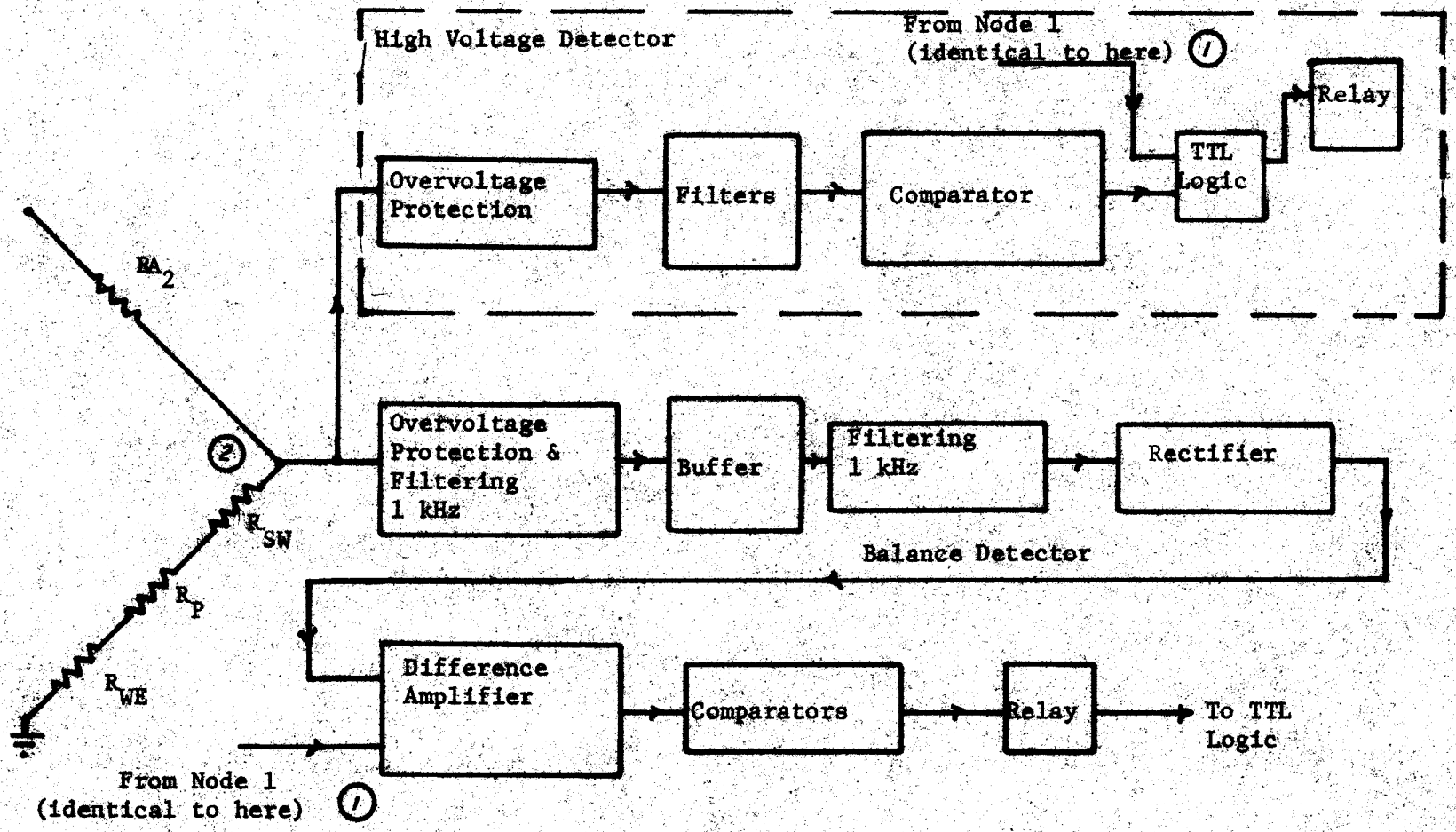

FIGURE 1.6. - Detector block diagram.

dropped across RA_1 and RA_2. Calculations and resistor sizing are done in the mathematical section.

1.3.4 Detector

The detector's primary function is to compare the voltages at nodes 1 and 2. The node 1 voltage will be constant and the node 2 voltage will be varying at a 10 Hz rate. (Refer to the block diagram of the detector in figure 1.6). The 1 kHz node voltage is first accepted through high voltage protection circuitry consisting of a 1 kHz transformer-capacitor bandpass filter and current-limiting resistors and zener diodes. This 1 kHz signal then passes through a buffer used to offset the losses of the high voltage protection circuitry, and then through a pair of active biquad 1 kHz bandpass filters. The filtered waveform is then rectified and passed into a difference amplifier. It compares this signal with the identically processed balance voltage from the other node and generates the difference between the two signals.

At this point, there is a sawtooth wave varying between zero (when the bridge is balanced) and a value depending on the value of R_{SW}. This is passed into a window comparator set at the required ground wire impedance tolerance (for details see calibration and use, Appendix A.2). As long as the difference waveform is within the correct tolerance, the comparators will be continuously exercised and their output will be a 10 Hz square wave. If the difference signal leaves the required tolerance range, the comparators will no longer be activated and a high or low dc voltage output will be produced. The comparator output is driven into a transistor-diode capacitor charge pump network that requires a constantly switching voltage to hold in a relay. TTL logic is used to display the condition of the relay.

Also connected to nodes 1 and 2 are the high voltage detectors. The block diagram of these detectors is shown in figure 1.6.

After being clipped by voltage suppression, the fault voltage is transformed down by a transformer. It is passed through a 60 Hz active filter and a rectifier, and is fed into a comparator that trips the relay at a fault level dependent on the comparator setting (discussed in Appendix A.2). In this way, trips can be set at different fault voltage levels and ground wire currents.

Three separate methods of tripping the relays have been described: the balance detector and the two high voltage detectors. TTL logic is used to coordinate the entire system. The output from the two high-voltage detectors is passed through TTL gates to determine which detector saw the fault and if either detector failed, which one it was. An indicator is also used to determine the condition of the balance relay.

1.3.5 Oscillator and Driver Circuitry

This circuitry consists of a 3 W power oscillator that drives the bridge, the oscillator and switch that removes R_{SW} from the Z_4 leg of the bridge, and the power supplies that supply all of the circuitry.

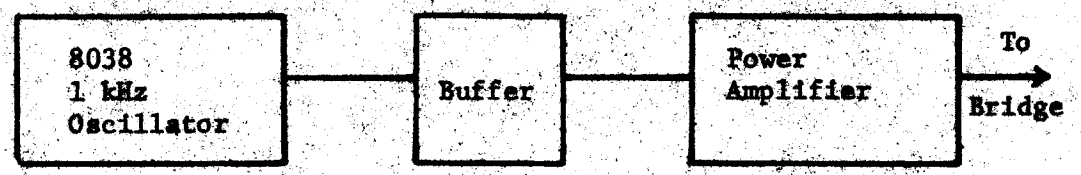

FIGURE 1.7. - Block diagram of bridge driver.

There are three separate power supplies for the monitor. An unregulated 70 V supply is used for the power drivers for the audio signal that drives the bridge. A regulated ±15 V supply used in the detector op-amps and filters, and a regulated +5 V TTL logic supply is used. Block diagrams for the supplies are shown in figures 1.10a), b) and c).

The bridge-driving supply is designed to supply 70 V at 0.4 A, although it actually supplies only 36 V_{PP} at 0.3 A. This allows changing the bridge resistors if necessary. Similarly, the ±15 V and 5 V supplies are over-designed to supply 1.0 A and 0.5 A, respectively. This is about four times their required level.

A block diagram of the bridge driver is shown in figure 1.7. A 1 kHz sine wave is derived from an 8038 waveform generator. This 1 kHz signal is then buffered and passed into the power amplifier. Here a boost of the signal to 12.8 Vrms (36 V_{PP}) drives the bridge.

The relay that switches R_{SW} in and out of the Z_4 leg is driven by a 10 Hz oscillator and placed across R_{SW} as shown in figure 1.8. This signal is used to saturate and cutoff a switching transistor that drives the coil of the relay. The 10 Hz switching frequency was selected because it is fast enough to detect a failed ground wire quickly, but is slow enough to allow the detector circuitry to respond.

1.4 FAULT AND FAILURE ANALYSIS

This section discusses the possible faults and component failures the bridge will be subjected to and how it will react to them.

Details of the power dissipation of the bridge components under fault conditions are covered in Appendix A.1.

Following is a list of hazardous conditions for the catagories of power line fault and component failure.

Faults

a) power line to frame or ground

b) power line to pilot wire

c) double power line to ground

Failures

a) bridge component RA_1 or RA_2 fails

b) pilot wire open

c) pilot-to-frame or ground short

d) grounding resistor opens or shorts

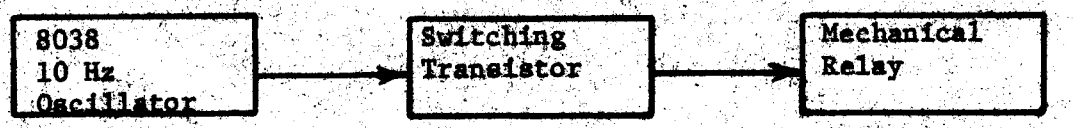

FIGURE 1.8. - Block diagram of balance switch.

e) ground wire impedance change

f) detector component faulty

g) bridge driving circuitry fails

h) switch fails

Fault conditions a) through c) will cause an identical reaction by the circuitry. The neutral of the transformer will shift, causing both the HV detectors to sense the fault. Faults of this type also saturate the balance detector at node 1 causing a trip there. Each of the three detectors is capable of tripping the breaker, so there is a large degree of redundancy.

If one of the failures a) through d) occurs, there is no danger and the bridge becomes unbalanced because each failure either opens or shorts a bridge component. The balance relay is therefore tripped and the display indicates that the bridge failed due to a bridge imbalance.

If the ground wire resistor changes its impedance, either up or down, (e), by approximately 50% (depending on the comparator settings), the bridge will trip due to imbalance.

If any detector components malfunction, (f), the relay will come out because the switching node voltage must propagate through the circuitry at the correct amplitude and balance for the relay to stay in. Similarly, a failure of the bridge driving circuitry, (g), will cause a trip, since both nodes will receive zero signal. Thus they will not be switched in and out of balance to drive the charge pump.

A failure of the switch across R_{SW}, (h), will cause the difference signal to cease driving the charge pump, allowing the capacitor that holds in the relay to discharge, and thus dropping the relay.

For details of how faults and failures affect the warning lights, refer to Appendix A.2.

1.5 CONCLUSIONS AND FURTHER RESEARCH

This monitor was designed as a prototype integrated ground check ground fault monitor for a substation supplying 7200 V_{L-L} (4160 V_{L-n}). Although designed for one system, every effort has been made to make the monitor as versatile as possible, in order to accomodate various ground wire impedance tolerances and voltage levels.

The system does seem to be feasible. It has monitored simulated faults and ground wires for weeks in the laboratory, during which time many faults and shorts were put on the circuitry. The circuits survived these instances and seem to be quite durable. Also, the system is as failsafe as possible.

The components of the design which must be the most carefully watched are the resistors that tie the transformer neutral to the frame. The problem here

is that the resistors involved must dissipate considerable power during faults. The duration of the fault should be rather short since it should be tripped out by the monitor. Further research along these lines could consider disconnecting the frame-to-neutral leg of the bridge during a fault with a self-resetting relay.

Another area of work could involve microprocessor monitoring of the bridge using saturable transistors at the bridge nodes and, in fact, a prototype using this idea has been designed and tested. An advantage of this method is that in most cases the exact source of failure may be pinpointed, including how the bridge component failed (open or short). The problem is that fault voltages at the nodes would destroy the transistors.

There are many advantages with the integrated bridge approach. There is redundancy, fail-safe design, and having all fault detection and monitoring circuitry in one enclosure coordinated with lamp indicators (many more of which could have been added) which aid in fault diagnosis.

CHAPTER II

DC GROUNDING SYSTEMS

2.1 INTRODUCTION

This task was to evaluate and compare grounding methods for dc-powered mine shuttle cars. Six presently used systems were investigated with special consideration given to their relative advantages and disadvantages.

To aid in this comparison, a computer simulation was made of four of the systems. The transients involved in starting the shuttle car and those caused by faults on the system were studied. This was done in an effort to determine the relative performance of each and thereby give mine operators a better idea of which method best suits their needs.

This chapter first summarizes each grounding system. The computer simulation procedures are then explained and the program results are given for the introduction of various faults to the systems. Finally, a more qualitative analysis is made of the effectiveness of each dc grounding method.

2.2 TYPES OF DC GROUNDING SYSTEMS

Six methods for grounding dc shuttle cars are explained below. A computer simulation of only four of these methods has been done and a further discussion of each can be found in section 2.5. SCR grounding was not modelled because of the complexity of the gating circuitry and also because of its similarity to diode grounding. The "Lectronic Sentry" was not modelled because the effectiveness of this system can best be determined experimentally.

2.2.1 Diode Grounding

A simplified drawing of the diode grounding system, with a grounded negative conductor, is shown in figure 2.1. For a grounded positive conductor the polarity of the grounding diode is reversed. The intent of this system is to provide a low-resistance path to ground for fault current (via the diode) when the hot conductor is shorted to the machine frame. In this sense, the diode merely replaces a ground wire (section 2.2.3). An overcurrent relay in series with the grounding diode picks up at 25% or less of the diode forward current rating and opens the main contacts, thus de-energizing the circuit. If a single diode is used, its current capacity must be 400 A. If a parallel connection of 2 diodes is used, their individual rating must be at least 275 A [7]. Therefore, the overload protection must be coordinated with the diode circuit.

Either the positive or the negative conductor may be grounded, but one must be grounded to ensure proper protection. Any resistive voltage drop in the grounded conductor will be blocked by the diode's high resistance when reverse biased. This provides shock protection for the machine operator and prevents arcing to grounded objects.

Most of the desirable features of the diode grounding system result from the elimination of the third (ground) wire. Some of the advantages of a

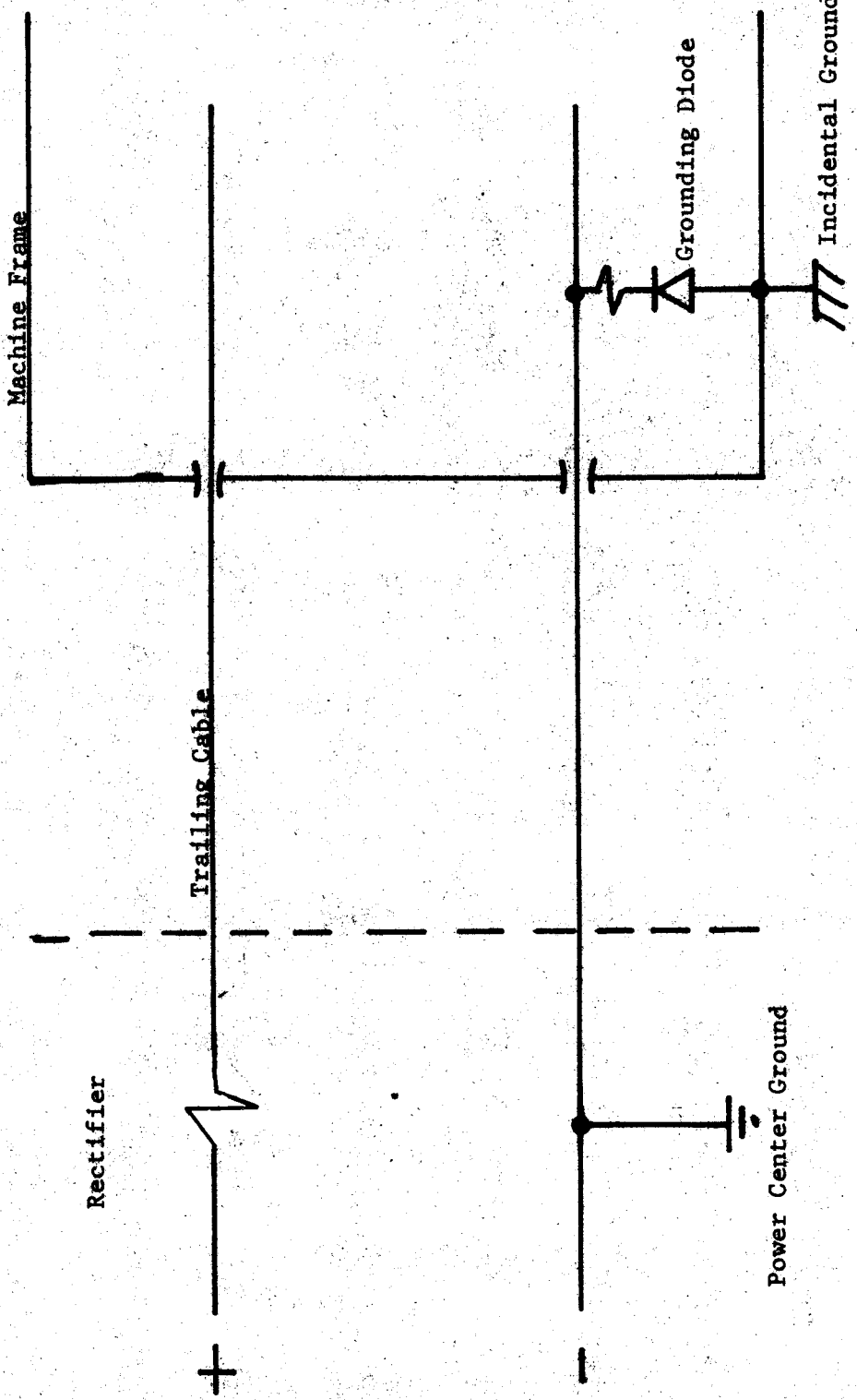

FIGURE 2.1.- Negative-grounded diode system.

two-wire system over a three-wire system (sections 2.2.3-2.2.5) are:

1. The cable cost and weight are reduced;

2. Splicing time and difficulty are reduced;

3. Better ground wire continuity is possible because the negative conductor is the ground-fault path;

4. The use of dual cable reels is possible (separate positive and negative conductors). This can reduce downtime, extend cable life, and make splicing easier [8].

A major drawback of the diode grounding system is that the integrity of the diode must be periodically checked. Almost all diode failures occur by shorting which means that this system "fails operative". It does not prevent machine operation and a short from the ungrounded conductor to the machine frame will still cause the main contacts to open. Diode failure can produce a shock hazard, however, since such a failure could go undetected indefinitely. Any voltage drop in the grounded conductor would appear on the machine frame and high current would not be blocked by the diode. For a further discussion of possible hazards with this grounding system, refer to section 2.5.2.

2.2.2 SCR Grounding

A variation of the diode grounding system is SCR grounding. The grounding diode is replaced by a controlled rectifier. It has an involved gating circuit which allows the SCR to turn on only if the machine frame voltage exceeds a threshold value for a period of time determined by a filter. A block diagram of this grounding method is shown in figure 2.2. The circuit itself contains two SCR's, a bidirectional breakdown diode (a diac), a transformer, and various other components. The need for this complicated controlling circuit for the SCR is a major drawback of this system.

SCR grounding has all the advantages a two-wire system has over a three-wire system explained in section 2.2.1. An important aspect of this grounding scheme is that the SCR is only "ON" when there is a ground fault; therefore there is no path for current to flow to cause intermachine arcing.

2.2.3 Basic Ground Wire System

Figure 2.3 shows the basic ground wire system. The negative power conductor is connected to the ground wire at the power center which is used as the ground-fault path. Any current produced by a short from the positive conductor to the machine frame will flow through the ground wire to the safety ground and the increased current caused by the short will trip an overcurrent relay in the positive conductor. Therefore, the sensitivity of this system is determined by the main overcurrent relay at the rectifier.

A major drawback with ground-wire systems is that an open in the ground wire could go undetected, leaving the machine operating in an ungrounded state. Monitoring the ground wire would eliminate this problem. Section 2.5.3 explains the computer simulation results for this system.

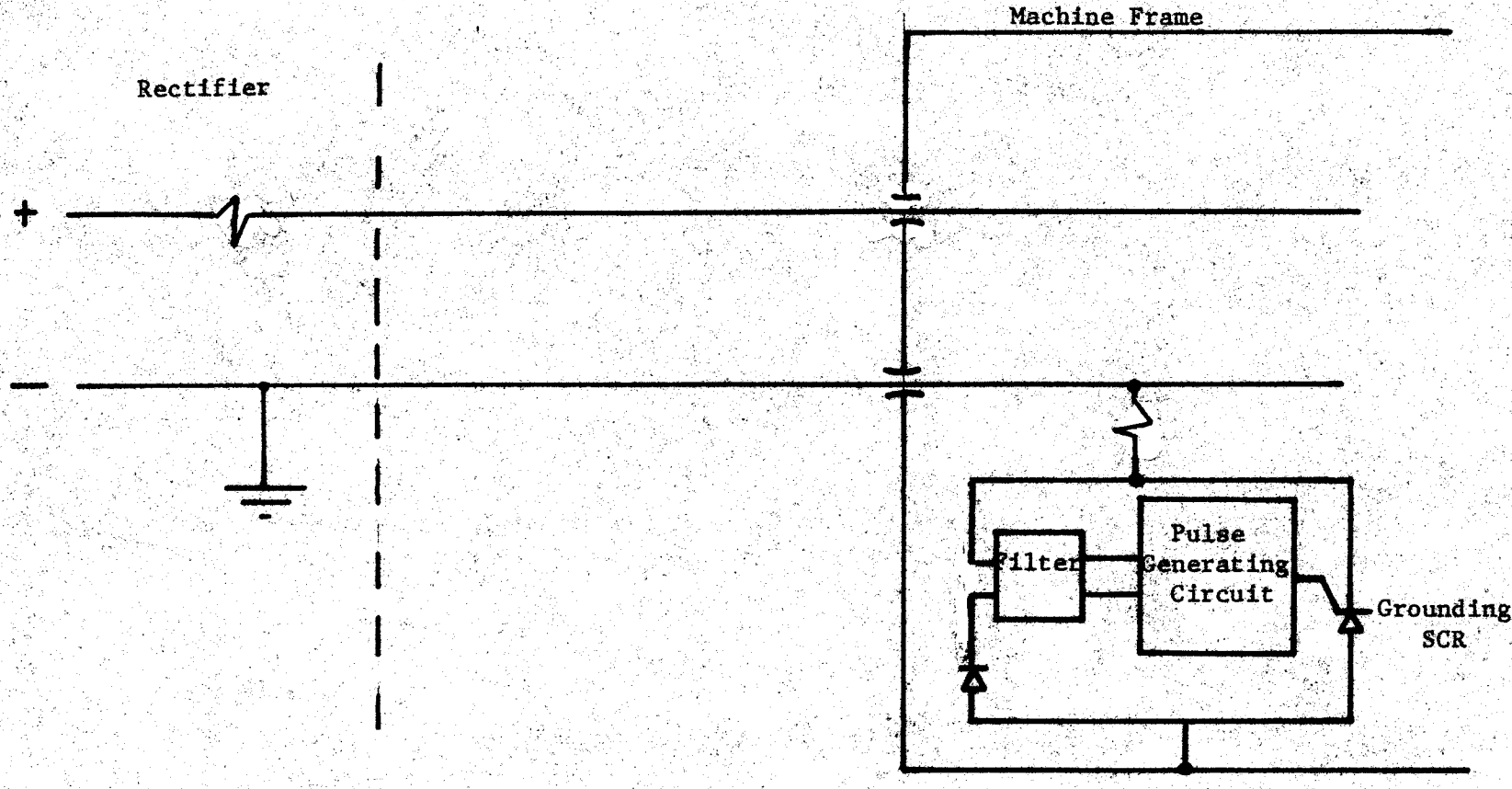

Figure 2.2. - SCR grounding system.

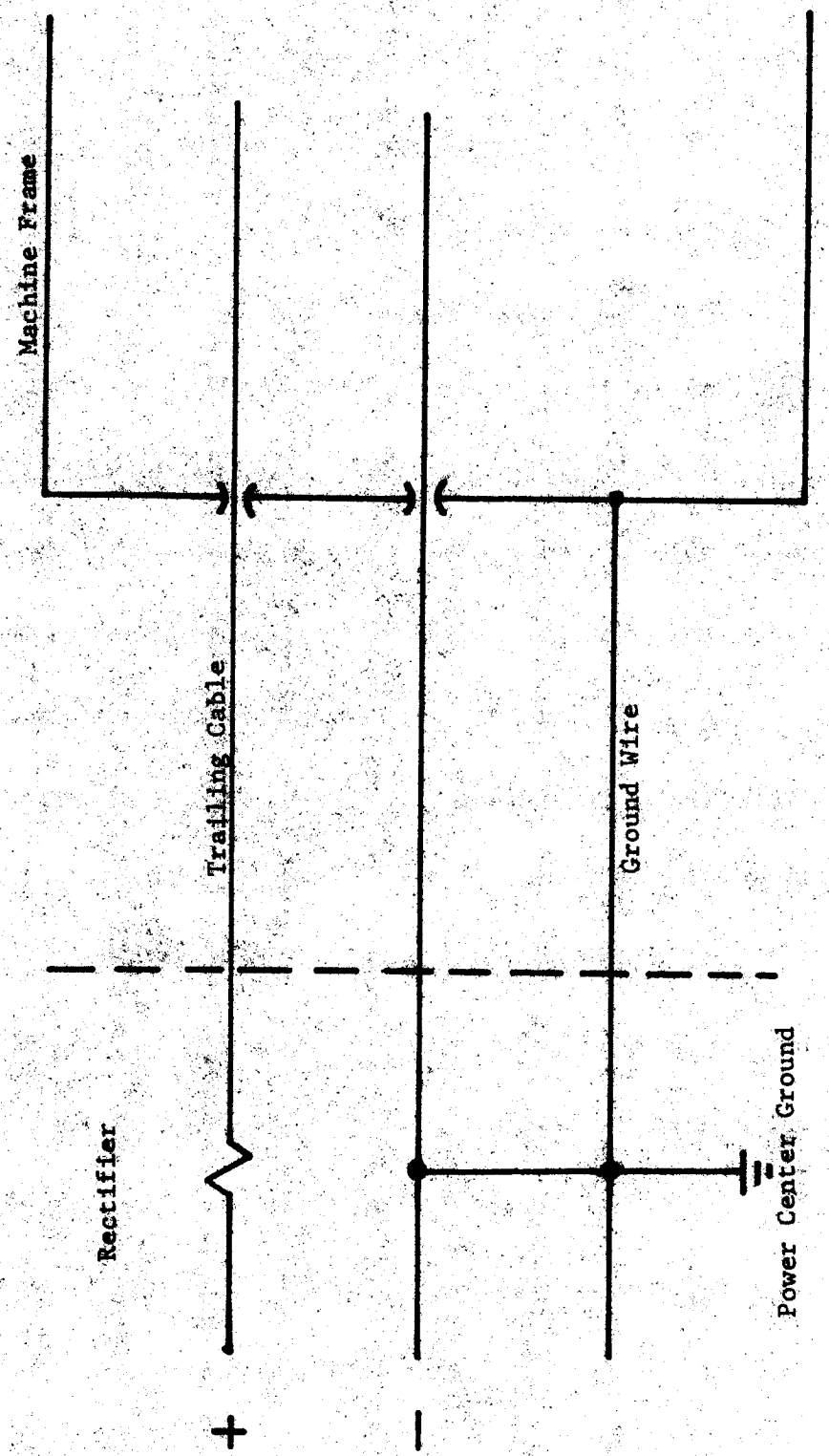

FIGURE 13. - Basic ground wire system.

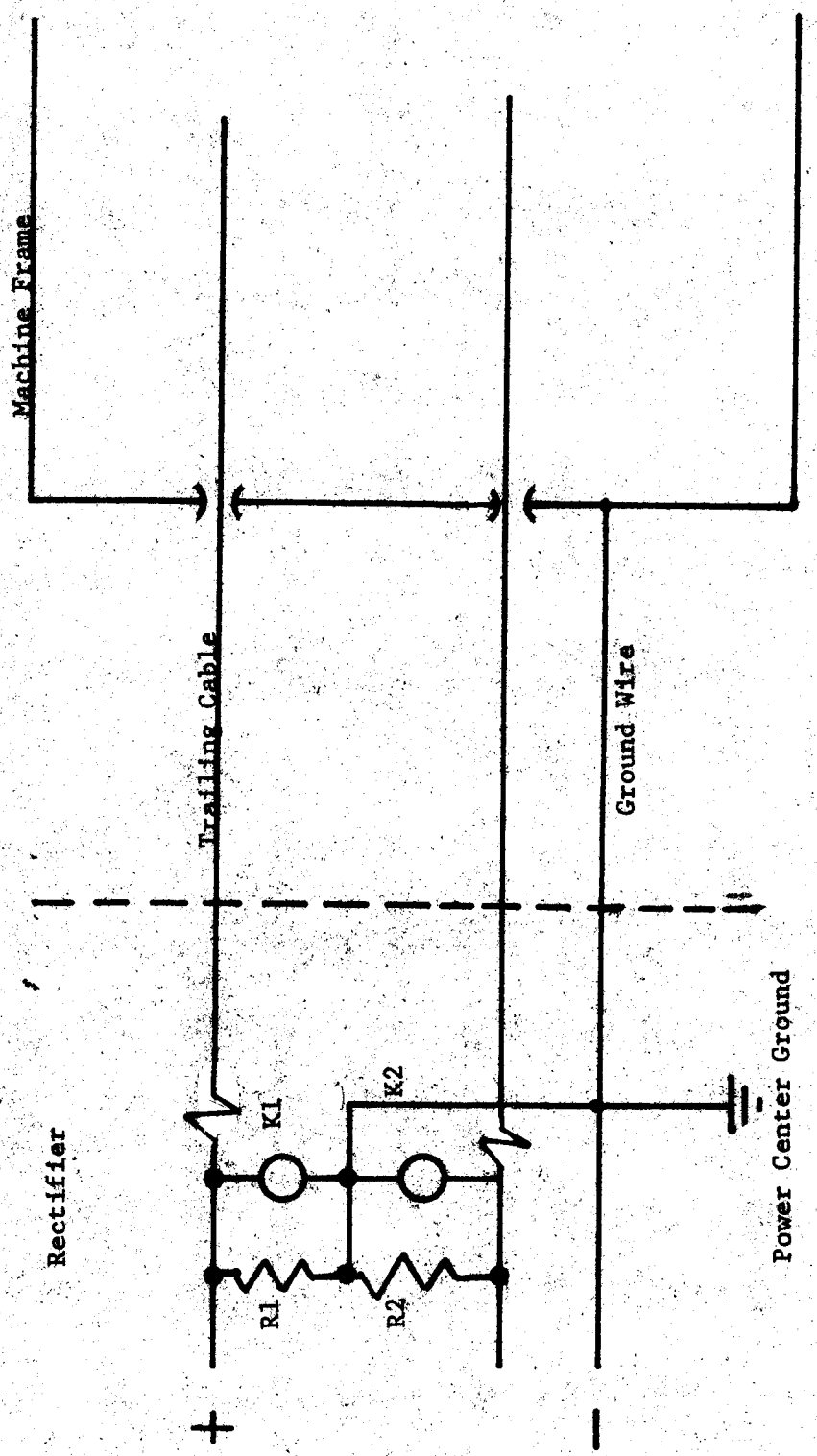

FIGURE 1.4.- Resistance-derived neutral system.

2.2.4 Resistance-Derived Neutral System

In the resistance-derived neutral system (figure 2.4) the neutral is established by the resistors R_1 and R_2. Voltage relays across each resistor sense any shift in the neutral caused by a ground fault on either conductor and open both conductors at the power center.

The overcurrent relays at the rectifier provide protection from a positive-to-negative conductor fault. The voltage relays are not sufficient, since there would be no shift in the neutral. No dangerous voltages would appear on the machine frame (since there is no current in the ground wire). Although the machine would be made inoperative, the conductor currents would be extremely high unless interrupted by the overcurrent relays.

2.2.5 Transformer-Derived Neutral System

Figure 2.5 shows a transformer-derived neutral system [9]. The neutral of the ac feeding circuit is connected through a resistor to the ground wire. The positive and negative conductors are passed through a saturable reactor controlled by an ac voltage. Only when the currents through the reactor are unequal (due to a ground fault) does its impedance to the ac control drop, and this will in turn activate an overcurrent relay.

An important advantage of this system is that it can provide selective tripping. If a fault occurs on one shuttle car which is powered from the same source as other machines, then the power to all the machines will not be cut off if there is one of these detectors for each machine.

2.2.6 Lectronic Sentry^R

The Lectronic Sentry System developed by Joy Manufacturing [10,11] is an active device which operates on a sender-receiver principle (see figure 2.6). An oscillator, mounted on the shuttle car, generates a low current signal (70mA, 25kHz). It is sent through one conductor where it is sensed by a pick-up coil and receiver and then returns through the other conductor. If a fault occurs in the cable or on the machine frame, the signal is interrupted which cuts off power to the UVR and the breaker will drop out.

This type of grounding has all the advantages that a two-wire system has over a three-wire system (see section 2.2.1). It is able to disregard normal operating overloads and it "eliminates possible severe arcing that can occur with a ground fault when a grounding conductor is employed" [12].

2.3 ELECTRONIC CIRCUIT ANALYSIS PROGRAM (ECAP)

2.3.1 Application

The IBM Electronic Circuit Analysis Program (ECAP) is a program system which can be used to show the dc, ac, or transient response of electrical circuits. The circuit under study must be reduced to an equivalent circuit using only voltage and current sources, resistors, inductors, capacitors, and an ECAP element known as a switch. When the current through the switch changes direction the values of specified elements switch to alternate values.

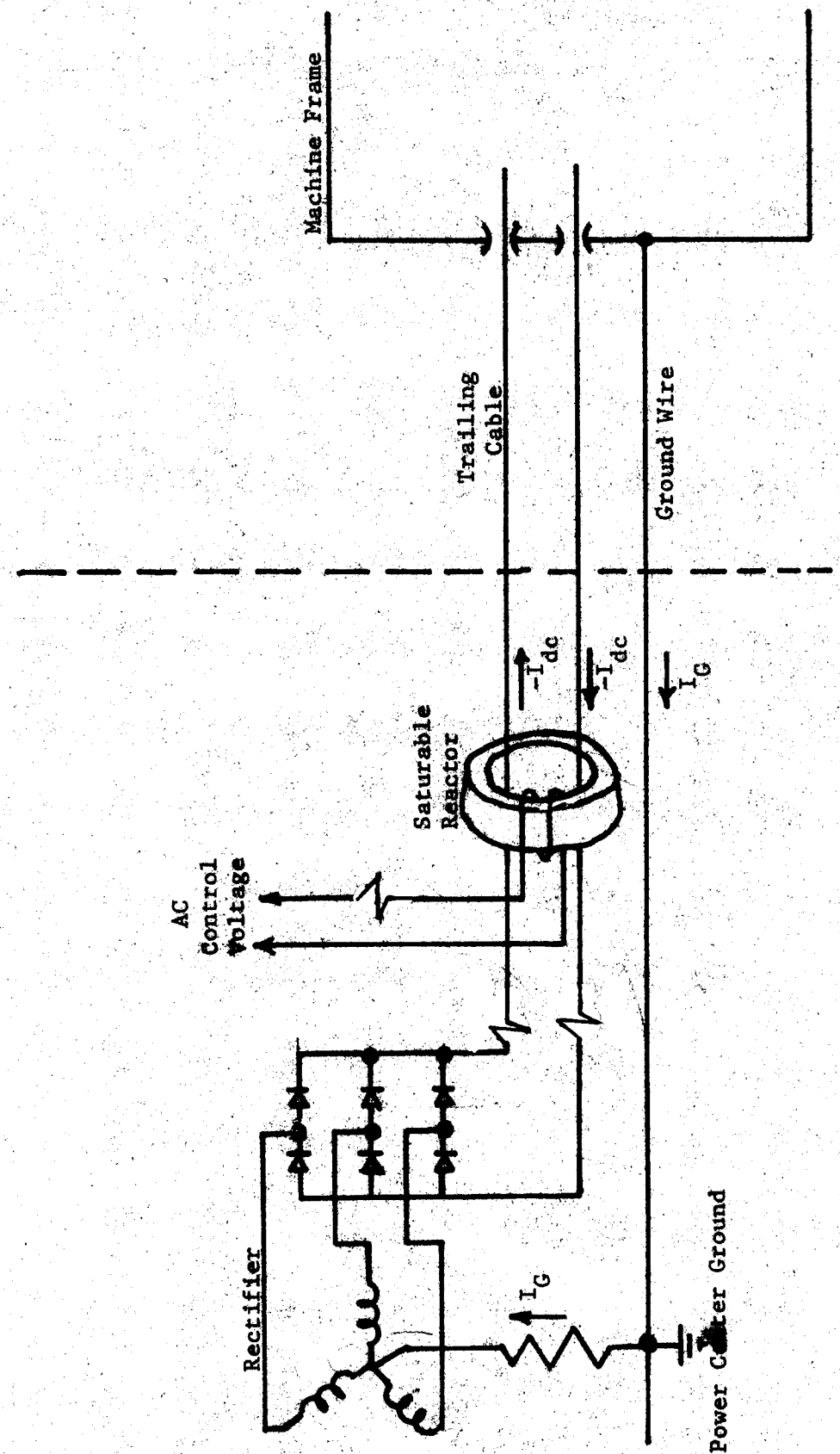

FIGURE 2.5. - Transformer-derived neutral system.

It is a very useful tool because it allows the modelling of nonlinear elements. Additional information on the program can be found in reference 13.

2.3.2 Limitations

ECAP allows the user to analyze a circuit fairly simply without manual solution of nth order differential equations. Although this saves time and effort, there are some limitations which must be considered. Three of these are discussed below.

1. The control and grounding circuits for dc shuttle cars contain such nonlinear elements as diodes, thyristors, transformers, contactors, etc. These elements require special attention in devising equivalent circuits with the same properties. Section 2.4.2 explains some of the models used in the computer simulation.

2. An important parameter of the ECAP solution is the time step. The time step indicates the number of computations made per second so there has to be a tradeoff between the accuracy of the solution and the length of time the program runs. The optimum time step for the circuits involved in this research seems to be 0.1 msec. Computations made less frequently yield longer lasting transients, and so the simulation does not reach equilibrium as quickly. The importance of choosing the right time step is illustrated in figure 2.7, where the same program (diode grounding with a positive to machine frame fault) is run at time steps of 0.1 msec and 1 msec. It can be seen from this graph that, although the initial transient of -9869 V occurs in both the simulations, the 1 msec time step gives the impression that the circuit has a longer time constant than it actually does.

3. Another problem encountered in the simulation is that there is no provision in ECAP for an open circuit. Very large resistance values can be used, but this still does not provide as much isolation as an actual open would. When contacts open, for example, their resistance changes instantaneously from 0.1 Ω to 10 MΩ. This causes extremely high voltages in the model since the current cannot change instantaneously in an inductive circuit. If 1 A is initially flowing through a closed contact, a voltage of 0.1 V appears across it. The instant the contact opens the voltage jumps to 10 MV but soon decreases once the current drops.

2.4 CONTROL CIRCUIT PROGRAM

2.4.1 The Control Circuit

The control circuit for a dc shuttle car consists of a number of relays which coordinate the shorting out of the motor starting resistors. It also contains a control diode which is used to prevent machine operation if the cable polarity is accidentally reversed. By using the same control circuit with various grounding systems a comparitive analysis between them can be shown.

The control circuit for the National Mine Service TORKAR is shown in

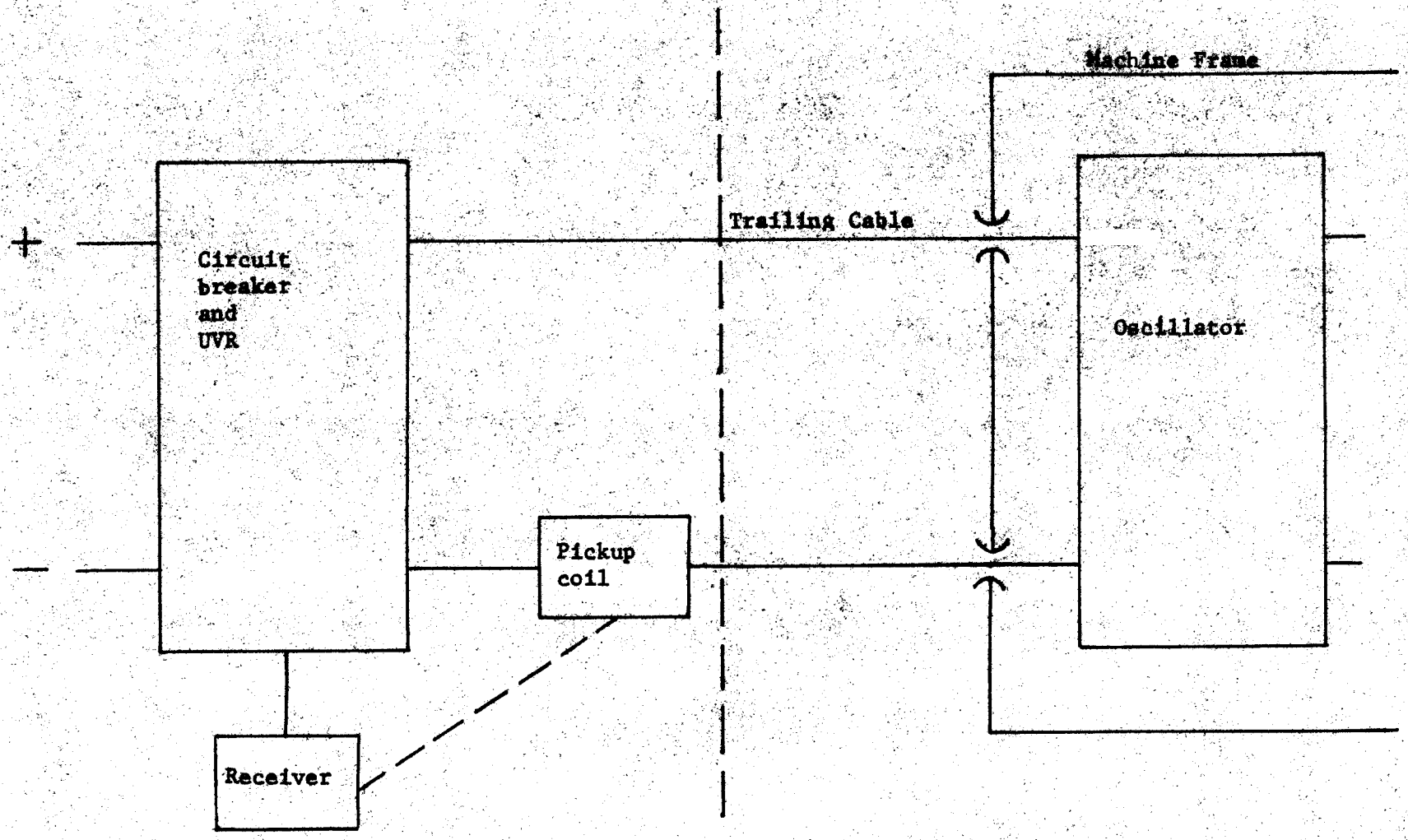

FIGURE 2.6. - Lectronic sentry dc system monitor (10).

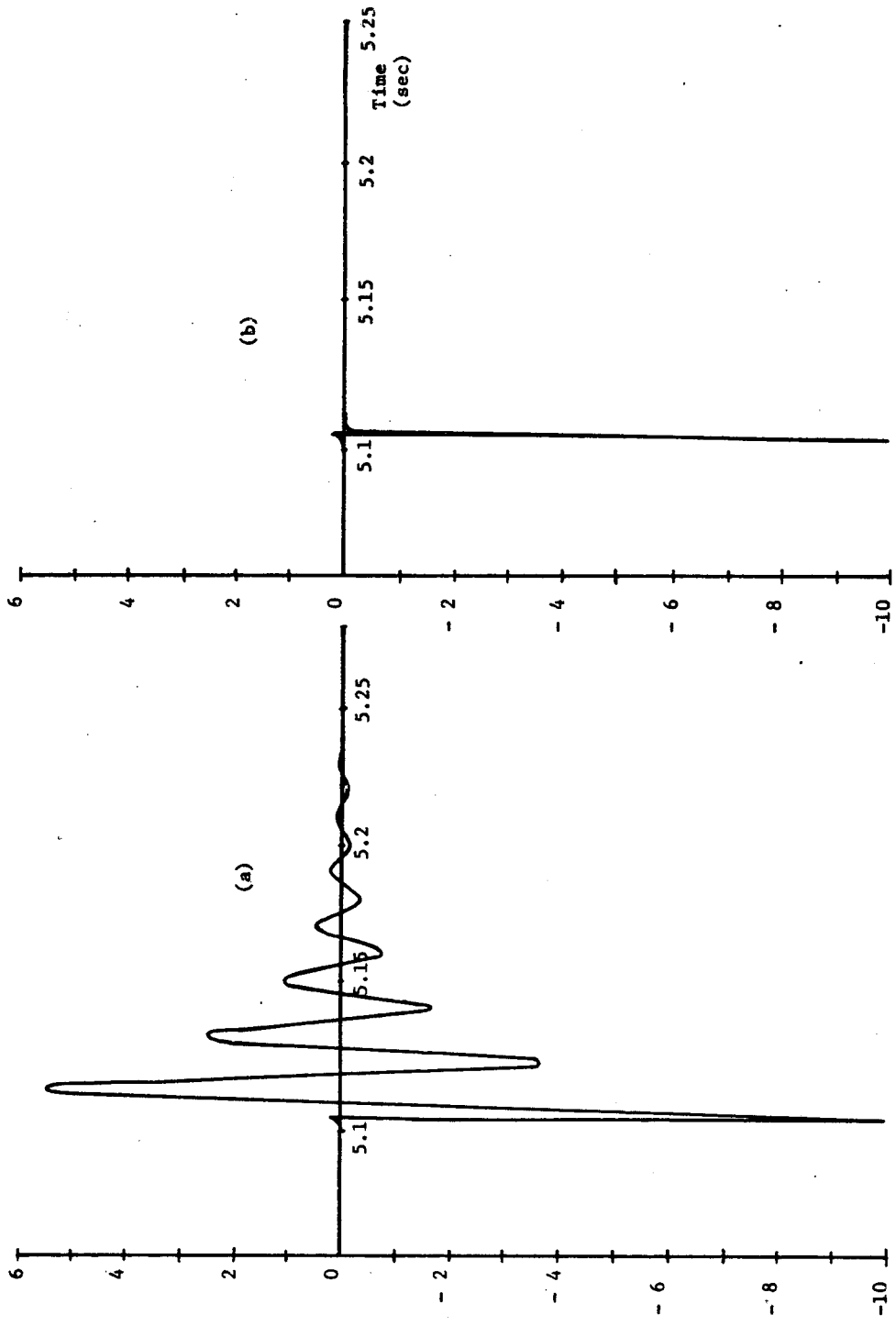

FIGURE 2.7. Comparison of same ECAP program using time steps of (a) 1 msec and (b) 0.1 msec.

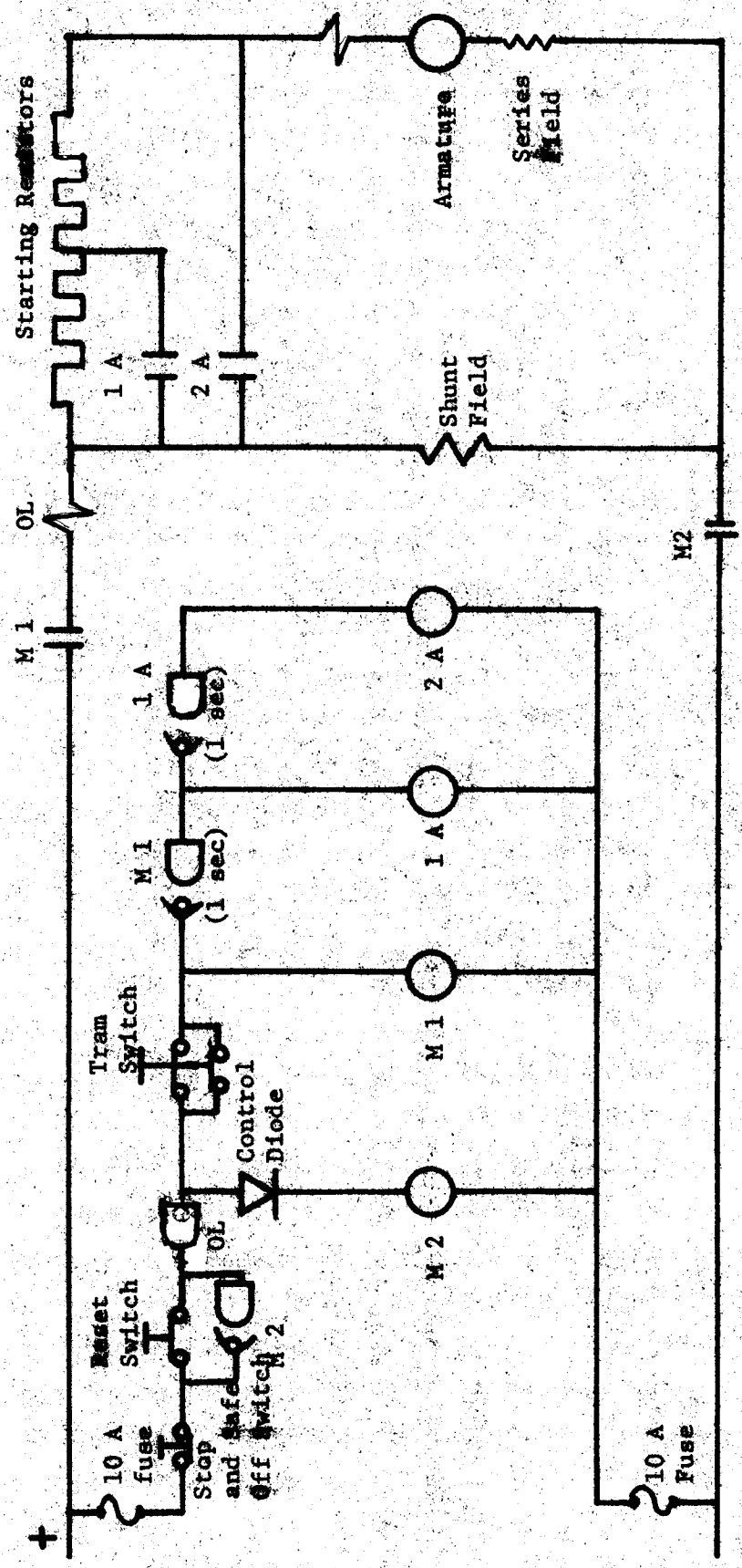

FIGURE 2.8.- Control circuit of the National Mine Service TORKAR.

figure 2.8. This is the standard used in the computer simulation. Its equivalent ECAP circuit is shown in figure 2.9a) and b). For specific element values refer to the programs in Appendix B.

2.4.2 Modelling Techniques for ECAP

Several elements of the control circuit require adjustments to make the circuit suitable for ECAP. These are each explained below.

1. Contactors - The contactors (M1, M2, 1A, and 2A) are coils which, after a sufficient amount of current is applied, activate their respective contacts. It was assumed that this amount of current is 0.1 A. A supplemental circuit for the ECAP model to test the level of current in the coil is necessary. Each contactor requires its own test circuit which are shown in figure 2.9b). Each consists of a constant current source of the test current magnitude, a dependent current source opposing it which duplicates the current in the actual contactor coil, and a switch which senses a change in current direction through the resistor to activate the contacts.

   Two of the contactors require a one-second delay before closing the contacts. These are the M2 and 1A contactors which control the shorting out of the motor starting resistors. The time delay circuits are shown in figure 2.9b). An R-L circuit is used with a unit step input activated by the contactor switch explained in the preceding paragraph. A separate current level test circuit is used in conjunction with the R-L circuit to activate the contact switches when the current through the inductor reaches the test current level. The element values used must satisfy the following equation where I_L is the current through the inductor:

   $$I_L = \frac{E}{R} (1 - e^{-tR/L}).$$

   For an inductor current of 0.9 A to be reached in one second the element values used in the circuit are: E = 10 V, R = 10 Ω, and L = 4.343 H.

2. Diodes - The control (polarizing) diode used in the control circuit and the grounding diode used in the Diode Grounding System are both modelled in the same manner. For the type of fault simulation being considered it is not necessary to model the reverse breakdown region of either diode. Figure 2.10a) shows the ECAP diode model and figure 2.10b) is its I-V characteristic using the RECAP plotting routine. The test current chosen is the value which yields a cut-in voltage of 0.75 V.

3. Overcurrent and Overvoltage Relays - The overcurrent relay used in the fault programs is simply modelled as a current level test circuit. Since there is no provision in ECAP for dependent voltage sources, the overvoltage relays must be modified to detect a change in current instead of voltage. The voltage relays, used in the resistance-derived neutral system, are placed across 1 kΩ resistors. The test

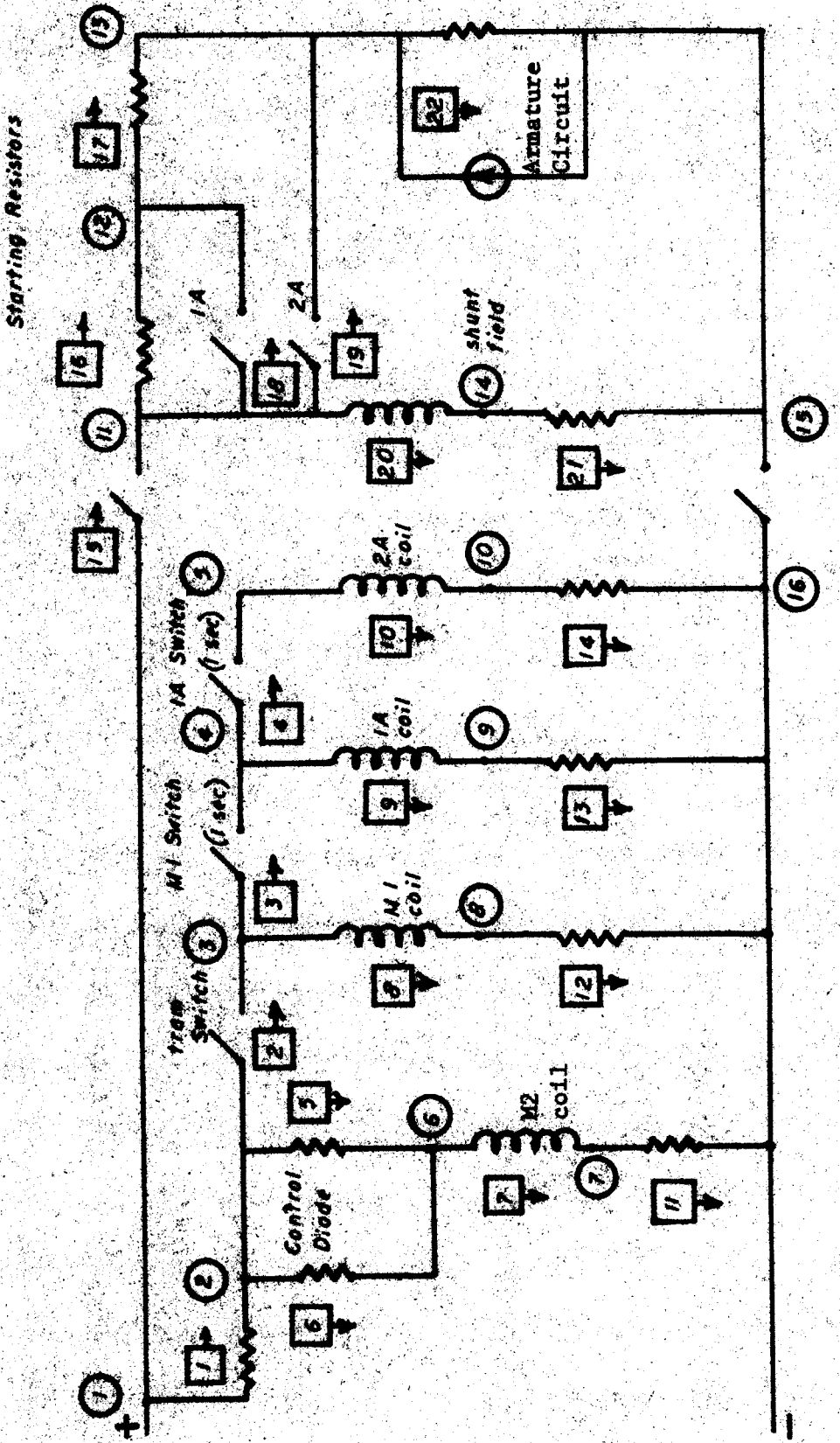

FIGURE 2.9a. - ECAP Model of the shuttle car control circuit.

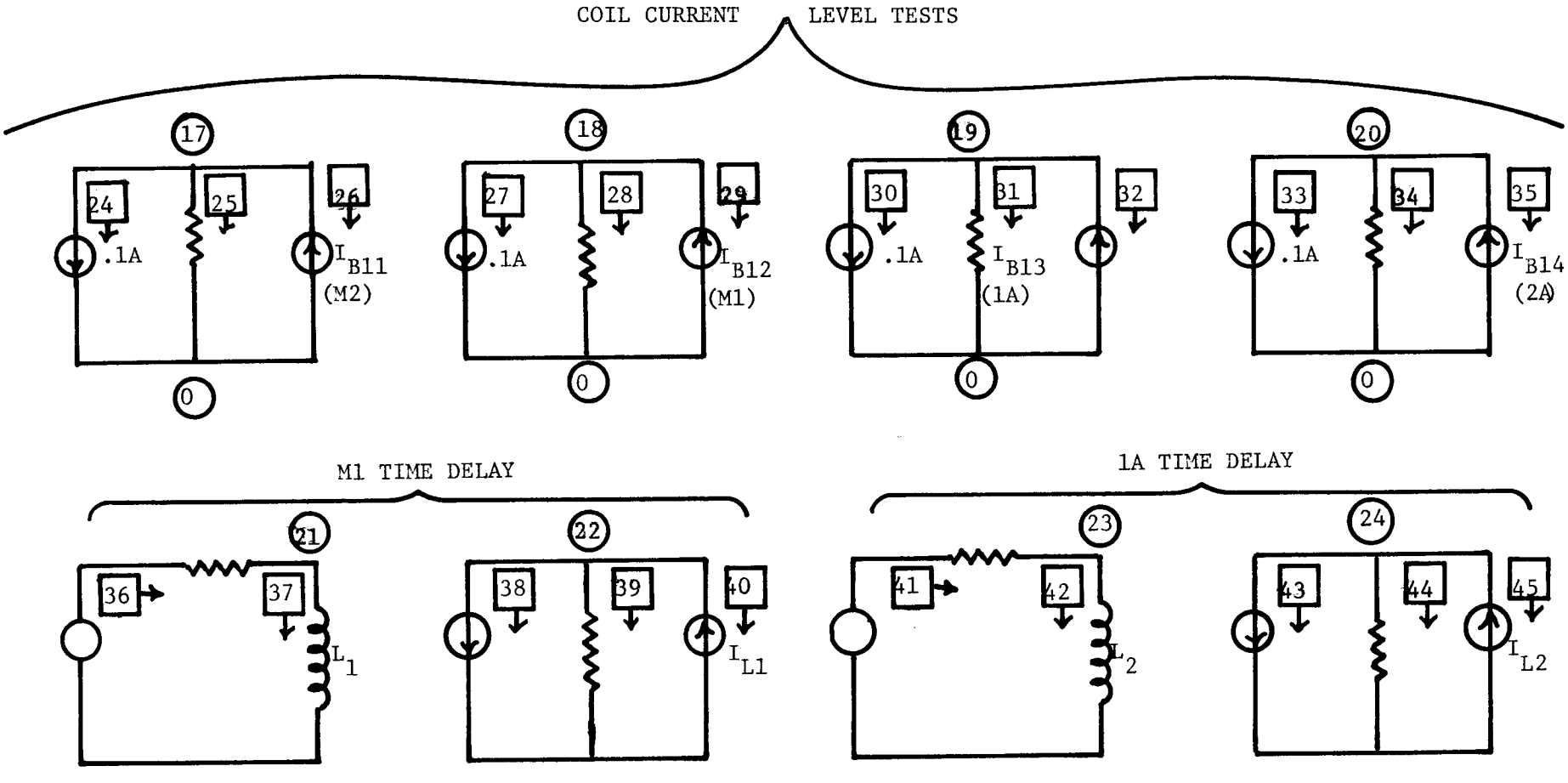

FIGURE 2.9b. - Supplemental circuits for use in conjunction with the control circuit model of Figure 2.9a.

(a)

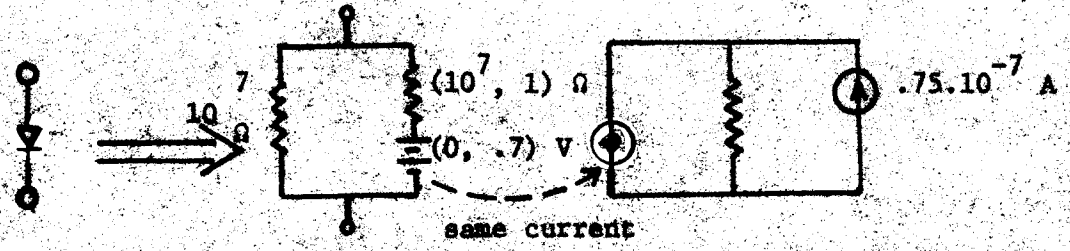

(b)

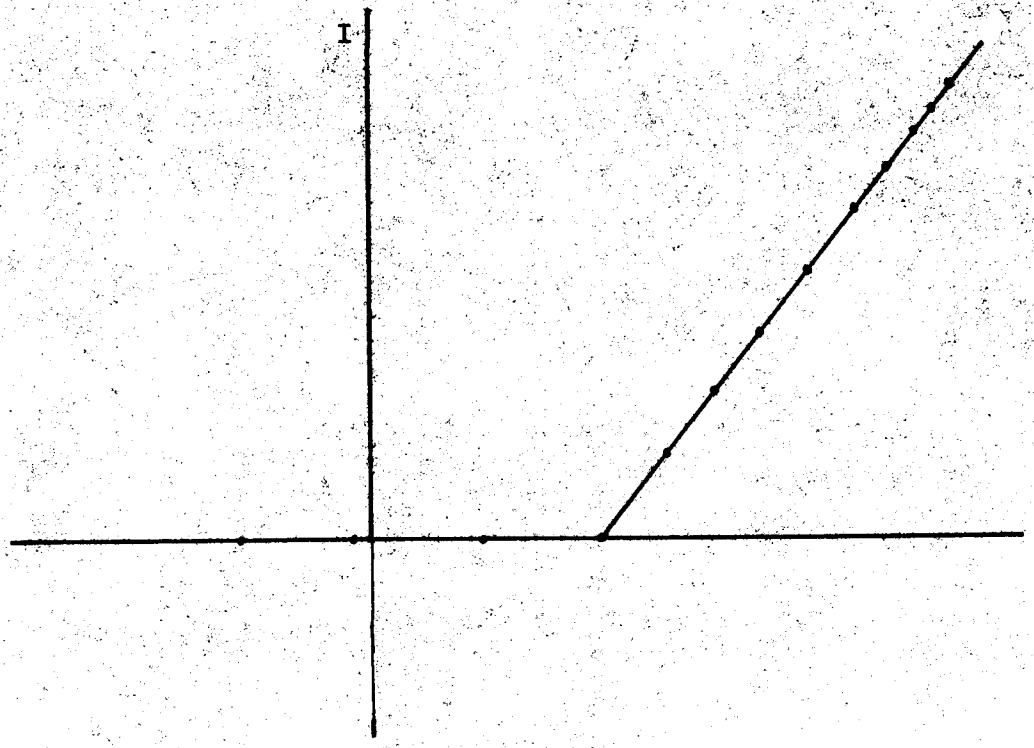

FIGURE 2.10a. - ECAP diode model:
b. - IV characteristic of the diode equivalent circuit using RECAP.

current level for each is then:

$$I_{test} = \frac{1}{1000\ \Omega} \quad (125 + \Delta V)\ V$$

where 125 V is the steady-state voltage across each relay and ΔV indicates the desired sensitivity of the relay.

4. Motor - The back emf of the motor is considered to be proportional to the shunt field current. Because a dependent voltage source is not an acceptable ECAP element, a Norton equivalent for the back emf has been used. A rather large shunt inductance simulates the motor inertia.

5. Other - The tram switch, which is actually a manual switch, is controlled in the program by the M2 contactor to simulate an activation time delay. The "stop and safe off" switch and the reset switch are assumed closed when the simulation is begun. The 10 A fuses are not modelled but the programs were checked to make sure that these currents always remained below this level.

2.4.3 Using the Control Circuit Model

The control circuit model shown in figure 2.9 is used as the basis for comparing the various grounding methods. Connections to this circuit for diode grounding, the basic ground wire method, the resistance-derived neutral system, and the transformer-derived neutral system are shown in figure 2.11a)-d). Because of the complexity of the transformer-derived neutral system discussed in section 2.2.5, a more simplistic system is used in the computer simulation. It contains no device to sense a shift in the neutral, so the only protection against faults is provided by the overcurrent relays at the power center. This is a "worst case" analysis for transformer-derived neutral systems to simply get an indication of the severity and consequences of various faults.

For the fault simulation under consideration it was unnecessary to fully model the rectifier, so a 250 V source with a 0.02 ohm resistance has been used. In the case of the transformer-derived neutral grounding system the rectifier is modelled as two 125 V sources with a 10 ohm grounding resistor at the neutral point.

The resistance for the positive and negative conductors is assumed to be 0.07 ohm (for 500 ft of #2 wire). The ground wire, which is usually one-half the area of the power conductors, has a resistance of 0.14 ohm. An inductance of 10 mH is used for each conductor which is considered to be a "worst case" value.

2.5 PROGRAM RESULTS

2.5.1 Introduction

It was desired to know about the severity of transients caused by starting the shuttle car motor for the different grounding systems. In grounding systems utilizing a ground wire the machine frame is not connected electrically

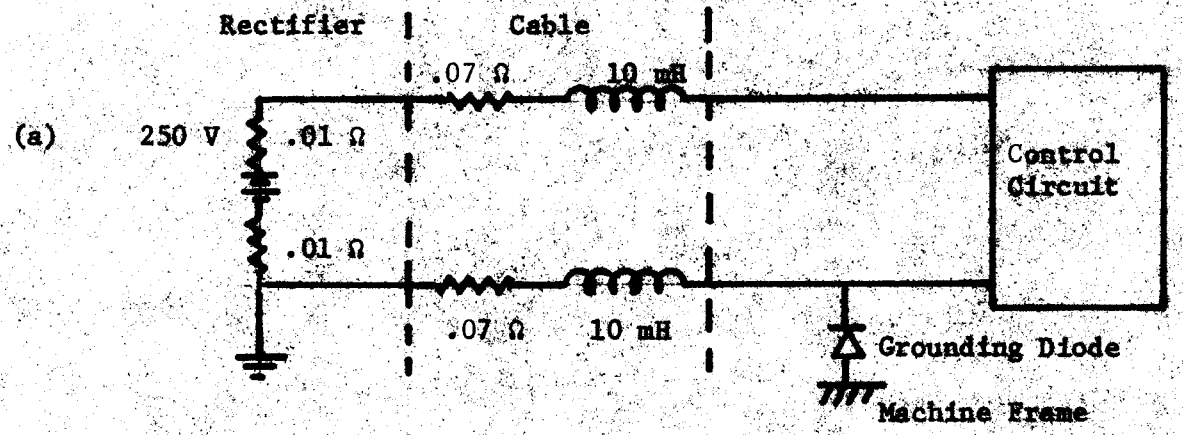

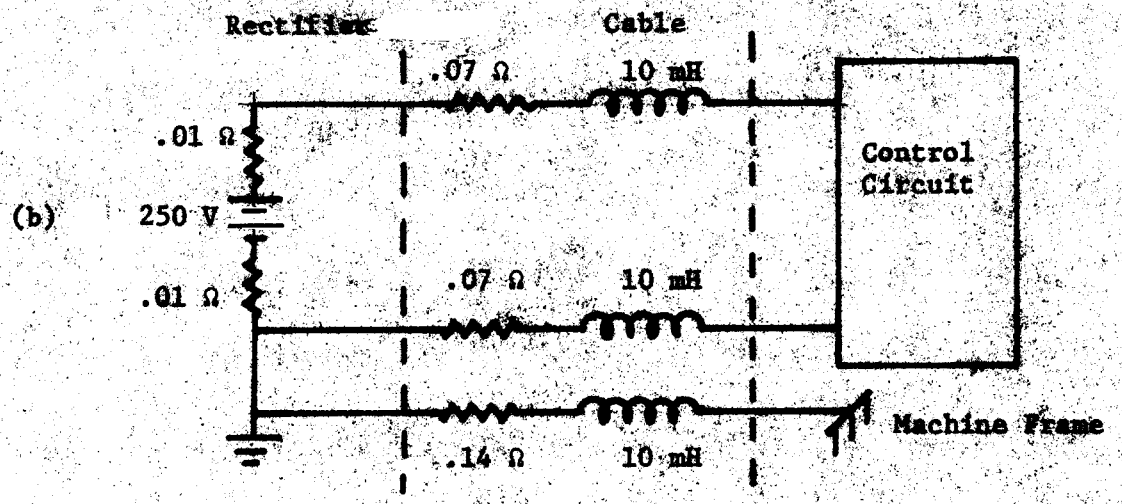

FIGURE 2.11. - Connection of the control circuit for (a) Diode grounding; (b) Basic ground wire system.

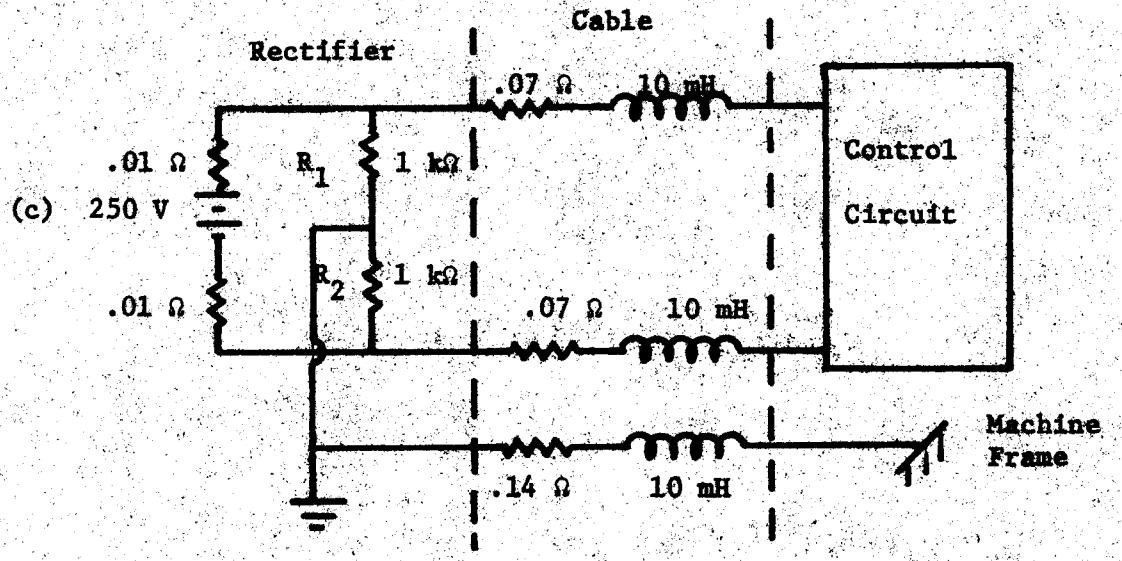

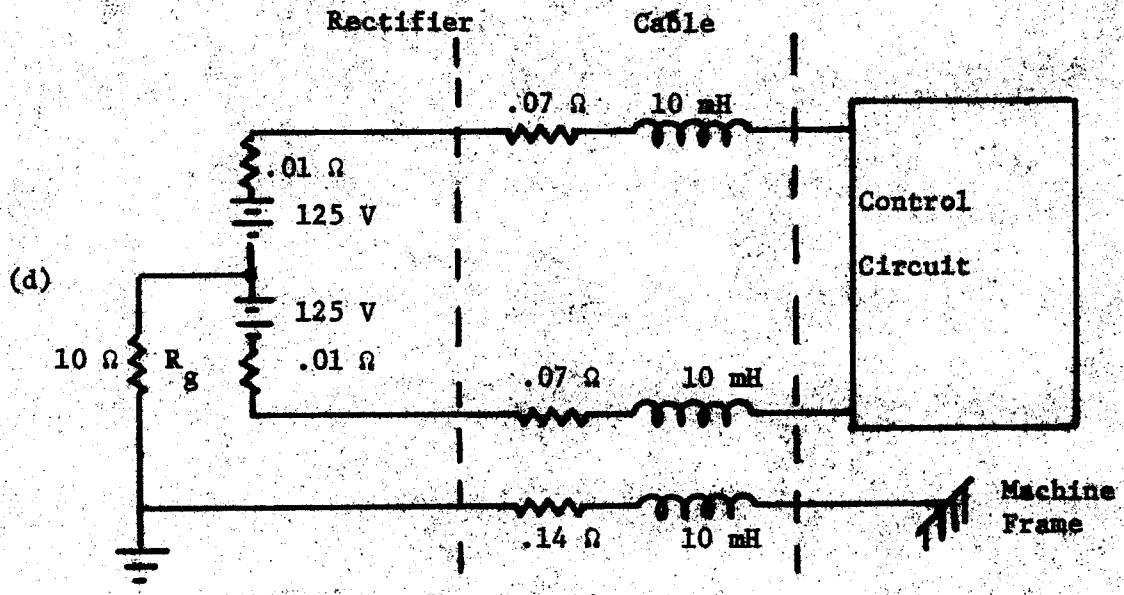

FIGURE 2.11. - (continued) - (c) Resistance-derived neutral system; and (d) Transformer-derived neutral system.

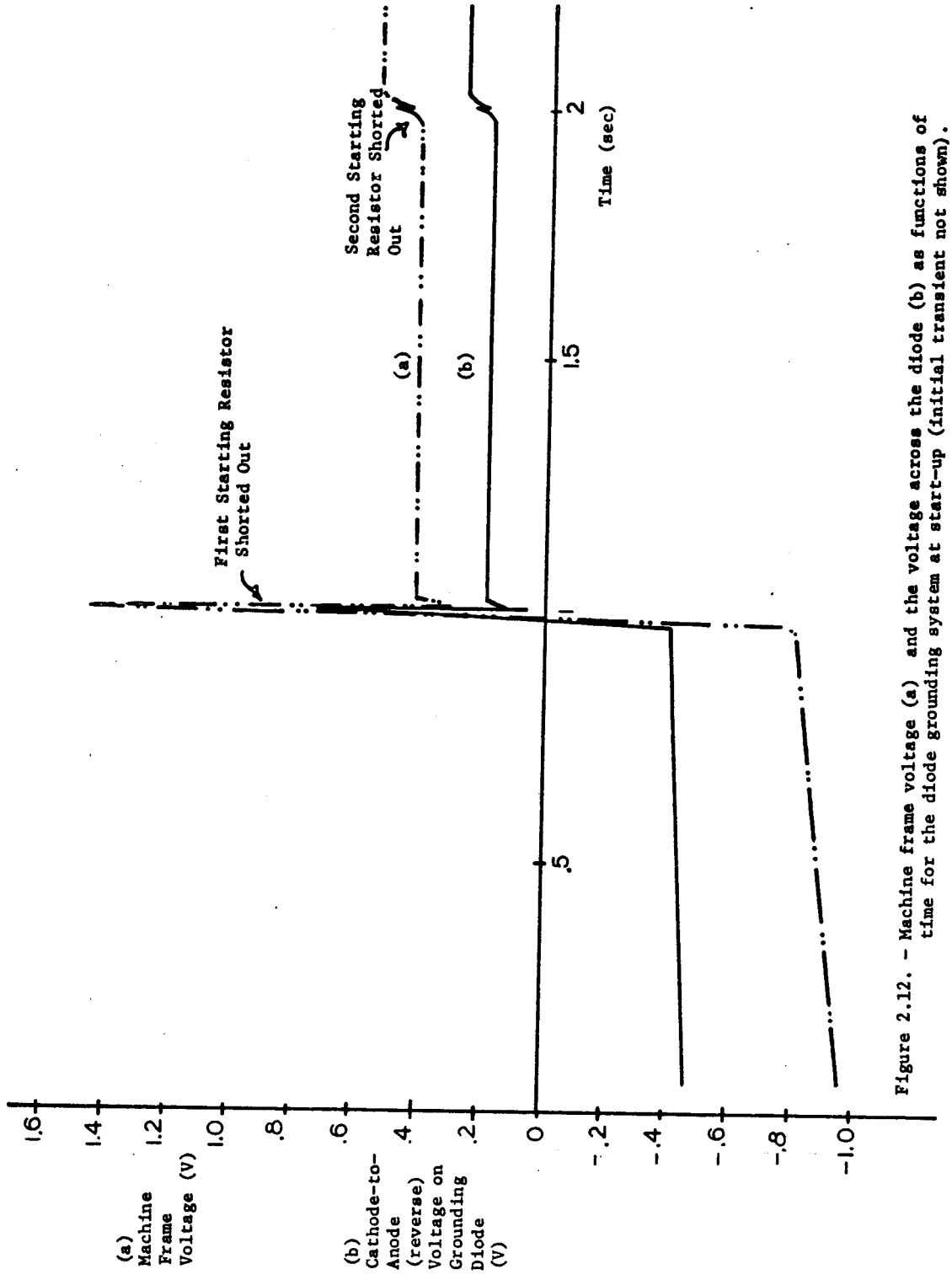

Figure 2.12. - Machine frame voltage (a) and the voltage across the diode (b) as functions of time for the diode grounding system at start-up (initial transient not shown).

to the control circuit unless there is a fault on the system. Therefore, only the diode grounding system can be simulated in the normal operating mode.

Faults are introduced to the systems after the machine is operating at steady state. Due to computer time considerations it was necessary to rerun the program using the steady-state current values as the initial conditions for the circuit inductances. The fault is then introduced 0.1 seconds after the program is started. This is done to make sure that the initial conditions yield appropriate equilibrium values.

Since there is no provision in ECAP for an open circuit, currents still flow through open contacts and often are high enough to cause the contactor coils to reclose the contacts even though the actual contacts would remain open. This problem was alleviated by altering the contactor current level test circuits. Once the contacts are opened, the test current is increased to a value that will no longer cause activation of the contacts.

There is another problem encountered because there is no open circuit in ECAP. The main overcurrent relays can only increase the resistance of the conductors and cannot completely isolate the circuit. For illustrative purposes, a resistance of only 1 kΩ was used to simulate this "open". Therefore, it must be noted that the machine frame voltage is actually at zero potential after the conductors are opened at the power center even though the graphs included in the following sections do not show this.

The following paragraphs explain the consequences of various system faults resulting from the computer simulation. Conclusions and a comparative analysis are then given in section 2.6.

2.5.2 Diode Grounding

2.5.2.1 Normal Operating Mode

Of all the grounding methods under consideration, only in diode and SCR grounding does the machine frame have direct electrical contact with the control circuit under a no-fault condition. Therefore, the transients occurring in the motor circuit are reflected on the machine frame. The voltages can be extremely high, but the current flowing to the machine frame is kept low due to the high resistance of the grounding diode in the "OFF" state.

To get an indication of the actual machine frame voltages and the voltages appearing across the diode, a connection was made from the machine frame to ground. A resistance of 10 MΩ was used. The graph in figure 2.12 shows both the machine frame voltage and the voltage across the diode as functions of time when the motor is started. It can be seen that small transients occur after the one second delays for the M1 and 1A contactors.

For graphing purposes, the initial transient has been ignored. It lasts less than 0.6 msec and during this time the M2 and M1 contacts are closed. The voltage on the machine frame (referenced to ground) in this time ranges from 46 V to 93 V. The reverse voltage on the diode is half of the machine frame voltage. This is because of a voltage division between the resistance

of the diode in its "OFF" state (10 MΩ) and the resistance from the machine frame to ground (10 MΩ). If this latter resistance is decreased, the transients appearing across the diode will be higher. Conversely, if the machine were completely isolated from ground there would be no reverse voltage across the diode.

2.5.2.2 Positive-to-Machine Frame Fault

After the machine has reached steady state operation, a short (0.1 ohms in ECAP) from the positive conductor to the machine frame is introduced. A plot of the machine frame voltage vs. time is shown in figure 2.7b).

At the instant the fault appears, the machine frame potential is elevated to 249 V. The grounding diode begins conducting, and the overcurrent relay in series with it activates. This opens the breaker that prevents current from flowing to the contactor coils (see control circuit diagram, figure 2.8). The machine frame voltage is then reduced by approximately half and all the contactors deactivate. This opens the motor contacts and, within 0.7 msec, the main overcurrent relays are tripped. This causes a large negative transient which decreases within 2 msec to a safe level. From the time that the fault occurs on the system to when the machine frame voltage is less than 40 V is approximately 3 msec.

2.5.2.3 Negative-to-Machine Frame Fault

There is essentially no change in machine frame voltage due to the occurrance of a short from the negative (grounded) conductor to the machine frame under otherwise normal conditions. However, this could present problems since there is no way to detect such a fault. Any voltage drop in the negative conductor appears on the machine frame. This could be dangerous if the resistance of the cable is higher than it should be due to a poorly-made splice. There would be a current division, however, between this resistance and the resistance of any grounded object that comes into contact with the machine frame.

2.5.2.4 Shorted Diode

As mentioned earlier (section 2.2.1), a shorted diode causes the machine to "fail operative". There is no change in machine frame voltage when all other conditions are normal because no current flows through the grounding diode regardless of its integrity. However, voltage drops in the negative conductor would appear on the machine frame. This condition is identical to having a negative-to-machine frame fault.

If a positive-to-machine frame fault occurs, there remains a low-resistance path to ground through the shorted diode. The machine frame voltage jumps to one-half the supply voltage and from this point on the consequences to this fault are the same as those given earlier for a positive-to-machine frame fault with an unfailed diode.

A negative-to-machine frame fault occurring when the diode is in a shorted condition presents the same problems it does when the diode is not failed.

2.5.2.5 Opened Diode

Under normal operating conditions, an opened diode (as with a shorted diode) does not present any problems since the negative conductor is essentially unconnected from the machine frame unless there is a fault.

If the positive conductor is shorted to the machine frame with the diode in an open condition, the full supply voltage will appear on the machine. Since the diode will not conduct, its overcurrent relay will not activate and the machine will remain operating. This dangerous situation is, therefore, undetectable unless a grounded object comes into contact with the machine frame.

A negative-to-machine frame fault with an opened diode poses the same problems described earlier, regardless of the integrity of the diode.

2.5.2.6 Open in Either Power Conductor

Machine operation is, of course, prevented in the event of an open in either power conductors. However, if the negative conductor is not completely open but merely has a very high resistance, and the positive conductor is intact, the voltage on the machine frame will approach the supply voltage. This occurs because the control diode still turns on and there is a voltage divider between its resistance (plus the M2 coil resistance) and the high resistance of the negative conductor. The current is kept low, however, because the diode remains in its high-resistance state. Therefore, this can only cause a shock hazard if the diode fails short.

2.5.2.7 Positive-to-Negative Conductor Fault

The consequences of a positive-to-negative conductor fault are almost identical to the case of a positive-to-machine fault with a shorted diode. The only difference is that if the resistance of the diode in the "ON" state is not the same when it is shorted.

2.5.3 Basic Ground-Wire System

2.5.3.1 Positive-to-Machine Frame Fault

At the instant a short occurs from the positive conductor to the machine frame, the voltage appearing on the machine jumps to approximately two-thirds of the supply voltage (166 V) because of a voltage division between the positive conductor (0.07 ohm) and the ground wire (0.14 ohm). Within 0.8 msec the main overcurrent protection is activated and a large transient of -3860 V appears on the machine frame. The voltage remains near this level for approximately 0.3 msec until all the contacts are opened. The voltage increases to around 25 V and then begins to decrease exponentially to near zero (see graph, figure 2.13). The magnitude of the machine frame voltage is greater than 40 V for less than 2 msec and the current in the ground wire reaches a peak of 13 A before the main overcurrent relays activate.

2.5.3.2 Negative-to-Machine Frame Fault

The machine will remain operating in the event of a negative-to-machine

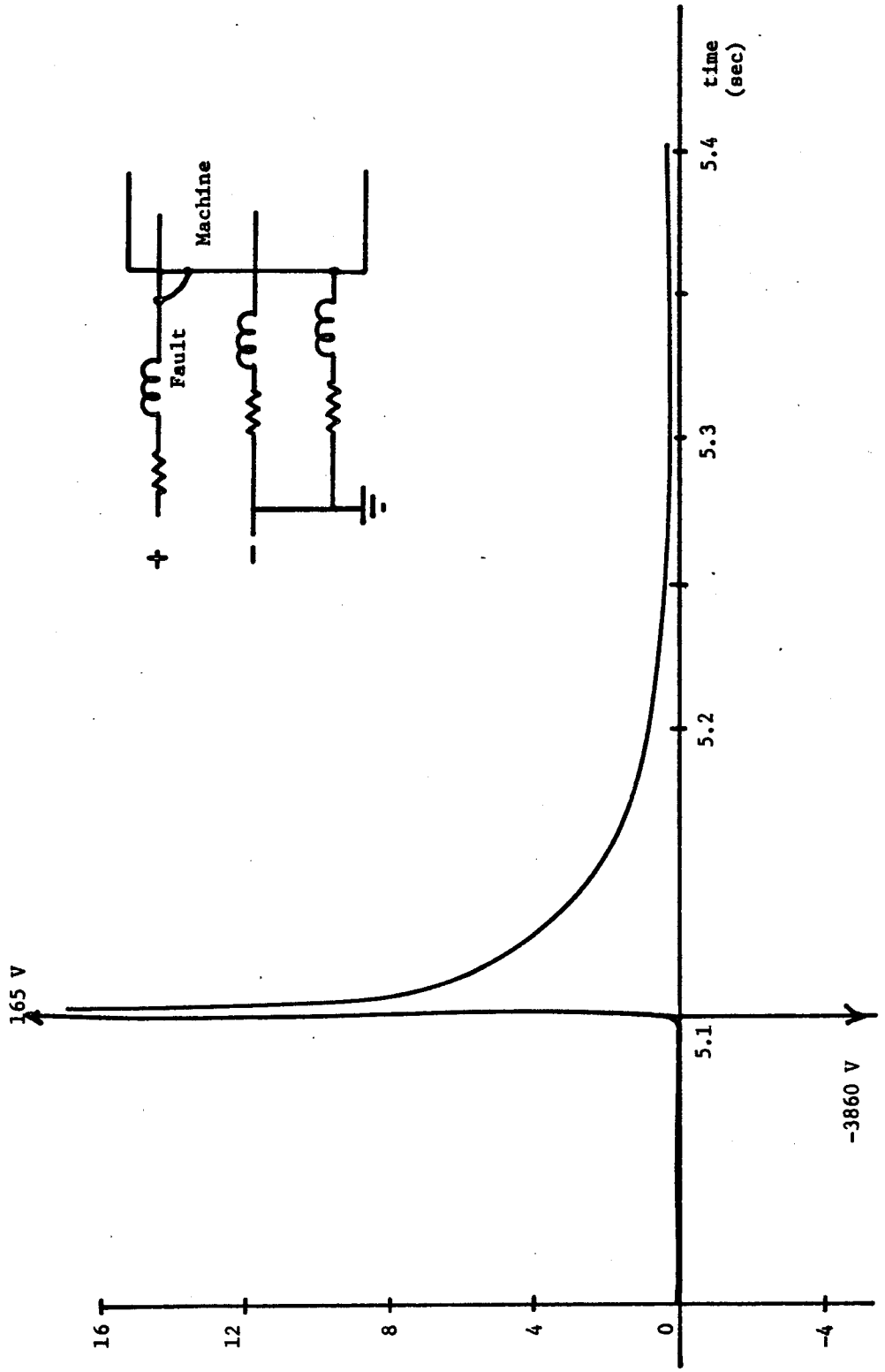

Figure 2.13. - Positive-to-machine frame fault for the basic ground wire system.

frame fault, and the voltage appearing on the machine frame stays at an acceptable value. The current in the ground wire increases, however, because of a current division between the negative conductor and the ground wire. A high resistance in either of these wires (due to poor splicing) does not cause high voltage on the machine frame because the parallel resistance of the two remain low.

2.5.3.3 Open Ground Wire

An open ground wire will go undetected unless there is a fault. This is similar to the case of an open grounding diode (section 2.5.2.5). With a positive-to-machine frame fault, the full supply voltage appears on the machine frame but no other significant changes in voltages or currents occur - the machine remains operating. A negative-to-machine frame fault with an open ground wire will have no effect on machine operation or on the machine frame voltage except that any voltage drop in the negative conductor would be reflected on the machine.

2.5.3.4 Positive-to-Negative Conductor Fault

This type of fault causes the current to be shunted away from the control circuit. This increase in current causes activation of the main overcurrent relays and the machine becomes inoperative. The ground wire is not involved and thus there is no voltage on the machine frame.

2.5.4 Resistance-Derived Neutral System

2.5.4.1 Positive-to-Machine Frame Fault

When a positive-to-machine frame fault occurs on a shuttle car grounded in this manner, the voltage on the machine frame jumps to approximately one-half of the positive-to-neutral voltage (62 V). This is caused by a voltage divider between the ground wire (0.14 ohm) and both the conductors (each 0.07 ohm). The voltage imbalance caused by this fault causes activation of one of the voltage relays which opens the conductors at the power center. Since this occurs before the conductor currents become very high, there is no large negative transient as in other systems. The graph in figure 2.14 shows how the machine frame voltage changes due to a ground fault from the positive conductor. The transient is dangerous for such a short time that it is immeasurable using ECAP and the current in the ground wire peaks at only 0.1 A.

2.5.4.2 Negative-to-Machine Frame Fault

In the event of a negative-to-machine frame fault, the same transient discussed above occurs. The only difference is that the fault is detected by the other voltage relay and the voltage appearing on the machine frame is opposite in sign.

2.5.4.3 Open Ground Wire

As with all ground wire systems, an open in the ground wire does not prevent machine operation and is not detected unless some form of ground-wire monitoring is used. If the ground wire is open when a positive-to-machine

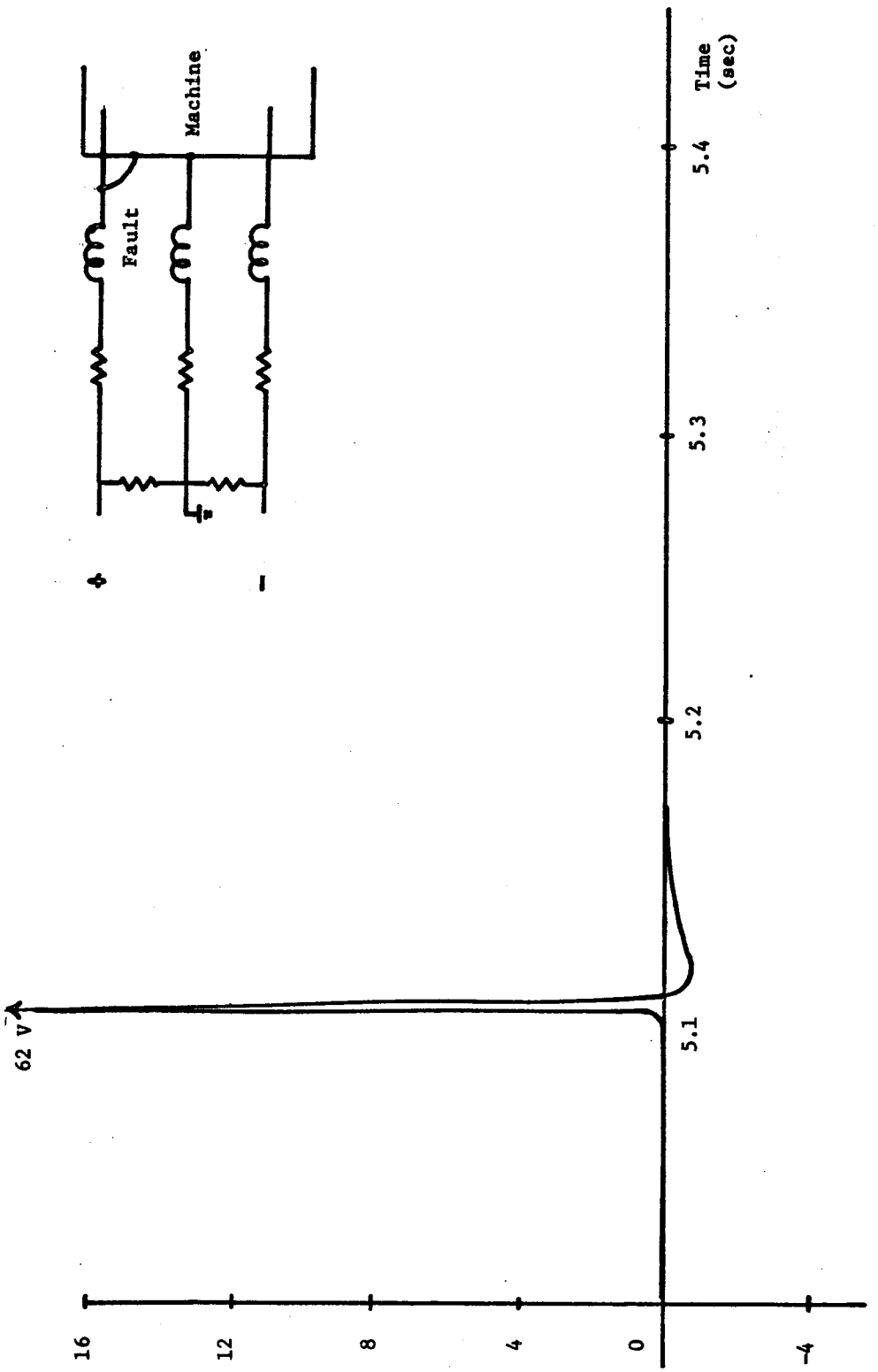

Figure 2.14. - Positive-to-machine frame fault for a resistance-derived neutral system.

frame fault occurs, the machine frame is elevated in potential to 125 V. Similarly, a negative-to-machine frame fault produces -125 V on the machine frame.

2.5.4.4 Positive-to-Negative Conductor Fault

A positive-to-negative conductor fault shunts current away from the control circuit and the increase in conductor current activates the overcurrent protection at the power center. When considering this type of fault, both the ground wire and the voltage relays are inconsequential--the only protection comes from the main overcurrent relays. The machine frame remains isolated from any dangerous voltages.

2.5.5 Transformer-Derived Neutral System

As previously mentioned, this simulation does not include the saturable reactor and its controlling circuit discussed in section 2.2.5. These program results show "worst case" transients, as if the circuitry for monitoring the neutral is inoperative.

2.5.5.1 Positive-to-Machine Frame Fault

A positive-to-machine frame fault causes the voltage on the machine frame to immediately increase to 82 V, which is approximately two-thirds of the positive-to-neutral voltage. Within 2.7 msec the conductor current increases to the tripping level of the overcurrent relays. A negative spike of -2262 V occurs as the overcurrent relays activate. The current to the control circuit decreases and all the contacts open. The machine frame voltage is at a dangerous level for less than 3 msec and the ground wire current reaches a maximum of 9 A. A graph of the machine frame voltage as a function of time when the fault occurs is given in figure 2.15. The dangerous transient would encompass a much shorter time interval and the conductor current would not reach so high a value if the shift in the neutral had been sensed by detecting circuitry.

2.5.5.2 Negative-to-Machine Frame Fault

As with the resistance-derived neutral system, a negative-to-machine frame fault yields the same results as a positive-to-machine frame fault. The only difference is in the sign of the machine frame voltage and the direction if the ground-wire current.

2.5.5.3 Open Ground Wire

An open ground wire is undetectable and does not present a dangerous situation unless there is a positive- or negative-to-machine frame fault. In this case the voltage on the machine frame reaches ± 124 V which is not detected by the circuitry.

2.5.5.4 Positive-to-Negative Conductor Fault

This type of fault yields the same results as it does in the other ground-wire systems. The overcurrent relays at the rectifier are activated

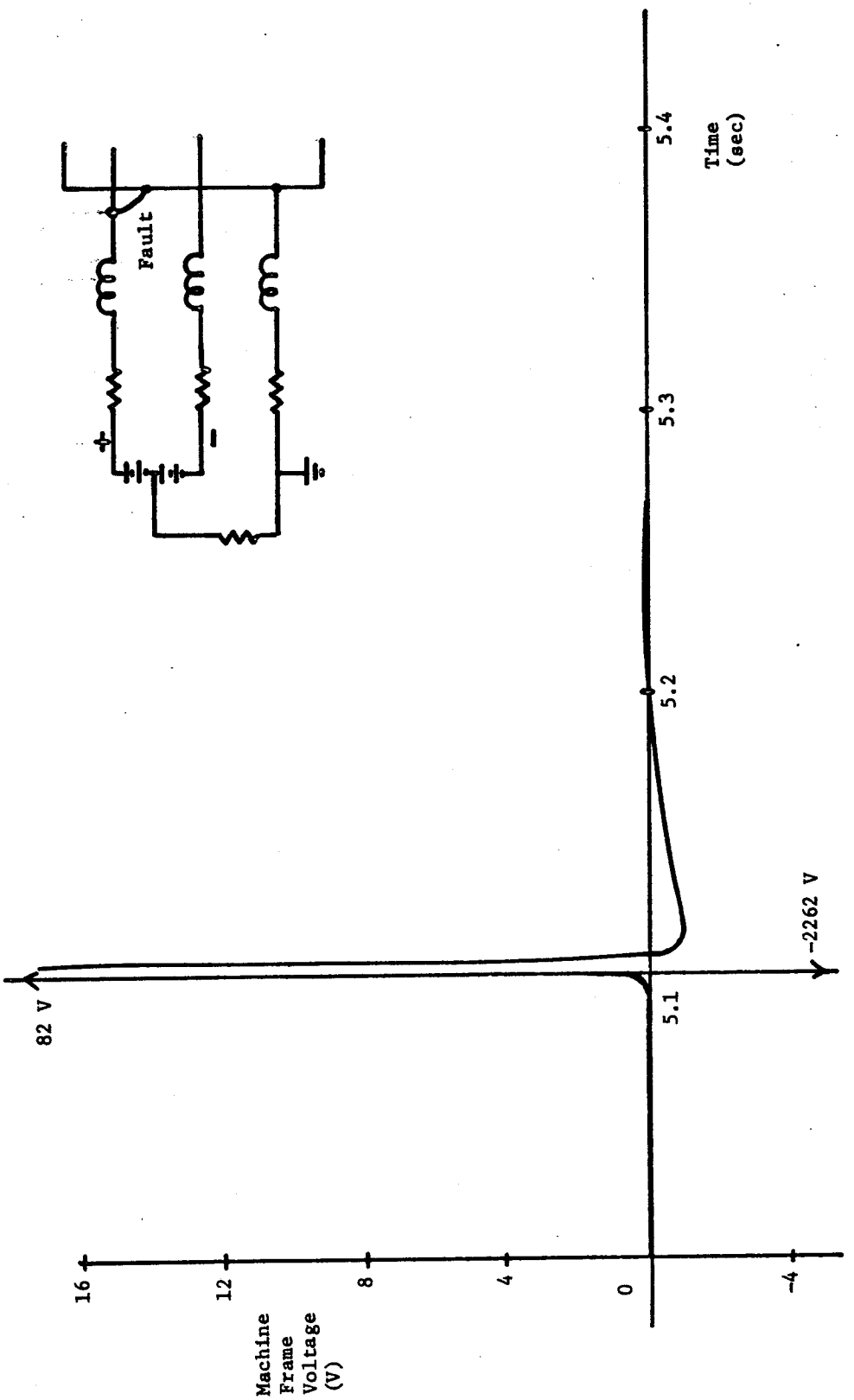

Figure 2.15. - Positive-to-machine frame fault for a transformer-derived neutral system.

TABLE 2.1. - Fault consequences for four DC grounding systems

FAULT	DC GROUNDING SYSTEM: DIODE GROUNDING	BASIC GROUND-WIRE SYSTEM	RESISTANCE-DERIVED NEUTRAL SYSTEM	TRANSFORMER-DERIVED NEUTRAL SYSTEM
Positive-to-Machine Frame Fault	Machine protected and becomes inoperative; dangerous transient lasts < 3 msec.	Machine protected and becomes inoperative; dangerous transient lasts < 2 msec.	Machine protected and becomes inoperative; dangerous transient lasts < 50 msec.	Machine protected and becomes inoperative; dangerous transient lasts < 3 msec without neutral sensing device.
Negative-to-Machine Frame Fault	Machine remains operating and no change in machine frame voltage. However, any voltage drops in negative conductor will appear on machine frame.	Machine remains operating and no change in machine frame voltage. Voltage drop in negative conductor or in ground wire is kept low.	Same as a positive-to-machine frame fault (opposite in sign only).	Same as a positive-to machine frame fault (opposite in sign only).
Positive-to-Negative Conductor Fault	Machine protected and becomes inoperative; machine frame voltages are not significantly different from when there is a positive-to-machine frame fault.	Machine protected and becomes inoperative; no ground-wire current or voltage on the machine frame.	Machine protected and becomes inoperative; no ground-wire current or voltage on the machine frame.	Machine protected and becomes inoperative; no ground wire current or voltage on the machine frame.
Open in Either Power Conductor	Machine becomes inoperative; if negative conductor is not completely open but has very high resistance machine frame voltage approaches 250 V though currents are blocked by diode.	Machine becomes inoperative; no ground-wire current or voltage on the machine frame.	Machine becomes inoperative; no ground-wire current or voltage on the machine frame.	Machine becomes inoperative; no ground-wire current or voltage on the machine frame.

TABLE 2.1. - Fault consequences for four DC grounding systems (cont'd)

FAULT	DC GROUNDING SYSTEM			
	DIODE GROUNDING	BASIC GROUND-WIRE SYSTEM	RESISTANCE-DERIVED NEUTRAL SYSTEM	TRANSFORMER-DERIVED NEUTRAL SYSTEM
Open in Ground Wire (Diode)* -normal operation	No problem though undetected.	No problem though undetected.	No problem though undetected.	No problem though undetected.
-with a positive-to-machine frame fault	Machine remains operating; 250 V on machine frame.	Machine remains operating; 250 V on machine frame.	Machine remains operating; 125 V on machine frame.	Machine remains operating; 125 V on machine frame.
Shorted Grounding Diode	Undetected in normal operation. Voltage drops in negative conductor are reflected on machine frame. Positive-to-machine fault identical to positive to negative conductor fault.			

* The consequences of an open diode (diode grounding system) are similar in nature to having an open ground wire since both are ground-fault paths.

as the conductor current increases. This causes all the contacts to open and the machine becomes inoperative. The machine frame and the ground wire are isolated from this type of fault.

2.6 CONCLUSIONS

2.6.1 Reliability of the ECAP Simulation

In analyzing the program results, it is important to note that the magnitudes of the transients were given only for illustrative purposes. Since there is no actual open circuit condition in the programs, the high voltages shown are due, in part, to the fact that current does flow through an "open" (see section 2.3.2 on the limitations of ECAP).

Although the voltage magnitudes given by the simulation cannot be taken literally, some comparative conclusions can be drawn. Positive-to-machine frame fault programs were run with everything constant except for varying the resistance of the "open" caused by activation of the main overcurrent relays. The resistance values ranged from 10 ohms to 1 MΩ. In every case, the negative transient found in diode grounding was much higher than that of the basic ground wire system. The length of time that dangerous voltages appear on the machine frame cannot be considered entirely correct either, for this is dependent on the time step selection. However, the time span of the transients given by the programs is greater than the actual value would be, simply due to the method of analysis which ECAP uses (refer to section 2.3.2).

It must be stressed that the fault programs were made solely in an effort to compare the grounding methods. The same control circuit and element values were used even though the actual circuits may vary considerably.

2.6.2 Comparative Analysis of the Grounding Systems

This analysis has shown that each grounding system considered has certain advantages but none consolidate solutions to all the problems. Table 2.1 shows the consequences of certain faults for each of the four grounding methods simulated. Table 2.2 summarizes the advantages and disadvantages of these four methods.

There are several elements or devices which might be added to the grounding systems outlined in section 2.2 to solve certain problems. Some of these are discussed below.

1. The addition of a diode at the rectifier can help in solving the problem of intermachine arcing in a two-wire system. The cathode is connected to the negative conductor and the anode to the safety ground. The negative conductor remains at zero potential and yet there is no path for intermachine arcing current to flow.

2. A diode testing device could be installed on a machine using the diode grounding system (this is discussed in Chapter 5). If the device is failsafe then there would be no dangerous voltages on the machine frame caused by ground faults.

TABLE 2.2. - Comparative analysis of four DC grounding systems

Diode Grounding System	
Advantages:	Two-wire system (see section 2.2.1) Protects the cable if fault is in by the main contactors
Disadvantages:	Integrity of the diode must be periodically checked because failed diode (open or short) may cause a shock hazard Voltage drops in negative conductor appear on the machine frame - dangerous if diode is shorted or if there is a negative-to-machine frame fault
Basic Ground-Wire System	
Advantages:	No extra devices are necessary - most simplistic system
Disadvantages:	Cable is not protected against a fault Sensitivity of system is determined by main overcurrent relays Open in ground wire presents potentially dangerous situation
Resistance-Derived Neutral System	
Advantages:	Protects the cable from a positive- or negative-to-machine frame fault Voltage relays can be set to desired sensitivity Fault currents are limited by the resistors
Disadvantages:	Requires resistors and voltage relays at the power center Open in ground wire presents potentially dangerous situation
Transformer-Derived Neutral System	
Advantages:	Selective tripping is possible Cable is protected against a positive- or negative-to-machine fault Relay in neutral sensing device can be set to desired sensitivity
Disadvantages:	Requires extra device for each machine on the system Open in ground wire presents potentially dangerous situation.

3. An added overcurrent relay in the ground wire could provide more sensitivity to ground faults [14]. The disadvantages with this are that an extra device is required and the probability of having an open ground wire is increased because of the probability of a failed relay.

4. As mentioned earlier, monitoring the ground wire would prevent machine operation in the event of an open ground wire. If unmonitored, an open can go undetected and dangerous voltage occurs on the machine frame when there is a ground fault.

This research cannot determine which grounding method is the "best"; it can only show the advantages and disadvantages of each. It is hoped that the information assembled here will aid in enlightening those involved with the grounding of dc equipment as to what systems are available and which one can best solve specific problems.

CHAPTER III

XIT-ROD^R EVALUATION

3.1 INTRODUCTION

The Xit-Rod^R is advertised as a "self-monitoring grounding electrode which functions anywhere, and is not subject to freezing or other variables" [17]. In order to substantiate or refute this statement, eleven Xit-Rods were installed in the Eastern Coal Fields in varying soil conditions (i.e. type, moisture content, slope, and resistivity). Resistance and resistivity measurements were made on these rods at different times over a period of nearly two years. The purpose was to monitor their resistance pattern over time and with seasonal changes. A comparison of this pattern with the theoretical model developed from the soil resistivity for a rod with the same dimensions, minus the salting effect was made. At the end of the test period, six rods were recovered to determine the amount of rod deterioration due to corrosion and galvanic influence. They were opened to discover the amount and condition of the salt remaining in the rod.

3.2 FIELD DATA

The classical "Fall-of-Potential" method was used to determine the earth resistance of the Xit-Rods. The 4-probe Wenner array, with electrode spacing being equal to rod length, was used to determine the soil resistivity. Table 3.1 gives a complete field data listing of all eleven rods for the period beginning Oct. 78 and ending June 80. It additionally gives a brief description of rod type, environmental conditions, and physical locations. Figures 3.1 through 3.11 are plots of rod resistance as a function of time. The theoretical resistance of a rod with like dimensions is shown for comparison. This resistance is determined from the soil resistivity by means of Equation 3.1.

$$R_{theoretical} = R_{th} = (\rho/2\pi L)\ \ln\ (4L/d), \qquad (3.1)$$

where ρ = observed soil resistivity (Ω-ft),

L = rod length (ft),

and d = rod diameter (ft).

Comparison of the measured resistance (R_∞) to the theoretical resistance (R_{th}) is a good indicator of the effectiveness of the self-salting process of the Xit-Rod. Figure 3.12 is reproduced from manufacturer's literature to serve as a comparative guide.

Figures 3.1 through 3.11 also provide a supplementary graph of the ratio (R_∞/R_{th}) to facilitate the understanding of rod operation. Theoretically, this graph should be a straight horizontal line of value one. A value less than one means that the salting phenomenon is lowering ground resistance.

TABLE 3.1. - Results of Xit-Rod measurements

Rod	Description & Location	Measurement Date	Measured Resistance (Ω)	Measured Soil Resistivity (Ω-ft)
1	8' Copper Philippi, WV Base of a Hill.	Oct. 78	22	
		Dec. 78	18.8	362
		Jan. 79	23.4	429
		May 79	18	226
		June 79	18.27	298
		July 79	16.73	255
		Aug. 79	16.13	229
		Apr. 80	18.58	456.5
		June 80	18.18	415.6
2	8' Copper Powhatan Pt, OH Swampy Fill	Oct. 78	5.5	74
		Apr. 79	5.2	78
		July 79	4.41	51.8
		Aug. 79	3.575	45.5
		June 80	4.349	66.2
3	8' Copper Keystone, WV Near Roadbed	Nov. 78	48	700
		Dec. 78	48.3	915
		Mar. 79	56.6	765
		June 79	53.6	736
		July 79	45.1	663.5
		Aug. 79	49.8	605.7
		Apr. 80	74.2	949
		June 80	70.36	1136
4	8' Copper Eccles, WV Hillside Road Grade	Dec. 78	172.7	3090
		May 79	120.9	2232
		July 79	111.8	2091
		Aug. 79	113.9	1779.4
		Mar. 80	164.6	2117
		June 80	163.55	2136
5	8' Copper Keystone, WV	Nov. 78	50.2	2268
		Dec. 78	70.9	2227
		Mar. 79	83	1632
		June 79	77.1	1246
		July 79	69.2	1126
		Aug. 79	68.1	1644
		Apr. 80	125.6	
		June 80	110	1900
6	8' Copper Bishop, VA Edge of Steep Slope	Mar. 79	215	1160
		June 79	122	1120
		July 79	130.4	904.8
		Aug. 79	146.7	1131
		Apr. 80	140.5	1319
		June 80	252	1204

TABLE 3.1 - (continued) - Result of Xit-Rod measurements

Rod	Description & Location	Measurement Date	Measured Resistance (Ω)	Measured Soil Resistivity (Ω-ft)
7	10' Galvanized	Oct. 78	4.8	74
		Apr. 79	4.1	78
	Powhatan Pt, OH	July 79	3.81	51.8
		Aug. 79	3.267	45.5
	Swampy Fill	June 80	3.93	66.2
8	10' Galvanized	Jan. 79	13.4	106
		Apr. 79	8.4	
		May 79	7.7	
	Waynesburg, PA	June 79		138.23
		July 79	5.71	
	In Fill Near Gulley	Aug. 79	5.67	87.34
		June 80	7.31	90.4
9		Mar. 79	245	1160
	10' Galvanized	June 79	101	911
	Bishop, Va	July 79	86.6	824
		Aug. 79	89.4	961
	Edge of Steep Slope	Apr. 80	108.7	1087
		June 80	136	1204
10	10' Galvanized	Dec. 78	154.4	3090
		May 79	217.9	2232
	Eccles, WV	July 79	113.1	2091
		Aug. 79	100.1	1779
	Hillside	Mar. 80	165.9	2117
	Road Grade	June 80	147.93	2136
11	8' Stainless Steel	Oct. 78	4.6	74
		Apr. 79	6.4	78
	Powhatan Pt, OH	July 79	4.48	51.8
		Aug. 79	3.807	45.5
	Swampy Fill	June 80	4.44	66.2

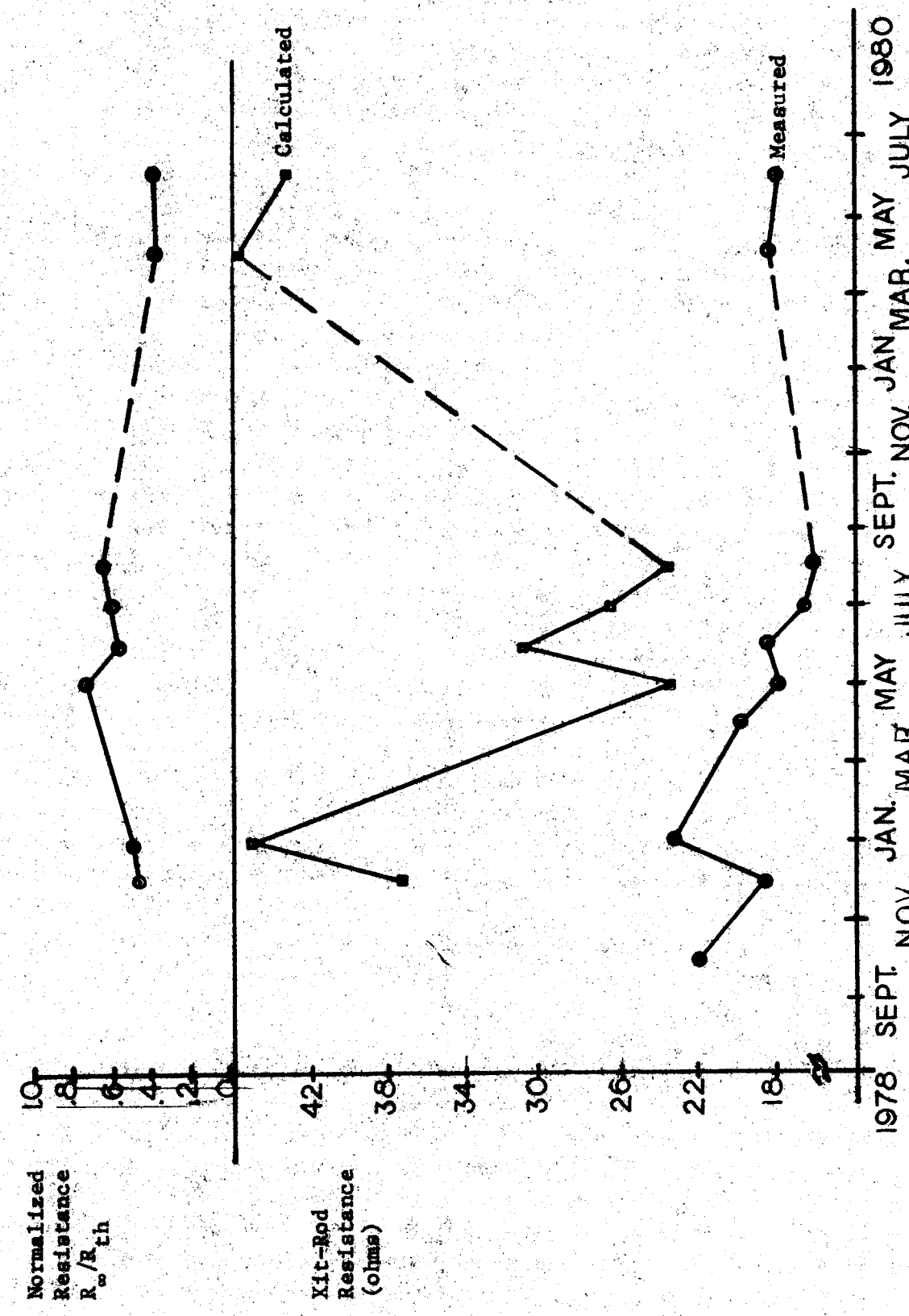

FIGURE 3.1. - Resistance of Xit-Rod number 1 as a function of time. Rod installed Oct. 78. Philippi, WV.

The positive and negative slopes correspond to decreasing and increasing rod effectiveness, respectively, relative to the previous measurement date. If the rods functioned as claimed, the normalized resistance curves would be mirror images of the theoretical resistance plot, after the rods had stablized at their low ohmic value. That is to say, if the measured resistance was a constant value, the curve produced by dividing R_{th} into R_{∞} (constant) would vary inversely to R_{th}, thus producing a mirror image.

Rod #1 was one of the most effective rods installed. It averaged close to 40 percent reduction of ground resistance over the theoretical resistance. However, its resistance pattern followed the same shape as the resistivity profile, as shown by Figure 3.1. Upon recovery, the bulk of the chemical salt was found to have leached out. (Note: All rods laid in a storeroom for nearly two weeks after initial recovery before they were opened.) A considerable amount of moisture was present inside the rod and the water-salt mixture retrieved was a pale lime green color. Also, the salt at the bottom of the rod was dryer and harder than at the top where the bulk of the water was concentrated.

Figures 3.2, 3.3, and 3.4 describe the behaviors of Xit-Rods #2, #7, and #11, respectively. All of these rods were located within 20 feet of each other and were connected together. As witnessed by the graphs, all three rods' resistances followed nearly the exact same shape as the resistivity profile. Also, a 30 percent resistance reduction was realized by each rod. It is important to note that they were installed in swampy ground. Considering the saturated conditions, most of the salt was expected to be gone from each rod. However, this was not the case. No salt could be retrieved through the top of rod #2 because of a coagulum of salt approximately one-fourth of the distance down the rod. Nevertheless, most of the salt, which was white, was removed from the bottom. In rod #7 (10' galvanized), the salt was solidified into such a hard mass the whole length of the rod that almost no salt was removed at all, and the small amount that was recovered was white and totally dry. The majority of salt in rod #11 (8' Stainless Steel) was removed from the bottom. It was blackish - turning to more of an orange color for the salt in the middle of the rod. This rod also had a glob of solidified salt that could not be removed. Both rods #2 and #11 had over 50 percent of original salt left in them and rod #7 had nearly 70-75 percent remaining in it.

Figure 3.5 describes the resistance behavior of rod #3. It is different from the ones previously discussed in that it does not follow the resistivity profile exactly. Four data points occur where an increase or decrease in resistivity creates expectations of a corresponding increase or decrease in measured resistance, when, in fact, the reverse is true. However, the salting has influenced the ground resistance by lowering it approximately 30 percent. No moisture was evident upon opening, and the fiberglass filler in the bottom of the rod was completely dry, which did not occur in any other rod. The salt in the top of the rod was blue in comparison to the white salt found in the bottom. This rod was also plugged by coagulated salt.

Rod #5 was installed in very high resistivity soil and the resistance values are correspondingly high. The normalized resistance plot of Figure 3.6 shows that rod effectiveness decreases for the first eight months after

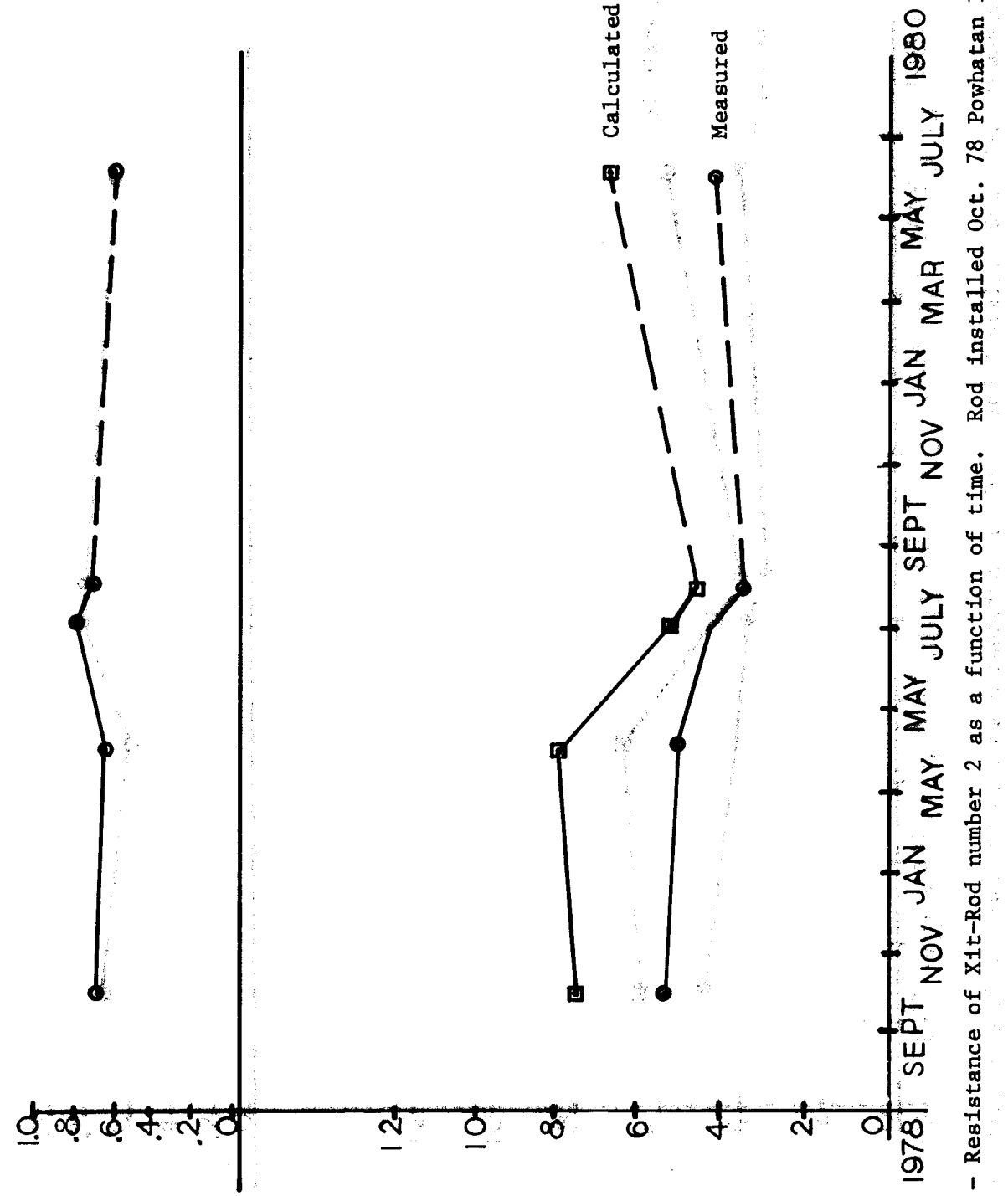

FIGURE 3.2. - Resistance of Xit-Rod number 2 as a function of time. Rod installed Oct. 78 Powhatan Pt. OH.

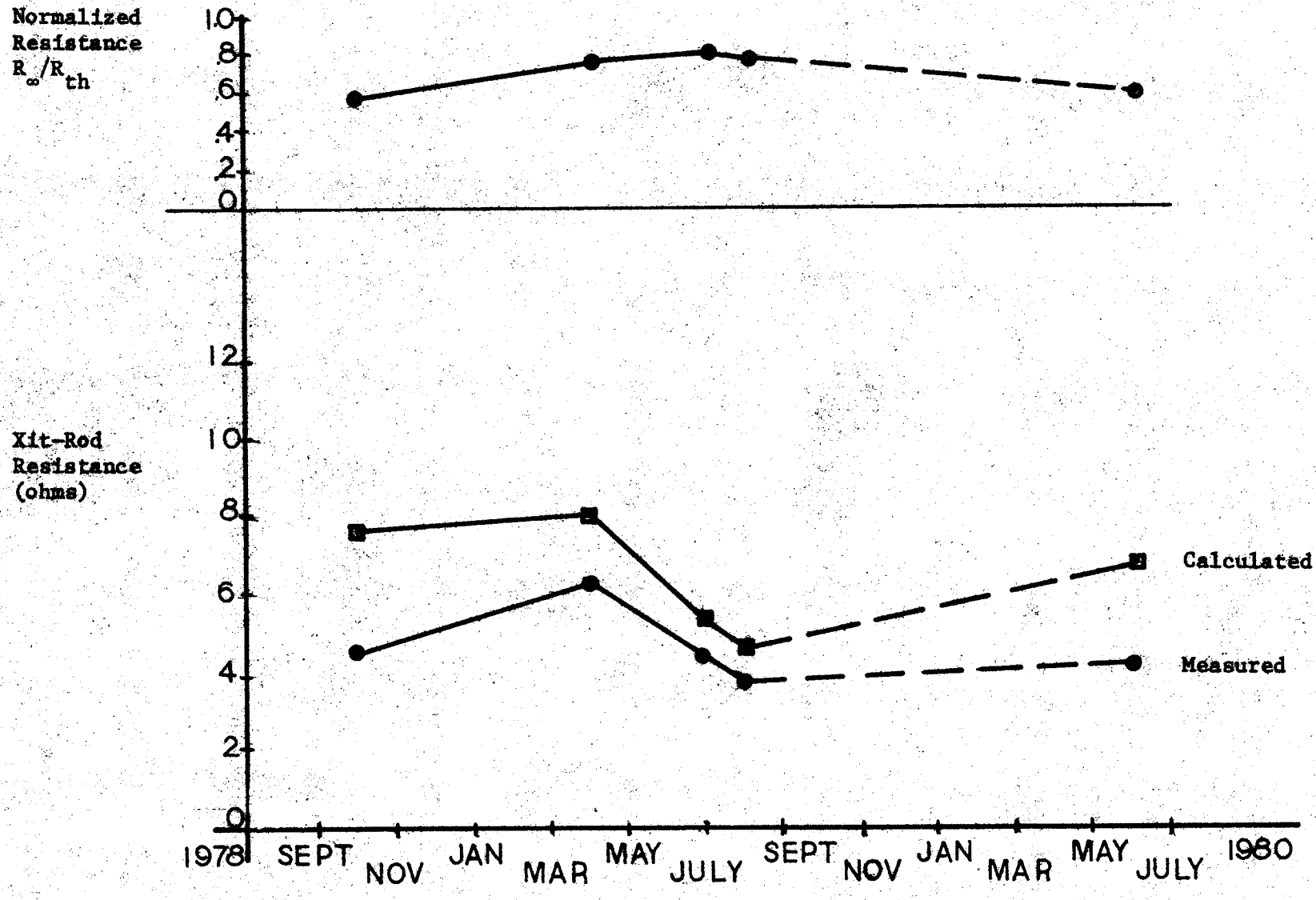

FIGURE 3.4. - Resistance of Xit-Rod number 11 as a function of time. Rod installed Oct. 78. Powhatan Pt. OH.

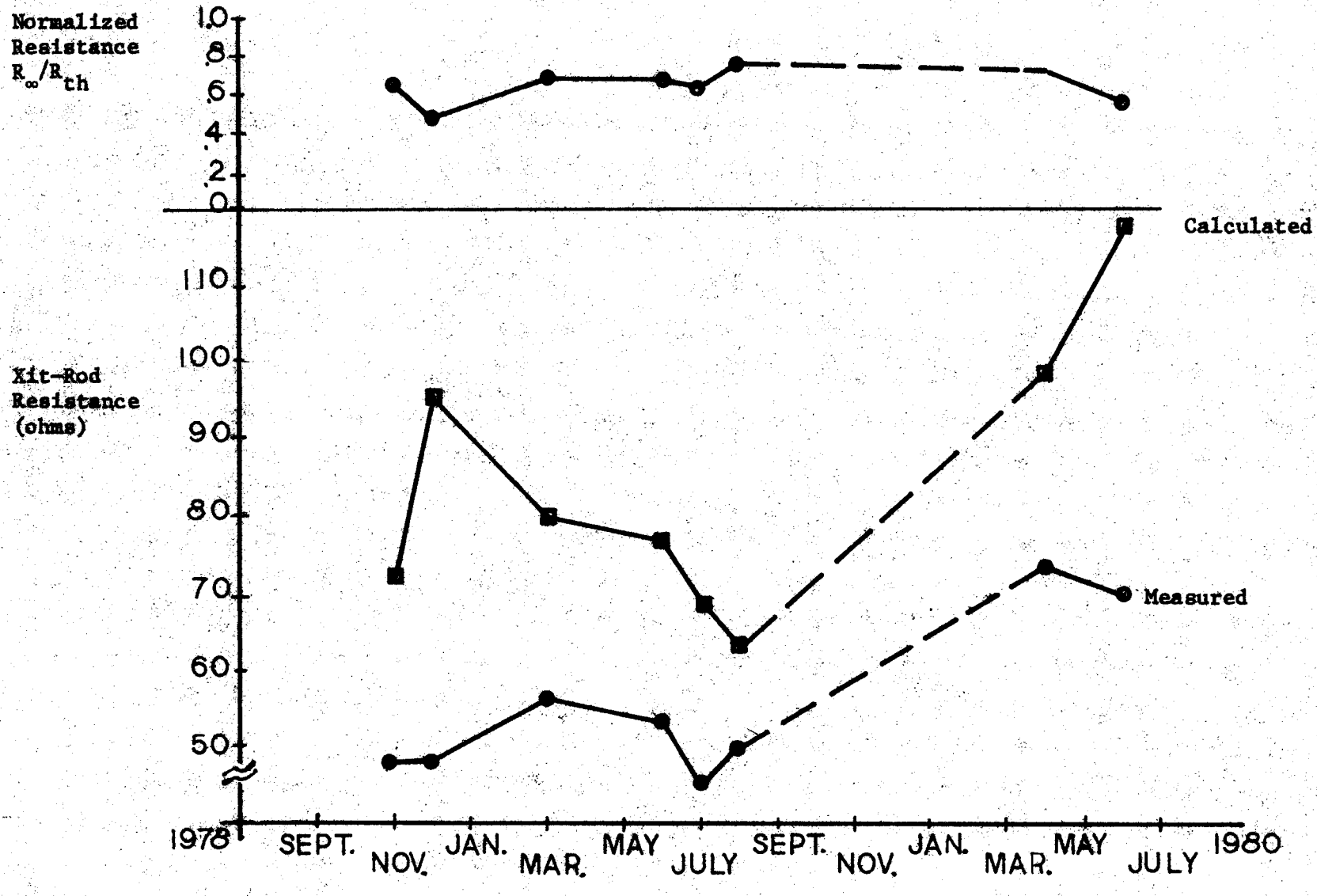

FIGURE 3.5. - Resistance of Xit-Rod number 3 as a function of time. Rod installed Dec. 78. Keystone, WV.

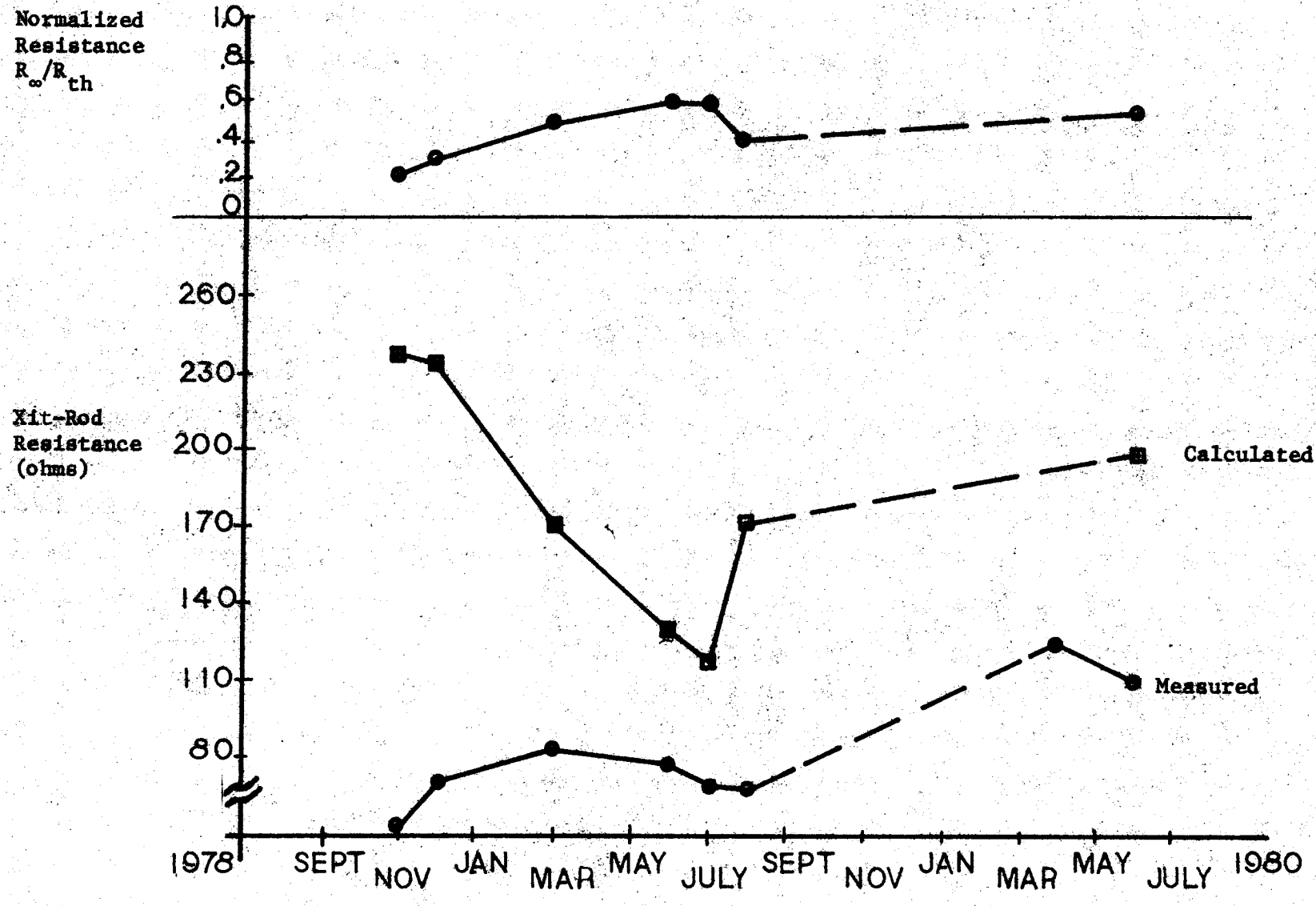

FIGURE 3.6. - Resistance of Xit-Rod number 5 as a function of time. Rod installed Dec. 78. Keystone, WV.

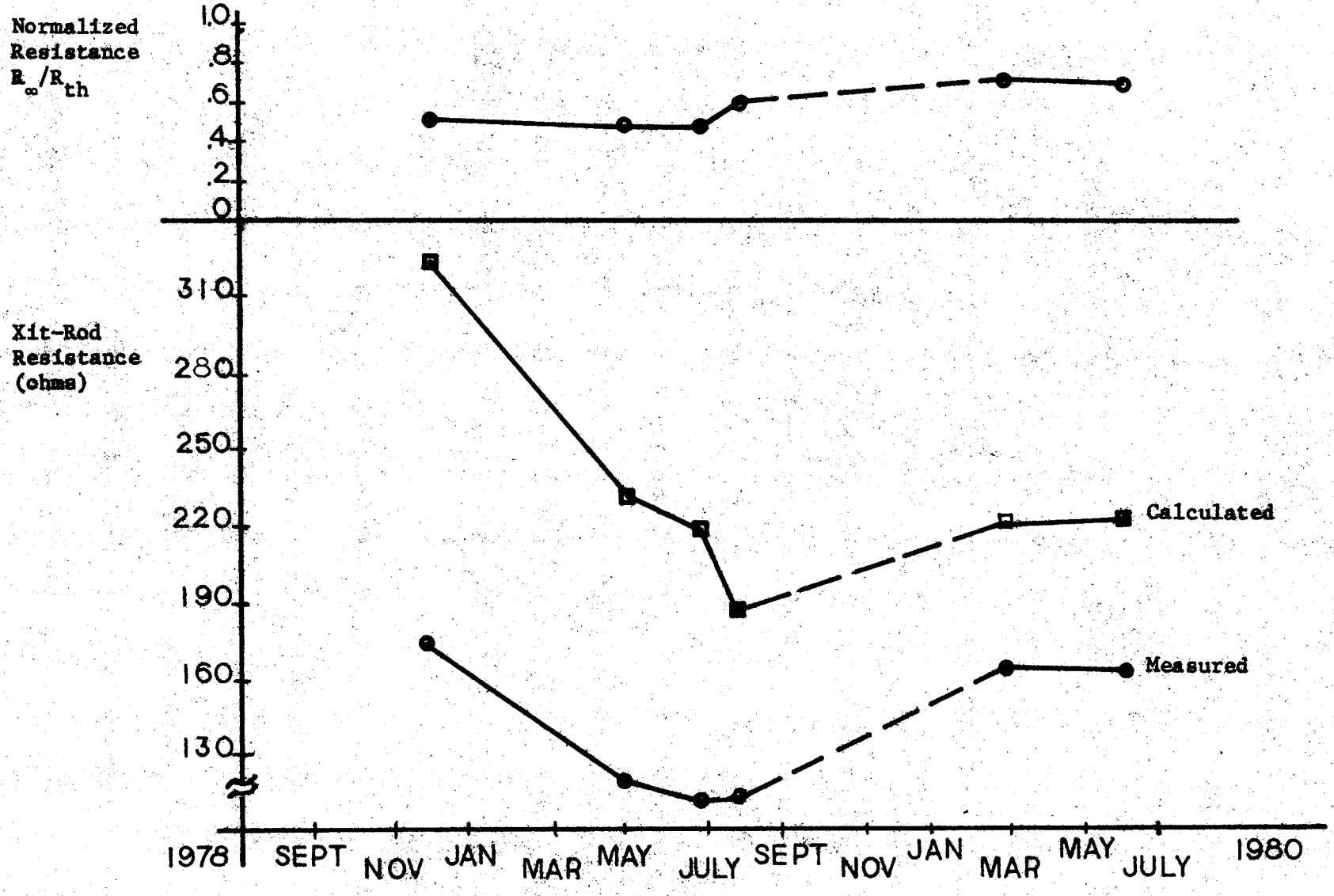

FIGURE 3.7. - Resistance of Xit-Rod number 4 as a function of time. Rod installed Dec. 78. Eccles, WV.

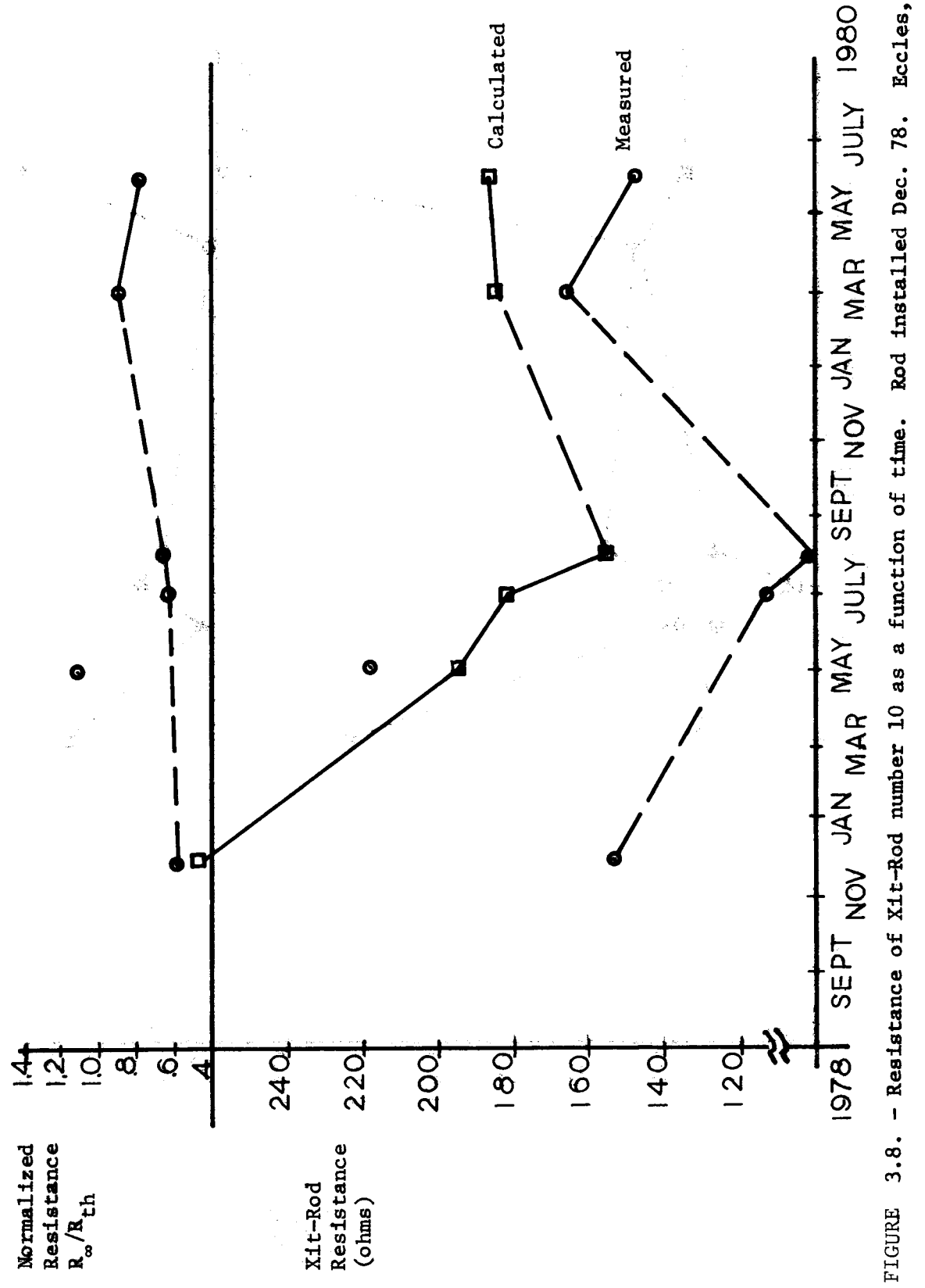

FIGURE 3.8. - Resistance of Xit-Rod number 10 as a function of time. Rod installed Dec. 78. Eccles, WV.

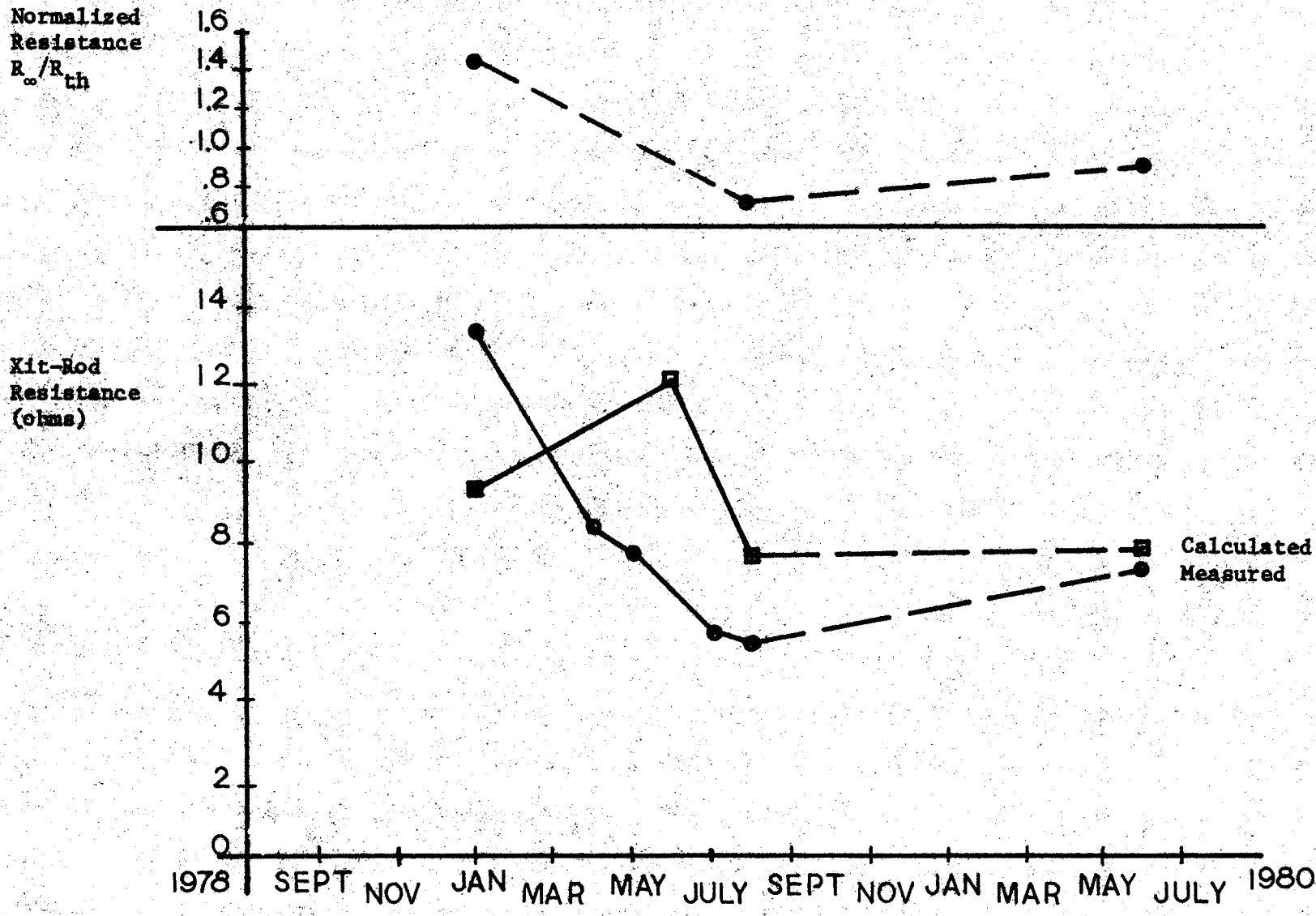

FIGURE 3.11. - Resistance of Xit-Rod number 8 as a function of time. Rod installed Jan. 79. Waynesburg, PA.

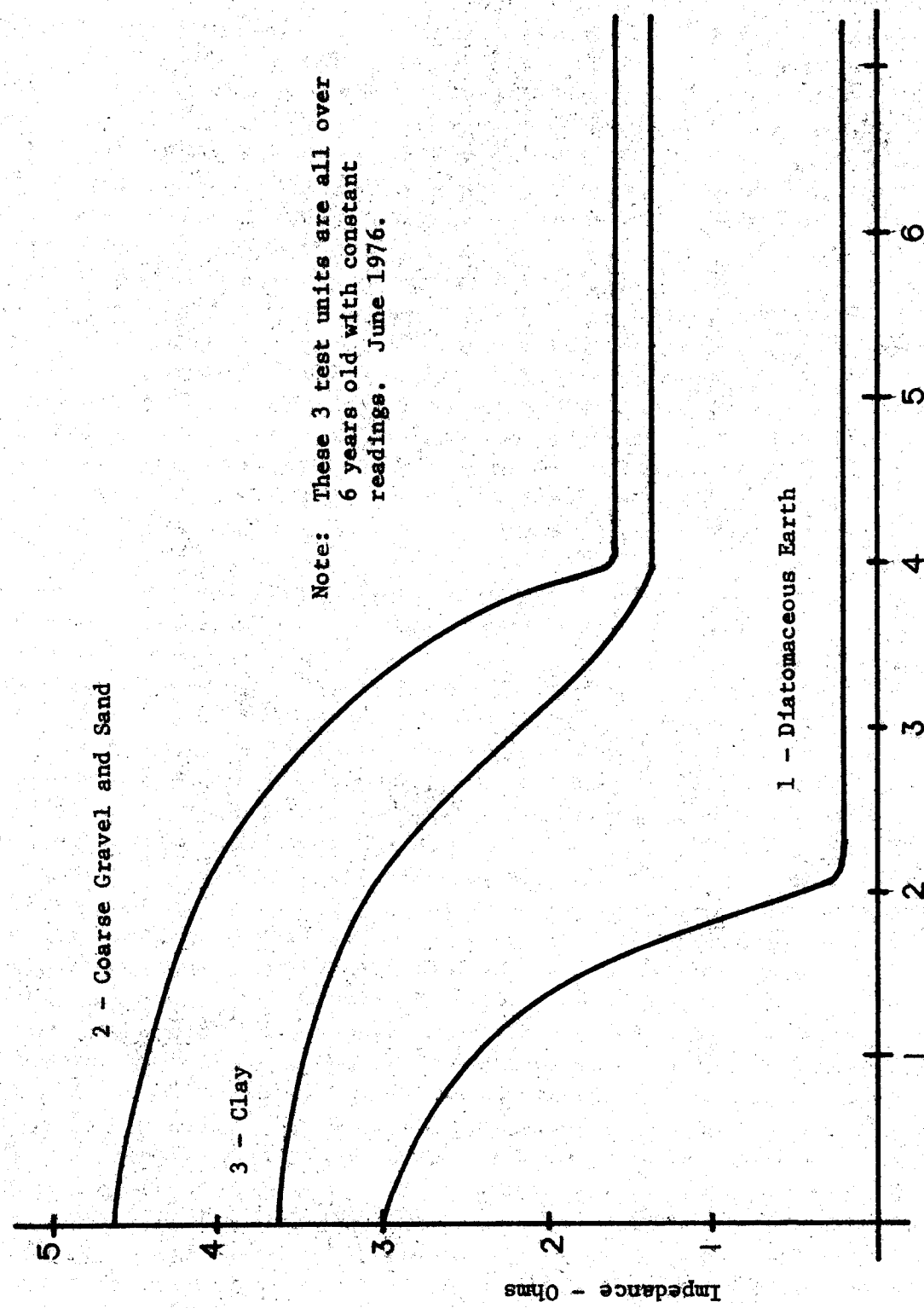

FIGURE 3.12. - Manufacturer's data on X-it Rod resistance.

installation. Upon removal, both top and bottom fiberglass fillers were wet, and approximately 30 percent of the salt originally present was massed solidly enough to prevent removal.

Figures 3.7 and 3.8 are plots of rods #4 and #10, respectively. Both rods were located in low conductivity soil approximately 25 feet apart and were connected together. Again, the rods' behavior patterns follow the resistivity very closely. Rod #4 has averaged approximately 40 percent reduction from the theoretical resistance as witnessed by the normalized resistance curve of Figure 3.7. Rod #10 closely follows the resistivity curve with the exception of one data point. This point is, however, questionable when the stray currents present at the time of measurement and the numerical values obtained are taken into consideration. This point is included on the graph for completeness, but is not included in the curve. Note that, although both rods were in spacial proximity, rod #10 consistently ran about 40-50 ohms less resistance. This agrees with theory as lower resistance is expected for a longer rod.

Rods #6 and #9 have higher measured resistance than that predicted by theory, as shown by Figures 3.9 and 3.10. However, this is realistic because of their location near the edge of a steeply-falling slope. The rods do not see a section of earth that equation 3.1 assumes is present. Thus, the equation predicts a lower resistance than should actually occur. Again the 10 foot rod runs at least 25-30 ohms less than the 8 foot rod except for the first data point.

Rod #8, plotted in Figure 3.11, was installed in low resistivity soil. Its resistance values were likewise low and steadily declined from installment for at least 7 months. The last data point is invalid because the rod was totally covered by 1-2 feet of dirt, thus negating the purpose of the Xit-Rod.

One of the recovered rods with the worst case of coagulated salt throughout its length was tested to determine how long it would take water to leach through from one end to the other. Both ends were cut off and the rod was hung vertically with the bottom end in a bucket. The top end had about 1.5 feet of salt removed from it, and this was filled with water on Friday. The following Monday the water had dropped approximately one-half inch in the rod. It was refilled that morning and the following morning it was down about one inch. For two days there was no change in the water level. On Friday seven days after the initial test was begun, there was slight evidence that a few drops had finally leached through to the bottom of the rod. The water leached out at a rate of about one-half inch per day for the next four days after which the test was terminated.

3.3 CONCLUSIONS

Of the eleven Xit-Rods installed, eight rods showed around 30 percent reduction in resistance over the theoretical predictions. Two of the rods had a higher than theoretical resistance, but this was anticipated because of their location. Of the rods recovered, there was no significant corrosion evident on either the stainless steel or the copper rods. However, the zinc coating on the galvanized rod was entirely gone except for a few patches. Considering the time necessary for water to permeate through the coagulated

salt in the one rod tested, serious doubt arises concerning the moisture drawing and leaching effect as claimed in manufacturer's literature.

Much of the data shows a large variation in rod resistance from measurement to measurement, so that rod behavior between data points is difficult to estimate. The 1980 data points are too far spaced in time from the previous points for the connecting line to have any particular significance about rod operation during this period. For this reason, the line is shown are broken instead of constant. Also, it should be noted that due to scheduling and availanle personnel, several different people were used in the data gathering process. However, this should not have a major effect on the data, because the measurement procedures and techniques are fairly straightforward. As a whole, the data is felt to be accurate and consistent with the actual conditions of the rods and soil.

Based on our data, serious questions are raised about the manufacturer's claims such as "freezing temperature has no effect on Xit-Rod or its function" and that "Xit-Rods are used . . . in arid and wet conditions, and their impedance to ground averages 5 ohms or less." They additionally claim that after a few months of service the rods will maintain a low ohmic value ("a small fraction of its low (3 to 5 ohms) initial value") for an indefinite period of time regardless of soil and resistivity conditions [19]. These statements appear to be unfounded for the conditions encountered in these field tests. Based on the data presented, varying resistivity had significant impact upon the resistance profiles of the rods tested. The manufacturer's statements cited above imply that regardless of soil resistivity, the Xit-Rod will have a resistance to ground of approximately 5 ohms and later stabilize at a lover resistance than this. This simply did not occur in the test applications. Several instances of rod resistances of up to 200 ohms were encountered and the resistance plots of most of the rods closely followed the pattern of the resistivity profile.

CHAPTER IV

COMPOSITE GROUND BEDS

4.1 INTRODUCTION

Mining operations are carried out in many areas where the soil resistivity is very high. The WVU research team has studied several locations where soil resistivity has been measured to be 3000 ohm-feet or more. To construct a 5-ohm safety ground bed in such soil would require a hemispherical electrode with a diameter of 191 feet or a bed of 100 10-foot rods covering 5 1/2 acres. Ground beds of this physical magnitude are impractical, and would be extremely expensive because of the quanity of materials needed.

Because regulations exist or are contemplated that require mines to meet specific low resistance values, a method to economically construct a large ground bed is necessary. Since large beds are needed only in areas of high soil resistivity, it may be possible to obtain adequately low resistance by burying a great quantity of an inexpensive semi-conducting material in contact with a relatively small electrode, rather than using a large electrode as discussed earlier. Another advantage of semi-conducting materials over metals as the electrode materials in high resistivity soil is that they will produce lower voltage gradients. This is particularly important in relation to substation ground mats, in which the magnitude of the gradients developed around the substation during lightning activity is directly proportional to the resistivity of the earth in which it is located. Therefore, the task of this research is to investigate the use of fill in conjunction with a metal electrode. The use of fill and an electrode will be referred to throughout this report as a composite ground bed.

4.2 MATERIAL EVALUATION

The fill material used in a composite ground bed must be of low cost and low resistivity. With these criteria in mind, several commonly available materials were evaluated for possible use as a fill material. The materials were first located in areas near to the mine site. If only a small sample could be made available for testing, and a Hewlett Packard Universal bridge was used to find the resistivity by the method shown in figure 4.1. The formula $\rho = AR/L$ was used, where ρ is resistivity, R is resistance, A is the area of the metal plates, and L is the length of the sample (figure 4.1). The bridge uses a 1000 Hz signal so that polarization is not a problem. If a larger sample were available, a Bison earth resistance meter was used to obtain the resistivity through the use of a Wenner Array (figure 4.2). Some material resistivities were found in a literature search and are identified by their references. Those materials considered and their resistivities are shown in the following table:

Material	Representative Resistivity Value
Waste Coal Pile	100 Ω-ft
Marconite Conducting Concrete	1 Ω-ft [20]
Fly Ash	1000 Ω-ft
Sanitary Land fill	
New fill	10 Ω-ft
Older fill	45 Ω-ft

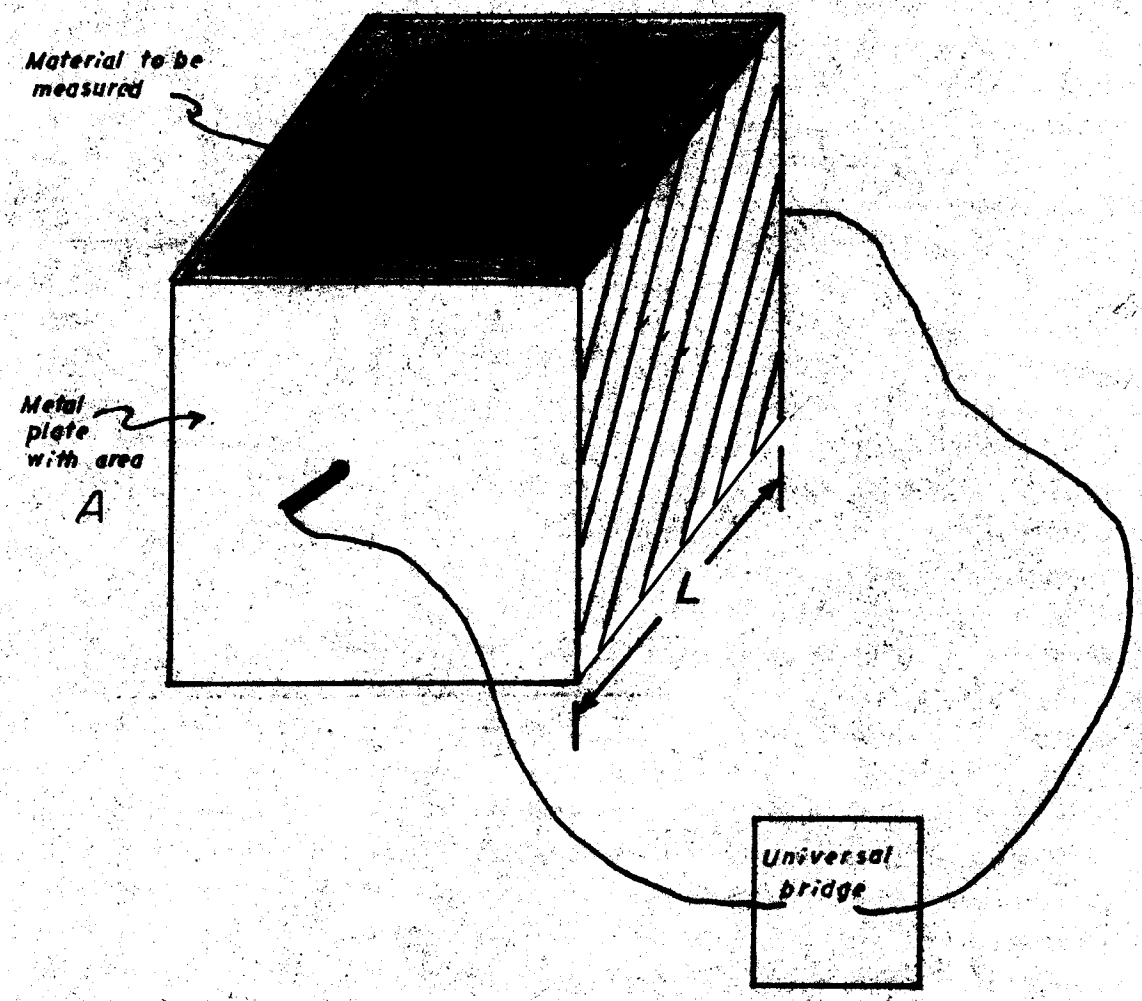

FIGURE 4.1. - Method to determine sample resistivity.

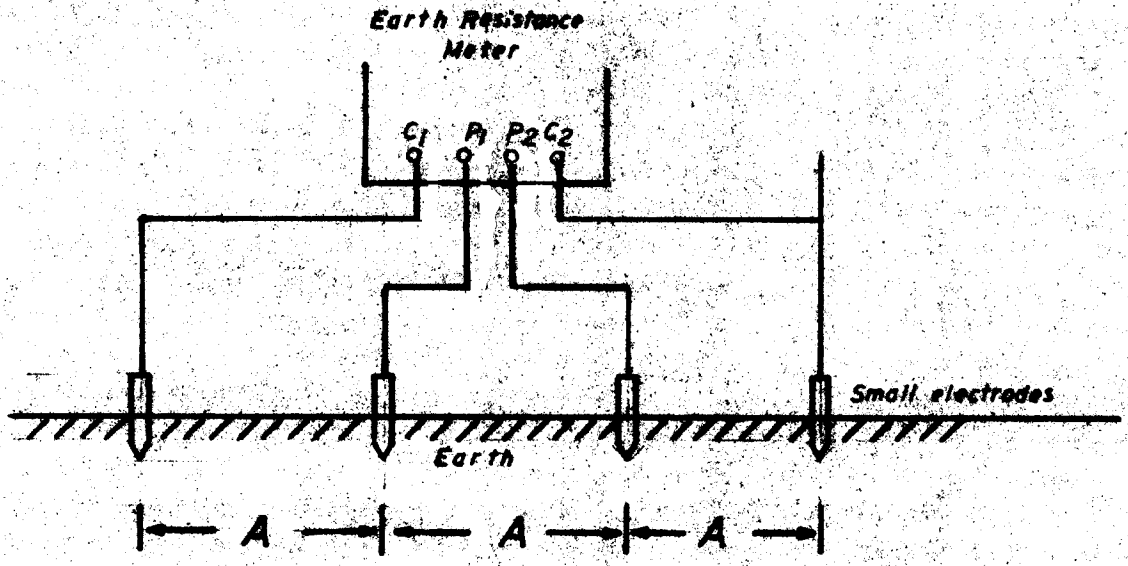

FIGURE 4.2. - The Wenner Array.

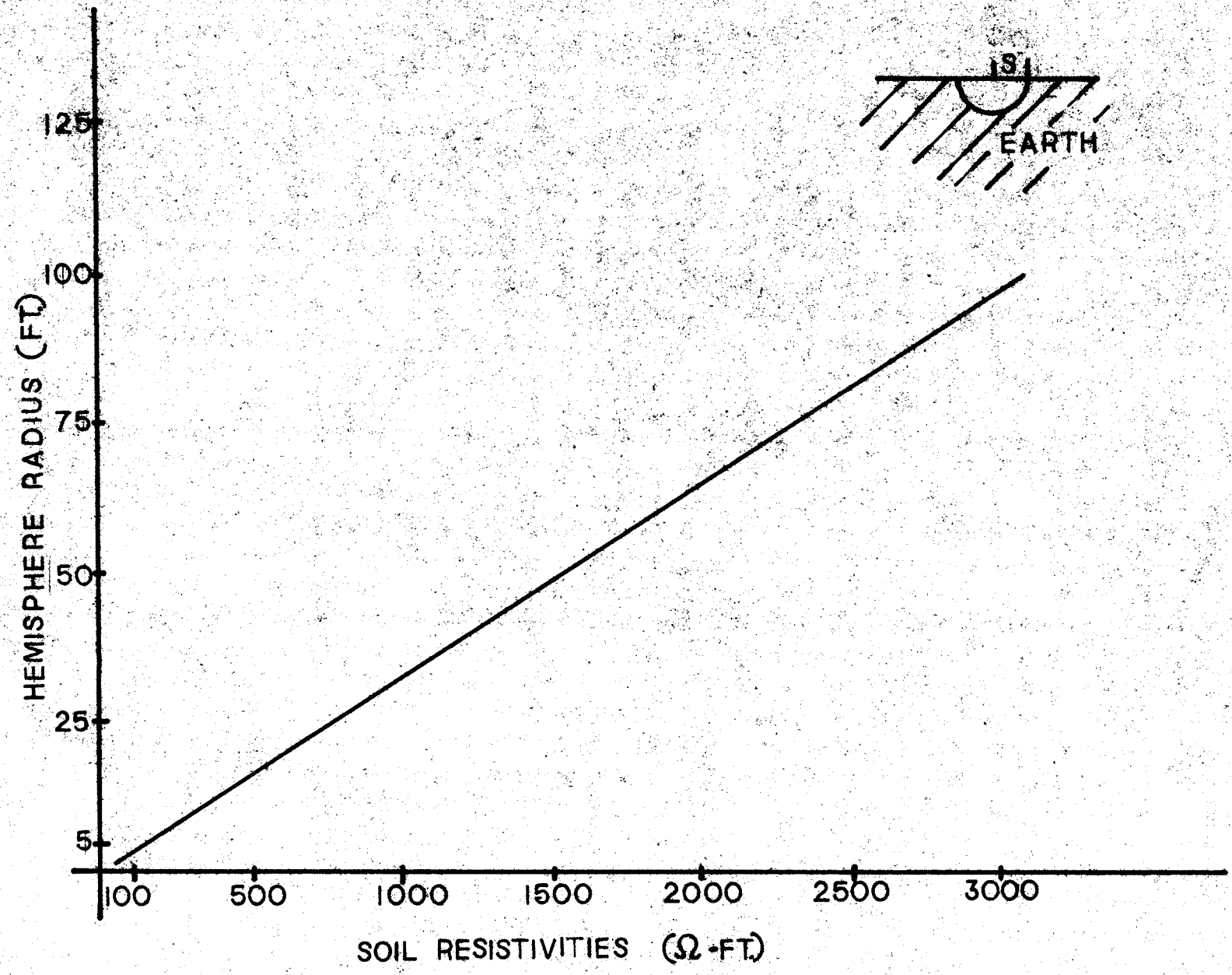

FIGURE 4.3. - **Hemispherical electrode radius for different soil resistivities.**

Slag pile	150 Ω-ft
Agricultural lime	5000 Ω-ft
Loams, garden soils, etc.	15 Ω-ft to 160 Ω-ft
Clays	26 Ω-ft to 160 Ω-ft [21]

The waste coal pile, conducting concrete, land fill, and slag pile all have electrical properties that make them suitable for use as a composite fill material.

With the exception of the Marconite conducting concrete, the major cost of all the fill materials examined would be for transportation. For example slag presently sells for $1.25/ton F.O.B. The sanitary land fill examined was one operated by the city of Morgantown, and consisted of normal wastes generated by the city. Since most of these materials can probably be found in close proximity to the mine, it would appear that fill materials can be obtained at relatively low prices.

The list, however, is not intended to be a complete list, nor is it intended to suggest the use of any of these materials. Rather, its purpose is to show that there are cheap, low resistivity materials available.

4.3 ELECTRODE CONFIGURATIONS

Several electrode configurations were studied for possible use in a composite ground bed. Among those analyzed were the hemispherical electrode, long wire surface conductor, and a ring of wire on the surface of the earth.

4.3.1 Hemispherical Electrode

The hemispherical electrode has a resistance which can be determined by the formula:

$$R = \frac{\rho}{2\pi S}, \quad [22] \tag{4.1}$$

where R = resistance,

ρ = earth resistivity,

and S = radius of hemisphere.

The required hemispherical radius to obtain a 5-ohm ground bed for a given soil resistivity can be seen in figure 4.3. To determine the resistance of a hemispherical electrode composite ground bed (figure 4.4) it is necessary to consider three different terms. The first term is the resistance of the hemispherical electrode in the fill. This is given by

$$R = \frac{\rho_2}{2\pi S}, \tag{4.2}$$

where ρ_2 is the resistivity of the fill.

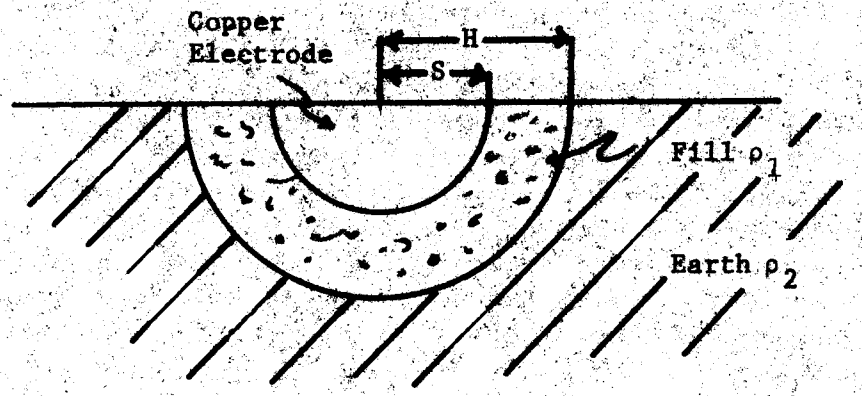

FIGURE 4.4. - Hemispherical electrode used in a composite ground bed.

It is also necessary to consider the resistance of the fill, which is now considered as the electrode in the earth.

$$R = \frac{\rho_1}{2\pi H} , \tag{4.3}$$

where H is the radius of the fill as shown in figure 4.4.

Whenever two electrodes, the metal electrode and the fill as an electrode are together, there is a mutual resistance between them. This mutual resistance is given by

$$R = \frac{\rho_2}{2\pi H} , \tag{4.4}$$

and must be subtracted from the sum of the resistances of the metal electrode and fill electrode cases to obtain the total bed resistance. Therefore, the total resistance of the hemispherical electrode composite ground bed is given by:

$$R = \frac{\rho_2}{2\pi S} + \frac{\rho_1}{2\pi H} - \frac{\rho_2}{2\pi H} , \text{ [23]} \tag{4.5}$$

where ρ_1 = earth resistivity,

ρ_2 = fill resistivity,

and H = radius of the fill.

All other terms are the same as those previously defined.

Using the Hewlett Packard 97 programmable calculator, results were fitted to equation 4.5 by choosing values for ρ_1, ρ_2, and S. Then a value for H was chosen and the equation was solved for R. If R was greater than the 5 ohms desired, H was incremented and the equation was again solved. This process continued until the desired R-value was obtained.

An infinite number of graphs could be generated from this resistance equation to cover all soil resistivities. Since this is impossible to do, only two soil resistivities, 1000 Ω-ft and 3000 Ω-ft, were chosen to demonstrate the use of the composite ground bed. These can be seen in figures 4.5 and 4.6.

To determine the economic feasibility of using the composite ground bed technique with the hemispherical electrode, the cost of installing a copper hemispherical electrode without fill was normalized and an allowable cost for the fill determined. Again, due to the large number of variables, it is necessary to concentrate on one example that can easily be extended to other cases.

To obtain a 5 Ω ground bed in 1000 Ω-ft soil without the use of fill, a hemisphere with a radius of 32' is needed (figure 4.3). The total cost for such a ground bed can be written as

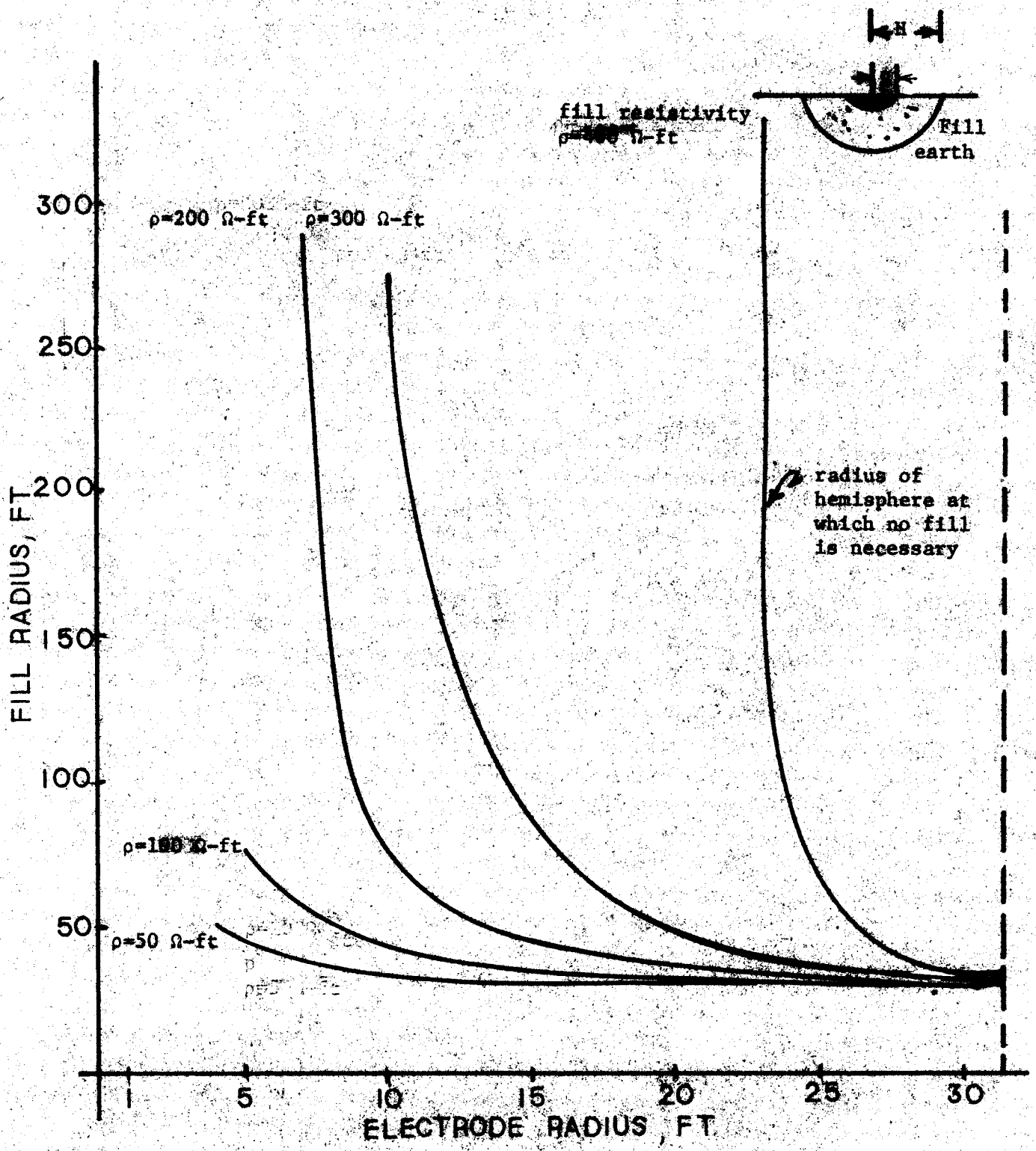

FIGURE 4.5. - Fill radius for composite ground bed hemispherical electrode in 1000 Ω-ft soil.

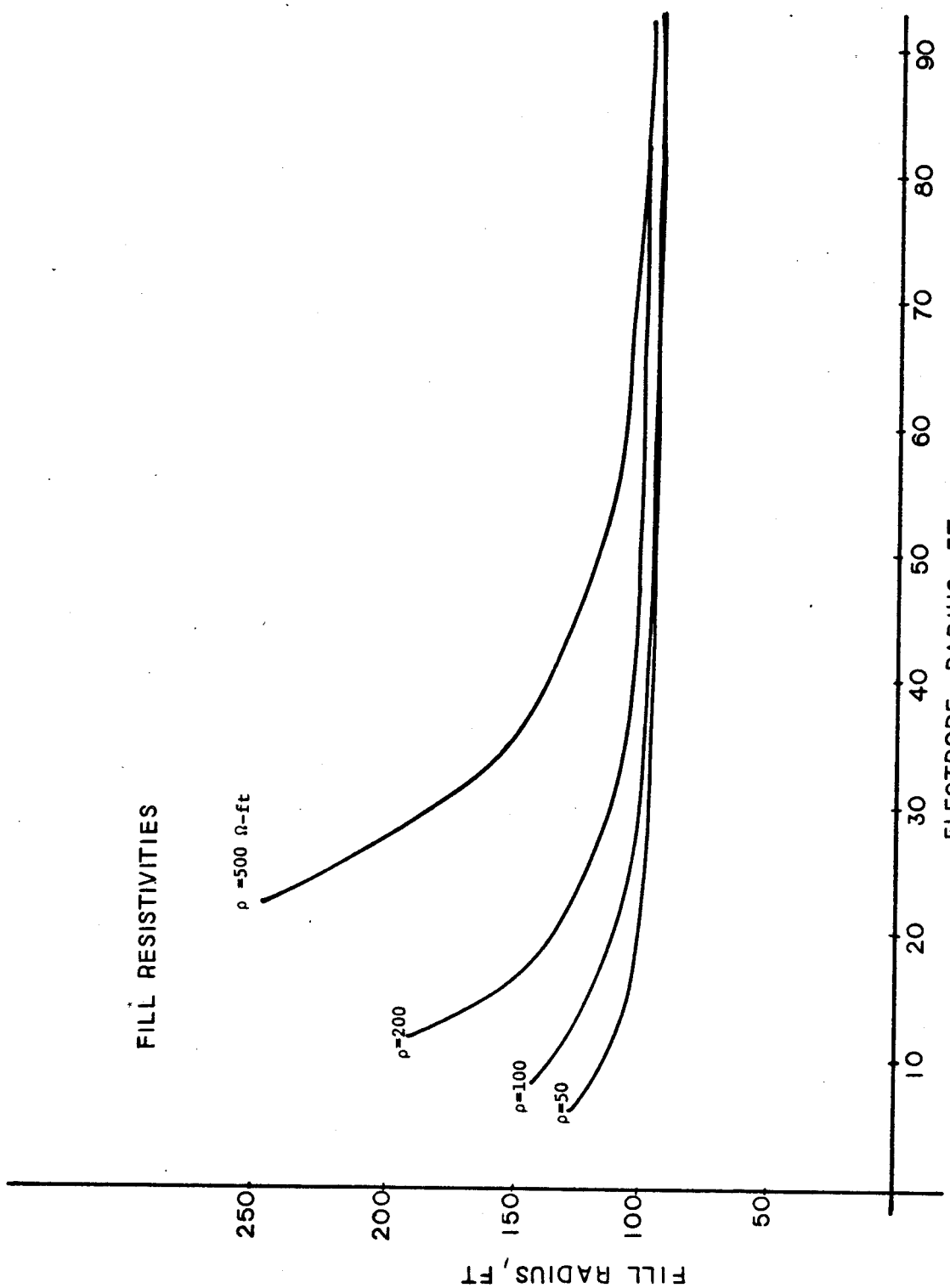

Figure 4.6. - Fill radius for composite ground bed hemispherical electrode in 3000 Ω-ft soil.

$$C_T = \frac{\frac{4}{3}\pi\,(32)^3}{2}\,(C_1) \tag{4.6}$$

where C_1 = cost/unit volume of excavation and copper,

and the remainder of the expression is the volume of the hemisphere.

For the composite ground bed case (figure 4.2), the additional cost to be considered is that of the fill material. The cost of this type of ground bed is determined by:

$$C_T = C_1 \frac{\frac{4}{3}\pi\,S^3}{2} + C_2 \frac{\frac{4}{3}\pi\,(H^3-S^3)}{2} \tag{4.7}$$

where C_2 is cost/unit volume of excavation and fill material.

All other terms are the same as those previously defined.

For the composite ground bed to be economically justifiable it can at worst have the same cost as the hemispherical electrode without fill. That is, when equations 4.5 and 4.6 are equal. By normalizing C_1 to 1 and setting these equations equal, the following expression results:

$$C_2' = \frac{32^3 - S^3}{H^3 - S^3} \tag{4.8}$$

where C_2' is the cost of fill relative to the cost of copper.

To obtain a 5-ohm ground bed, however, H and S are dependent upon each other as well as the fill resistivity (equation 4.5). By referring to figure 4.5 and choosing values of H and S, the cost of the fill relative to the cost of copper can be determined.

In more general terms, to consider the interdependency of H, S, fill resistivity, and earth resistivity simultaneously, equation 4.7 is solved for H.

$$H = \left(\frac{C_T - \frac{2}{3}\pi\,S^3\,C_1 + C_2\,\frac{2}{3}\pi\,S^3}{C_2\,\frac{2}{3}\pi} \right)^{1/3} \tag{4.9}$$

Substituting this result into equation 4.2 and solving for C_2 gives

$$C_2 = \frac{3\left(\left(R_T - \frac{\rho_2}{2\pi S}\right)\frac{2\pi}{\rho_1-\rho_2}\right)^3 \left(C_T - 2/3\,\pi S^3\,C_1\right)}{C_1\,2\pi\left(1-\left\{\left(R_T - \frac{\rho_2}{2\pi h}\right)\frac{2\pi}{\rho_1-\rho_2}\right\}^3 S^3\right)} \; . \tag{4.10}$$

For the more general case, equation 4.6 can be written as

$$C_T = \frac{4}{3}\,\Pi\,\frac{(r)^3}{2}\,(C_1), \tag{4.11}$$

where r is the hemisphere radius required when no fill is used.

Again, to economically justify the composite ground bed, its cost (equation 4.11) must at worst be equal to the cost of the no-fill ground bed (G in equation 4.10 and equation 4.7). By normalizing C_1 to 1, substituting the value of G into equation 4.10, and solving for C_2/C_1 (C_2'), the following equation was developed:

$$C_2' = \frac{3\,\{(R_T - \frac{\rho_2}{2\Pi S})\,\frac{2\Pi}{\rho_1 - \rho_2}\}^3\,(\frac{2}{3}\,\Pi\,r^3 - \frac{2}{3}\,\Pi\,S^3)}{2\,\Pi\,(1 - \{(R_T - \frac{\rho_2}{2\Pi S})\,(\frac{2\Pi}{\rho_1 - \rho_2})\}^3\,S^3)},$$

where R_T is the ground bed resistance desired,

and all other variables are the same as defined earlier. Results of this equation for a 5-ohm ground bed in earth with a resistivity of 1000 Ω-ft can be seen in figure 4.7. An example can best demonstrate the use of figure 4.7. If a hemispherical electrode with a 15' radius was used with a 100 Ω-foot fill, the allowable cost/unit volume of the fill could be as high as about 0.63 times the cost/unit volume of copper (see figure 4.7). That is to say, if a cubic foot of copper sells for $100, then it would be economically justifiable to spend as much as $63 for a cubic foot of fill material.

At today's price for copper, it would appear that fill could easily be obtained within the price limits given by figure 4.7 or equation 4.8. Therefore, it appears that the composite ground bed could be economically justified when used in a hemispherical electrode ground bed.

4.3.2 Surface Conductor

The next electrode analyzed was a long conductor on the surface of the earth (figure 4.8). The resistance of such a ground bed is given by:

$$R = \frac{\rho}{\Pi \ell}\,\ln\,\frac{2\ell}{d}\,, \quad [24] \tag{4.13}$$

where ℓ is the conductor length,

and d is the conductor diameter.

The conductor lengths necessary to obtain a 5-ohm ground bed using several different conductor sizes in various soil resistivities can be seen in figure 4.9. As can be seen, there is not a significant change in required conductor lengths for large changes in conductor sizes.

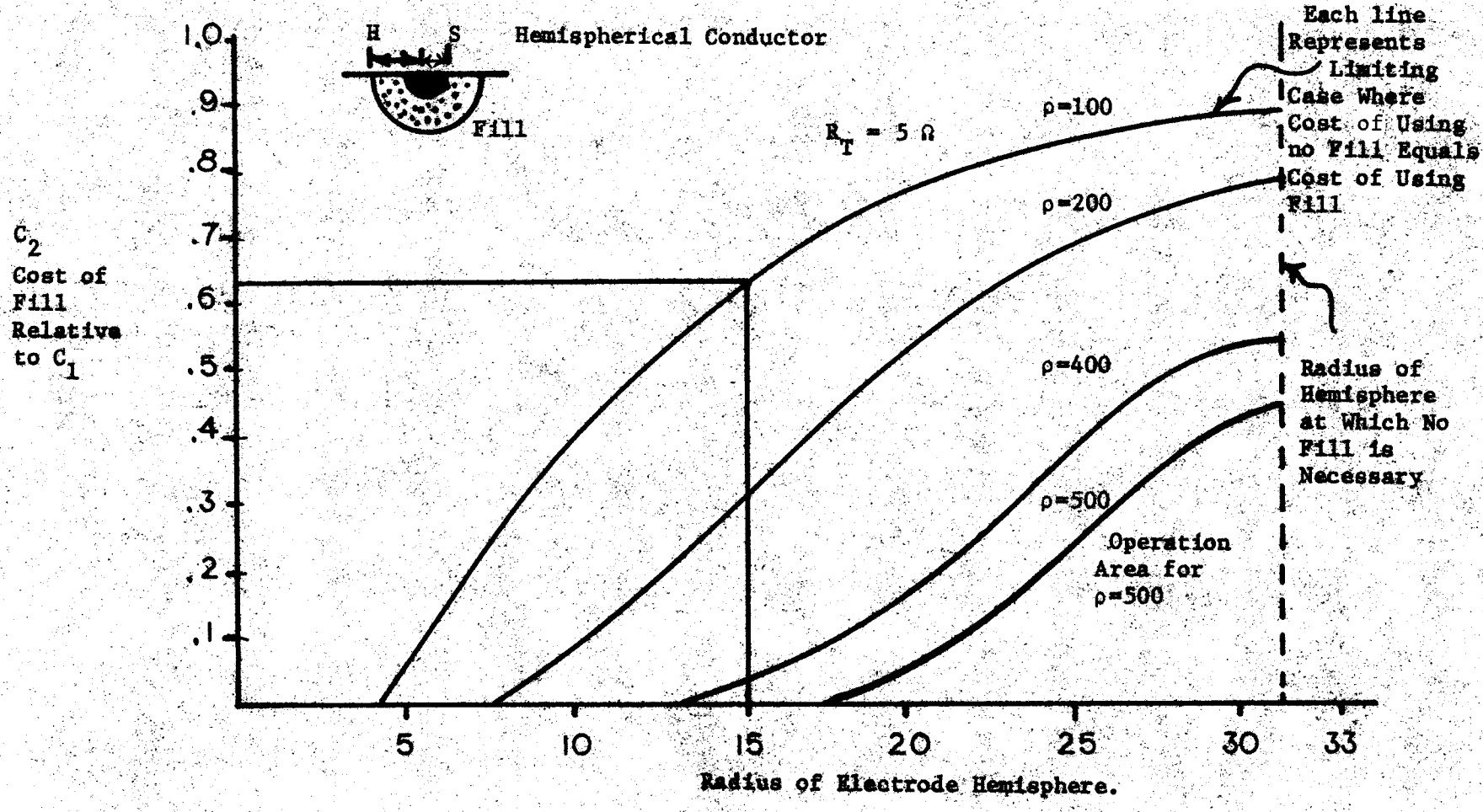

FIGURE 4.7. - Cost versus size for a hemispherical composite ground bed.

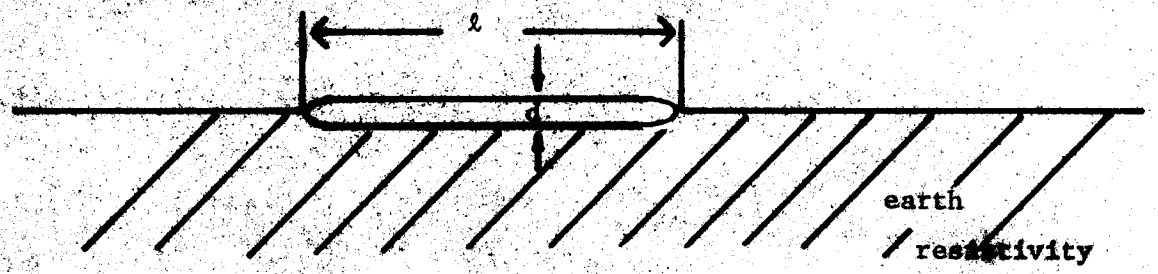

FIGURE 4.8.6 - Surface Conductor

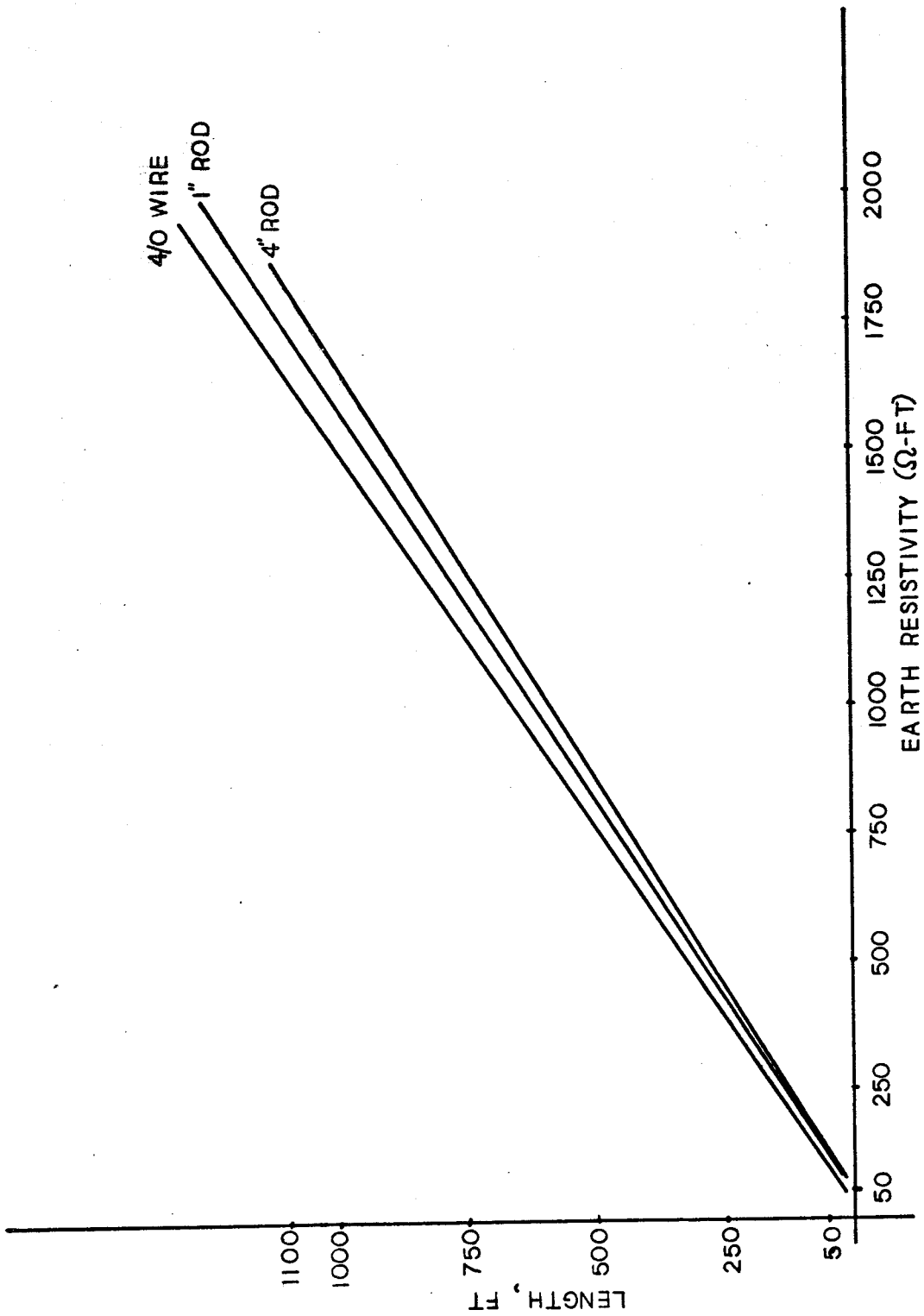

Figure 4.9. - Surface conductor lengths for a 5Ω ground bed .

When the surface conductor is used in a composite ground bed (figure 4.10) the resistance equation becomes:

$$R = \frac{\rho_2}{\pi \ell} \ln \frac{2\ell}{d} + \frac{\rho_1}{\pi L} \ln \frac{2L}{D} - \frac{\rho_1}{\pi \ell} \ln \frac{2\ell}{D} , \tag{4.14}$$

where L is the fill length,

D is the fill diameter,

and all other variables are as previously defined. The term $\frac{\rho_2}{\pi \ell} \ln \frac{2\ell}{d}$ represents the resistance of the electrode in the fill material, and $\frac{\rho_1}{\pi L} \ln \frac{2L}{D}$ is the resistance of the fill as the electrode in the earth. Again, since there are two conductors there is a mutual resistance between the two that is given by $\frac{\rho_1}{\pi \ell} \ln \frac{2\ell}{D}$, the total resistance is, as shown in equation 4.14, the sum of the resistances of each electrode with the mutual resistance term subtracted.

However, there is an inter-relationship between D, L, and ℓ. This relationship can be shown to be:

$$D = \sqrt{L^2 - \ell^2} . \tag{4.15}$$

Substituting equation 4.15 into equation 4.14 gives

$$R = \frac{\rho_2}{\pi \ell} \ln \frac{2\ell}{d} + \frac{\rho_1}{\pi L} \ln \frac{2L}{\sqrt{L^2 - \ell^2}} - \frac{\rho_2}{\pi \ell} \ln \frac{2\ell}{\sqrt{L^2 - \ell^2}} . \tag{4.16}$$

A numerical analysis of this expression was performed to find the required fill length (L) to obtain a 5-ohm ground bed, given a fill resistivity (ρ_2), earth resistivity (ρ_1) conductor length (ℓ), and conductor diameter (d). This was accomplished by using the Hewlett Packard 97 programmable calculator. Values were chosen for ρ_2, ρ_1, ℓ, and d, then a value was chosen for L. The resistance was then calculated and checked to see if it was 5 ohms. If not, L was incremented and the process continued until the resistance was lowered to 5 ohms. The results of this analysis for various conductor lengths and fill resistivities with a given earth resistivity of 1000 Ω-ft can be seen in figure 4.11.

Applying these results to equation 4.15, the diameter of the fill necessary to obtain the 5 ohm ground bed can be determined. The volume of fill can then be determined by:

$$V = \frac{1}{3} \pi \frac{D^2}{2} L, \tag{4.17}$$

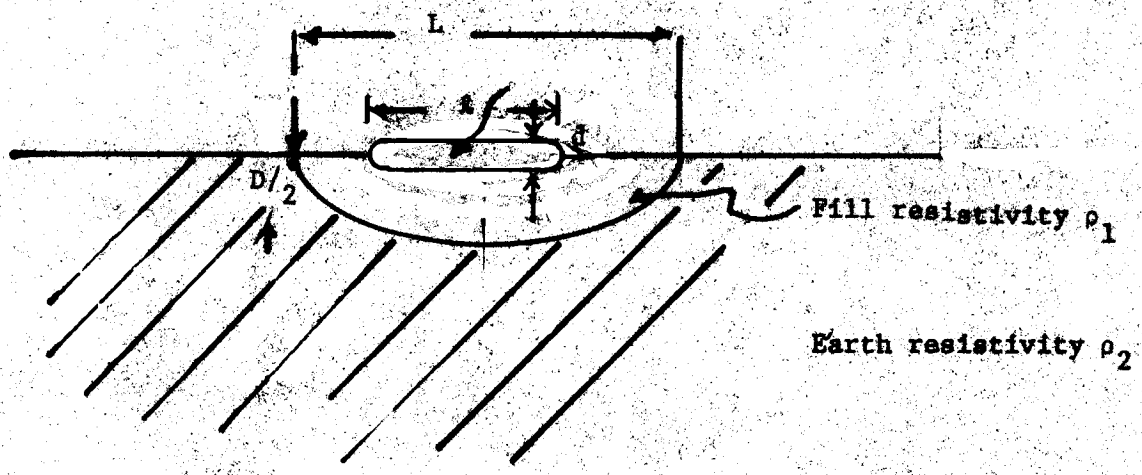

FIGURE 4.10. - Surface conductor composite ground bed.

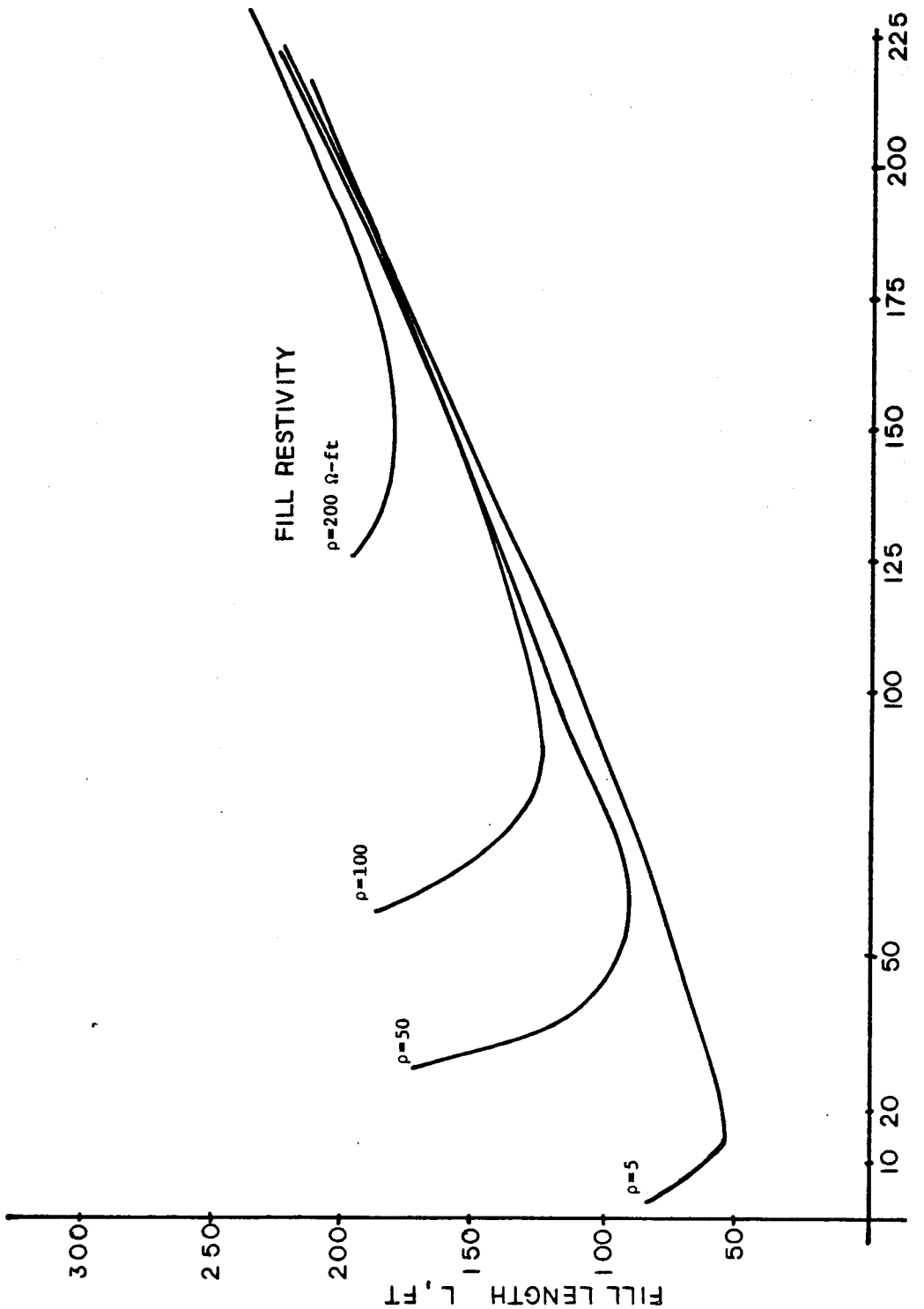

Figure 4.11. - Length of fill necessary to obtain a 5 Ω composite surface conductor ground bed.

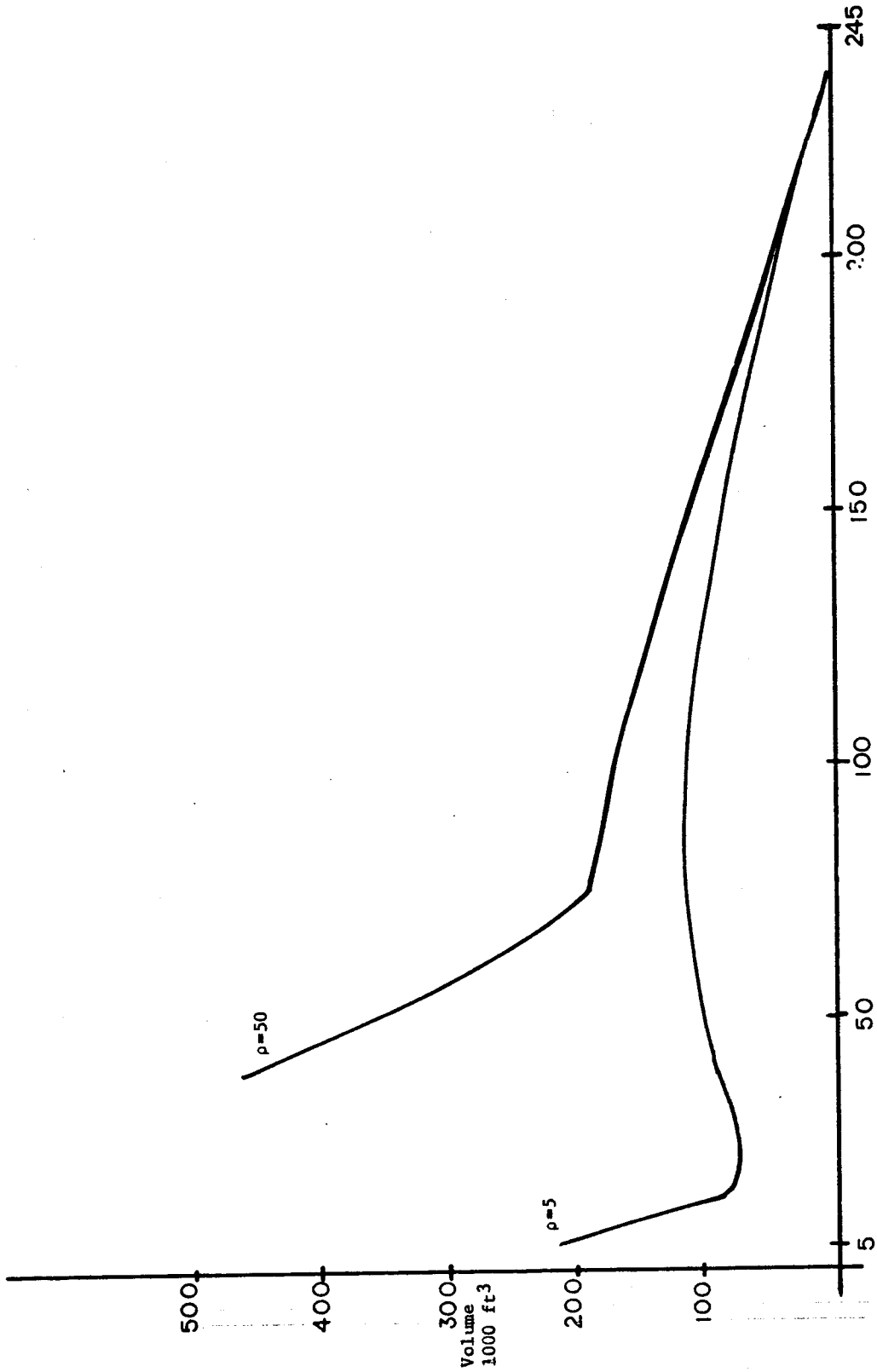

Figure 4.12. - Fill volume required to obtain a 5 Ω ground bed for varying conductor lengths.

where all terms are the same as those previously defined. These results are recorded in figure 4.12.

To do the cost analysis for the long wire case, it is first necessary to make three basic assumptions:

a) minimum excavation to be a ditch that is 2 feet in width

b) backfill costs will be the same regardless of amount of fill used

c) conductor cost is negligible compared to excavation costs.

Using the first assumption, the volume of earth that must be removed for each case in figure 4.11 can be found. This limit affects only the extreme right hand portion of figure 4.16, and limits it to 4 times the conductor length at each point.

A cost comparison between the composite long wire surface conductor and the long wire surface conductor without fill was then conducted.

To obtain a 5-ohm ground bed in earth with a resistivity of 1000 Ω-feet a 660 foot length of 4/0 conductor would be needed (figure 4.9). The total cost for this case can be written as

$$C = C_1 \ (4) \ 660, \tag{4.18}$$

where C is total cost, C_1 is cost/unit volume to excavate and backfill, 4 represents the minimum ditch area that can be dug (2' x 2') and 660 is the length of the ditch.

For the composite ground bed, the cost equation becomes

$$C = C_1 \ V_1 + C_2 \ V_2, \tag{4.19}$$

where C_1 is as defined for equation (4.17),

V_1 is the volume of the earth that must be removed,

C_2 is the cost/unit volume of the fill,

and V_2 is the volume of fill needed.

The limit for economical feasibility for the long wire surface conductor composite ground bed occurs when its cost reaches the cost of a no fill ground bed. By normalizing the common cost (C_1) of excavation to 1, and setting equation 4.18 equal to 13, the following relationship was established:

$$2640 = V_1 + C_2' \ V_2, \tag{4.20}$$

where C_2' is the cost/unit volume of fill relative to the cost/unit volume of excavation.

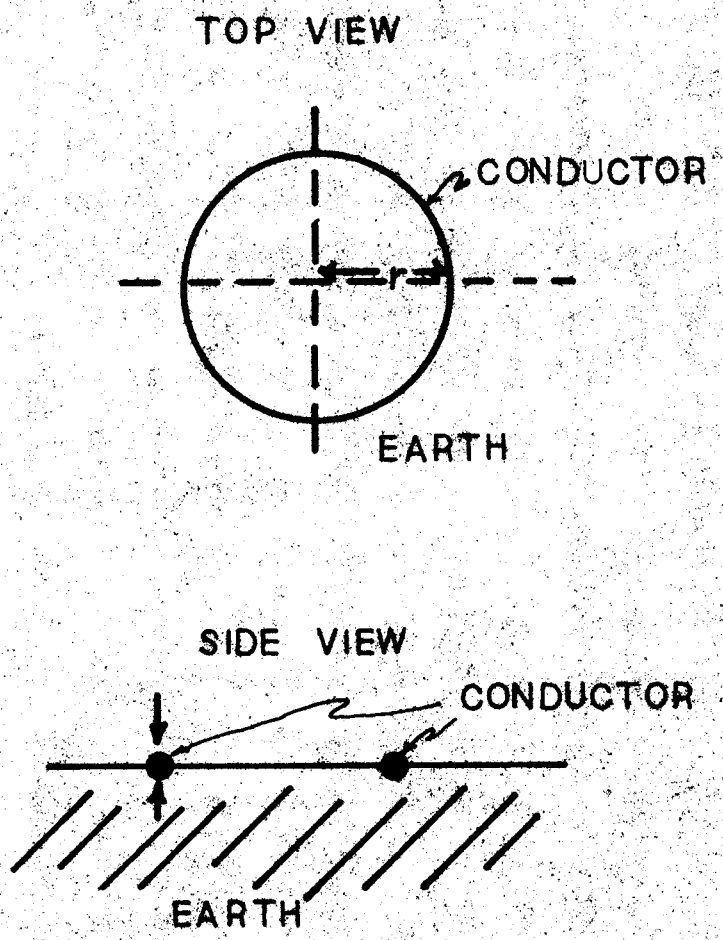

FIGURE 4.13. - Circular ring ground bed.

However, V_1 and V_2 (equation 4.20) are directly dependent upon L and ℓ, respectively, (equation 4.17 and assumption 1). Furthermore, L and ℓ are inter-related as can be seen by referring to equation 4.14).

Rather than attempting a numerical solution of this complex relationship, a brief graphical analysis can be performed. From equation 4.20, it can be shown that the largest volume of earth that can be economically removed is 2640 cubic feet. This situation requires that the fill, including transportation and installation, have a net cost of 0 to satisfy the equality. By referring to figure 4.12, the volume of earth to be removed is found to reach the 2640 cubic feet level only for an extremely large conductor length. Although this is an improvement over the original conductor length, the problem of voltage drop on the analysis and the high gradients associated with the long wire conductor are not alleviated. For these reasons further analysis of the long wire conductor was terminated.

4.3.3 Circular Wire Ring

The final geometry studied is shown in figure 4.13. The resistance of the circular ring is given by

$$R = \frac{V(x,z)}{I} = \frac{\rho}{2\Pi} \cdot \frac{2}{\Pi} \frac{F(k)}{[(r+x)^2 + z^2]^{1/2}} \quad [25] \tag{4.21}$$

for x = r and z = a,

where r is the conductor radius,

x is the distance from the center of the ring,

z is the distance up from the center of the conductors,

$$k = \left[\frac{4 \times r}{(x+r)^2 + z^2}\right]^{1/2} \tag{4.22}$$

and

$$F(k) = \int_0^{\Pi/2} (1-k^2 \sin^2 \psi)^{-1/2} \, d\psi. \tag{4.23}$$

Since a << r, (r is at least 20 times a), k will approach unity and the elliptic integral is then given by

$$R = \frac{\rho}{2\Pi} \frac{1}{\Pi r} \ln \frac{8r}{a}. \tag{4.24}$$

The required ring radius to obtain a 5-ohm ground bed using a 4/0 conductor for various earth resistivities can be seen in figure 4.14.

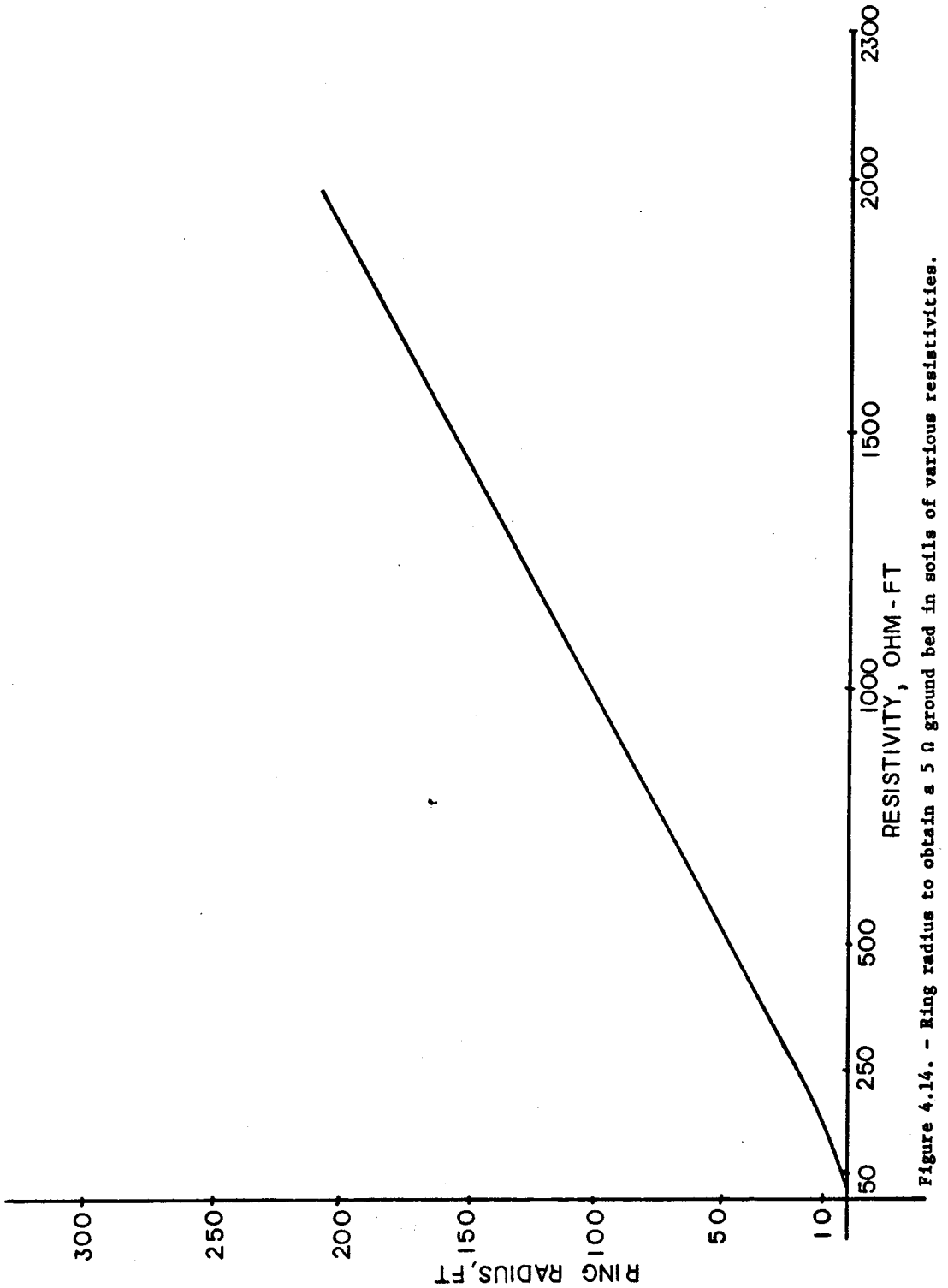

Figure 4.14. - Ring radius to obtain a 5 Ω ground bed in soils of various resistivities.

The circular ring composite ground bed (figure 4.15) has a resistance that can be determined by:

$$R = \frac{\rho_2}{2\pi\pi r} \ln \frac{8r}{a} + \frac{\rho_1}{2\pi\pi r} \ln \frac{8r}{c} - \frac{\rho_2}{2\pi\pi r} \ln \frac{8r}{c}, \qquad (4.25)$$

where a = conductor radius

r = the wire ring radius,

ρ_1 = earth resistivity,

ρ_2 = fill resistivity,

c = fill radius,

$\frac{\rho_2}{2\pi\pi r} \ln \frac{8r}{c}$ = mutual resistance,

$\frac{\rho_2}{2\pi\pi r} \ln \frac{8r}{a}$ = conductor electrode resistance, and

$\frac{\rho_1}{2\pi\pi r} \ln \frac{8r}{c}$ = fill as electrode resistance.

By combining the mutual resistance term ($\frac{\rho_2}{2\pi\pi r} \ln \frac{8r}{c}$) with the conductor resistance term ($\frac{\rho_2}{2\pi\pi r} \ln \frac{8r}{a}$), equation 4.19 can be simplified to:

$$R = \frac{\rho_2}{2\pi\pi r} \ln \frac{c}{a} + \frac{\rho_1}{2\pi\pi r} \ln \frac{8r}{c}. \qquad (4.26)$$

A numerical analysis was then performed on the HP-97 calculator by choosing ρ_1 to be 1000 ohm-feet, a as 0.022', by varying the value of r and solving for the necessary fill radius to obtain a ground bed resistance of 5 ohms. This was done for several fill resistivity (ρ_2) values. Results can be seen in figure 4.16. It should be noted that the simplifying assumption $a << r$ is not violated in the results shown in figure 15.

To do the cost analysis for the circular ring, the assumption that the same amount of excavation is needed for both the composite and no-fill ground beds is made. This is justified by the low fill radius that is required. Conductor cost is again considered to be negligible as compared to the cost of excavation.

Using the guidelines established, the following cost equation was developed for the no-fill circular ring ground bed:

$$C = \pi\ 2\ r_1\ C_1,$$

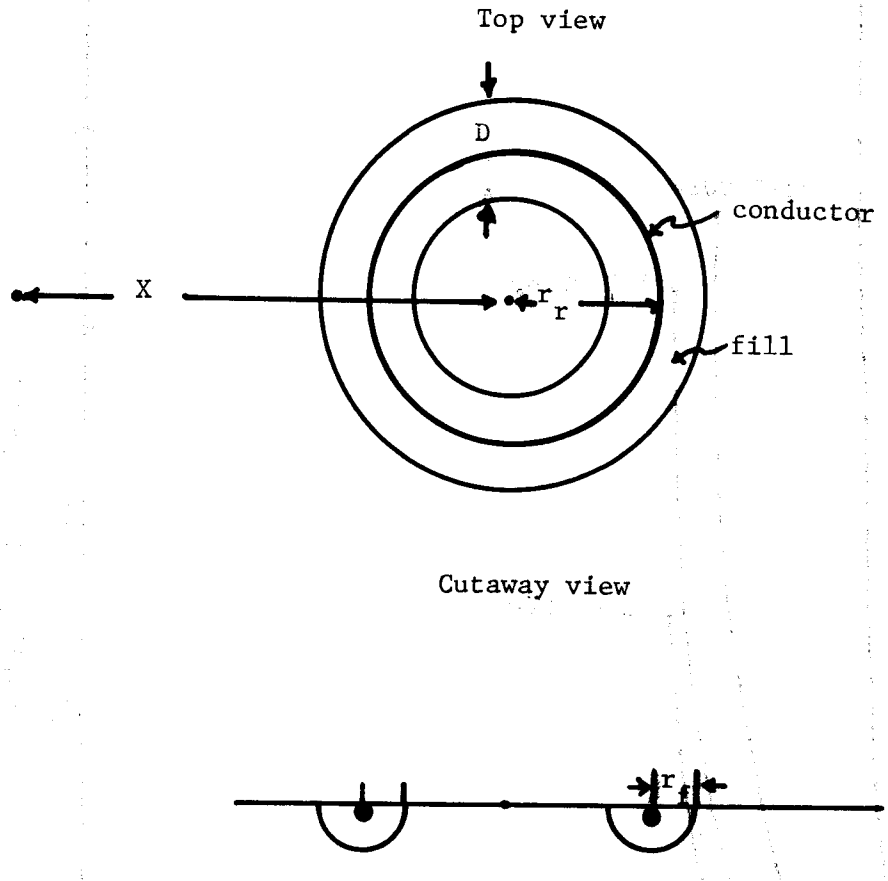

FIGURE 4.15. - Circular ring composite ground bed.

where $2\Pi r_1$ is the circumference of the ring,

and C_1 is the cost/unit length of excavation and backfill.

For the composite circular ring ground bed, the cost equation is given by:

$$C_T = \Pi 2 r_2 C_1 + \frac{\Pi^2 C^2}{2} 2 r_2 C_2, \tag{4.28}$$

where r_2 is the radius of the metal ring in the composite ground bed,

and C_2 is the cost/unit volume (including purchase price and transportation costs) of the fill.

The limiting economically justifiable case occurs when the cost of the composite ground bed equals the cost of the non-composite ground bed. By normalizing C_1 to 1, equations 4.27 and 4.28 can be simplified to give

$$C_2' = \frac{2 (r_1 - r_2)}{C^2 r_2 \Pi} \tag{4.29}$$

where C_2' is the cost of fill relative to the cost of excavation.

This equation has been graphed for a few specific fill and earth resistivities and can be seen in figure 4.17. As can be seen in the graph, the cost/unit volume of fill can exceed the cost/unit volume of excavation by as much as 25 times. It would appear that if a suitable fill material was in close proximity to the mine site, a composite ground bed could prove to be economically suitable.

As a specific case, consider an earth resistivity of 1000 Ω-feet and a fill resistivity of 200 ohm-feet (slag, as mentioned under material evaluation). The required ring radius can be obtained from figure 4.14 as 107.5 feet. For a ring radius of 80', the necessary fill radius is about 0.2' as can be seen in figure 4.16. Applying equation 4.29, the relative cost of fill is found to be 5.47 times the cost of excavation/unit length.

If the cost/unit length of excavation is $1.30, as one estimation showed, then the allowable cost/volume for the fill is $7.11. The volume of fill needed is 31.58 cubic feet, which was approximated to be 3/4 ton. The cost of slag, as reported under materials evaluation is $1.25/ton, or about $1 for the amount needed. The cost/unit volume of the fill is then about .04, which leaves $7.07/unit volume for transportation costs.

For 31.58 cubic feet of fill, a total cost of $223 ($7.07 X 31.58) is allowed for transportation. Since this amount of fill can be hauled in a pick-up truck, $.45/mile is allowed for use of the vehicle and driver. This is based on $.20/mile for the vehicle, and $10 an hour for the driver, considering

he can drive 40 miles/hour. The maximum total distance to be driven can then be 495 miles for a round trip or 247 miles one way. With slag piles in Wheeling and Pittsburgh for example, this means that the mines in northern West Virginia and southern Pennsylvania could use this as an economical alternative.

Of the geometries reviewed, it appears that the circular ring has the properties best suited for practical application. The hemispherical electrode is not practical, due to installation and electrode availability. The long wire surface conductor would have large gradients associated with it. For these reasons, only the circular ring analysis was extended.

4.4 CIRCULAR RING VOLTAGE GRADIENTS

The voltage with respect to infinite earth for a circular ring of wire is given by:

$$V(x) = \frac{I_f}{\pi^2} \rho \frac{F(k)}{r+x} , \quad [25] \tag{4.30}$$

where I_f is the fault current,

r is ring radius,

x is distance from the center of the ring,

and $F(h)$ is the elliptic integral (equation 4.22).

Applying this to the composite ground bed case, the following equations were developed. For $x \geq r + r_f$, (figure 4.15)

$$V(x) = \frac{I_f}{\pi^2} \rho_1 \frac{F(k)}{r + r_f} + \frac{I_f}{\pi^2} \rho_2 \frac{F(k)}{r + x} , \tag{4.31}$$

where $F'(k)$ is the elliptic integral evaluated at $x = r + r_f$, and all other variables are the same as those previously defined.

For $x \leq r + r_f$, (in the fill)

$$V(x) = \frac{I_f}{\pi^2} \rho_2 \frac{F(k)}{r + x} . \tag{4.32}$$

To solve for the voltages associated with the circular ring ground bed during a fault current, it is necessary to evaluate the elliptic integral of the first kind:

$$F(k) = \int_o^{\pi/2} (1-k^2 \sin^2 \psi)^{-1/2} \, d\psi, \quad \text{(eq. 4.23)}$$

$$\text{where } k = \left[\frac{4 x r}{(x+r)^2 + Z^2} \right]^{1/2} . \quad \text{(eq. 4.22)}$$

On the earth's surface Z goes to 0, so that

$$k = \left[\frac{4 \times r}{(x+r)^2} \right]^{1/2} .$$

Elliptic integral tables are tabulated for $\theta = \sin^{-1} k$, and usually in only 5° increments of θ. Since the area of highest gradients will be occurring close to the ring, the value of k, and hence the value of θ will be varying only a small amount. For this reason it became necessary to write a program for the HP-97 that could numerically evaluate the result of the elliptic integral for a given value of k.

As an example, the gradients associated with the circular ring ground beds were graphed for a soil resistivity of 1000 Ω-ft. Using a 4/0 conductor and no fill, $\frac{\text{potentials}}{\text{Ampere of fault current}}$ over 2' intervals can be seen in figure 4.18. For the composite ground bed case in 1000 ohm-foot soil and a 50 ohm-foot resistivity fill, the gradients over 2' for a 5-ohm ground bed and a ring radius of 60' can be seen in figure 4.19. As can be seen in the graphs, the gradients associated with the composite ground bed are considerably lower than for the no-fill ground bed. By increasing the fill diameter, and thus lowering the resistivity of the ground bed, a further reduction in the gradients can be obtained (figure 4.20).

4.5 DRIVEN ROD GROUND BED

To construct a 5 ohm driven rod ground bed in 1000 ohm-foot soil, a 9 by 9 array of 8' length 1/2" diameter rods with a 12'8" spacing is needed (figure 4.21) [27]. If the assumption is made that a minimum amount of excavation can be accomplished when connecting the rods in the circular ring case, it is found that the total length to be excavated in 1014 feet. This is nearly twice the amount of excavation (660') required for a no-fill circular ring ground bed. Also, the cost of the rods (total length of 648') is much more than the cost of the same length of wire.

A program was developed that calculates the mutual resistance for any location around a given driven rod ground bed. By taking the difference in resistances associated with any two points around the ground bed and then multiplying by the fault current, the absolute voltage gradient is determined. If the resistance is not multiplied by the fault current, the result can be viewed as volts/amp of fault current. The results of the investigation for the 5-ohm driven rod ground bed can be seen in figure 4.22. The circles in figure 4.21 show where the step potentials were taken, and the numbers on the figure correspond with the numbers listed on the gradient graph.

4.6 GROUNDING MESHES

The most common means of gradient control in ground beds today is through the use of grounding meshes. The resistance of a ground mesh is given by:

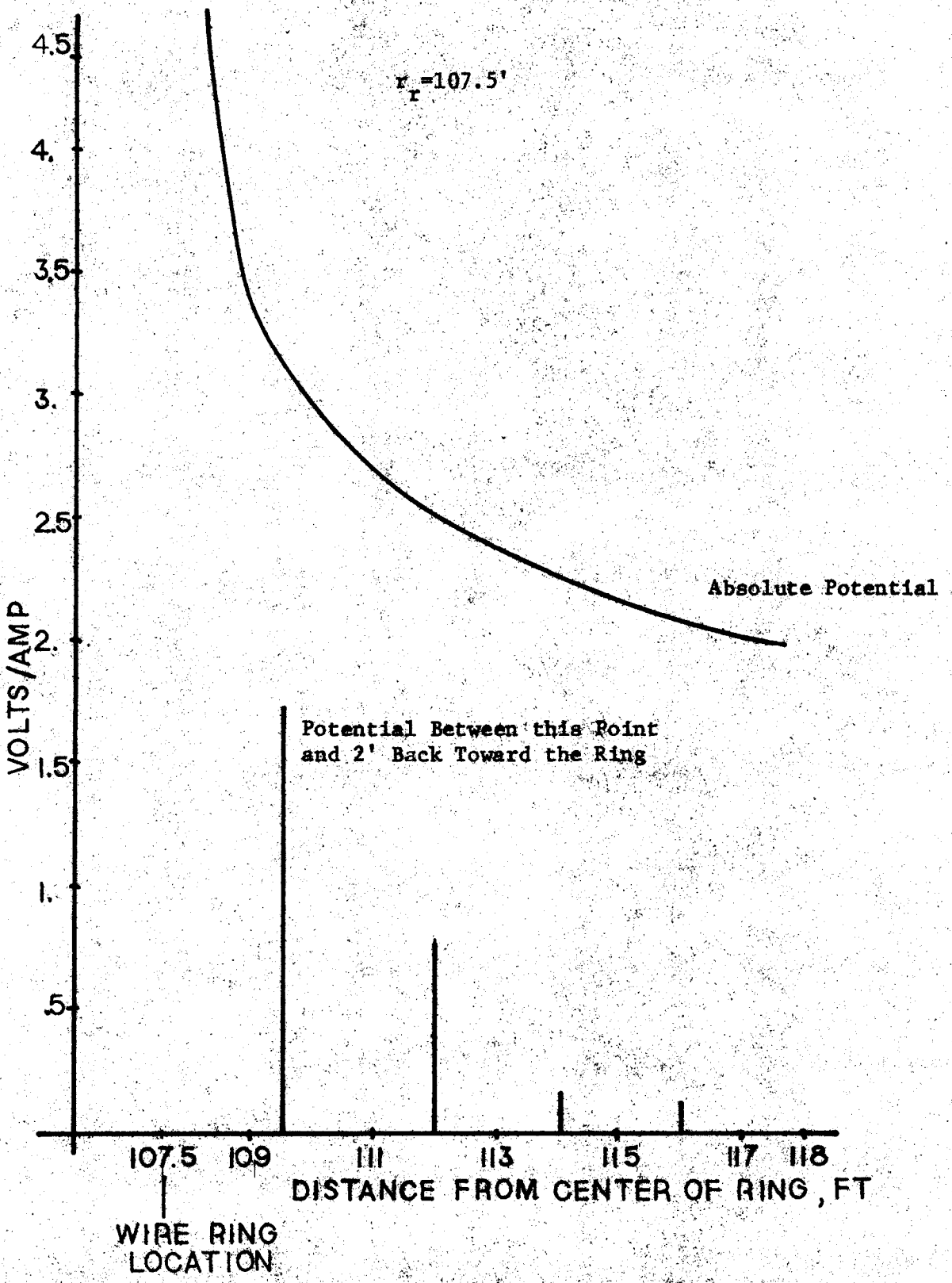

FIGURE 4.18. - Voltage per ampere of fault current at various points from no fill ring.

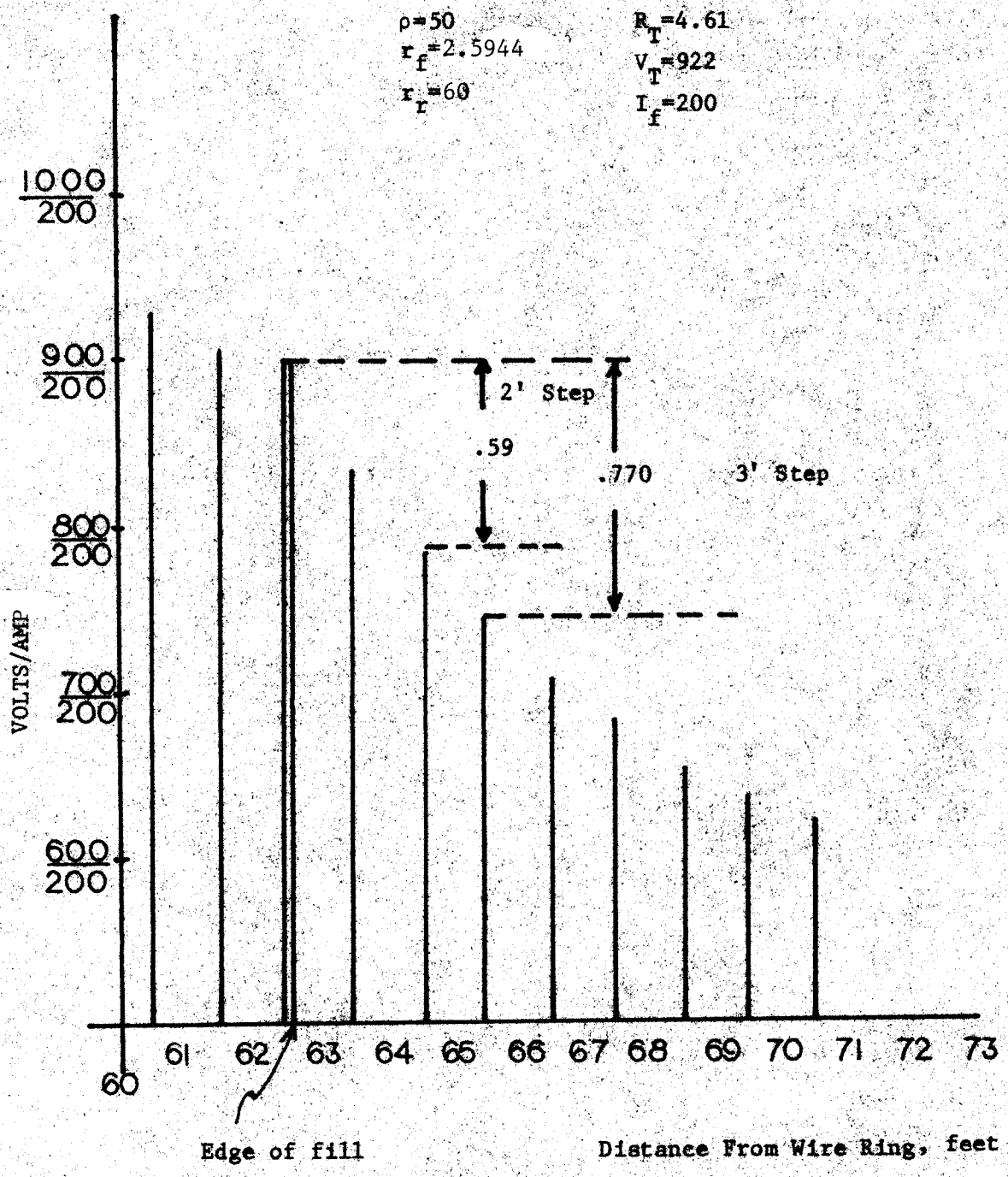

FIGURE 4.19. - Step potentials for the composite circular ring ground bed.

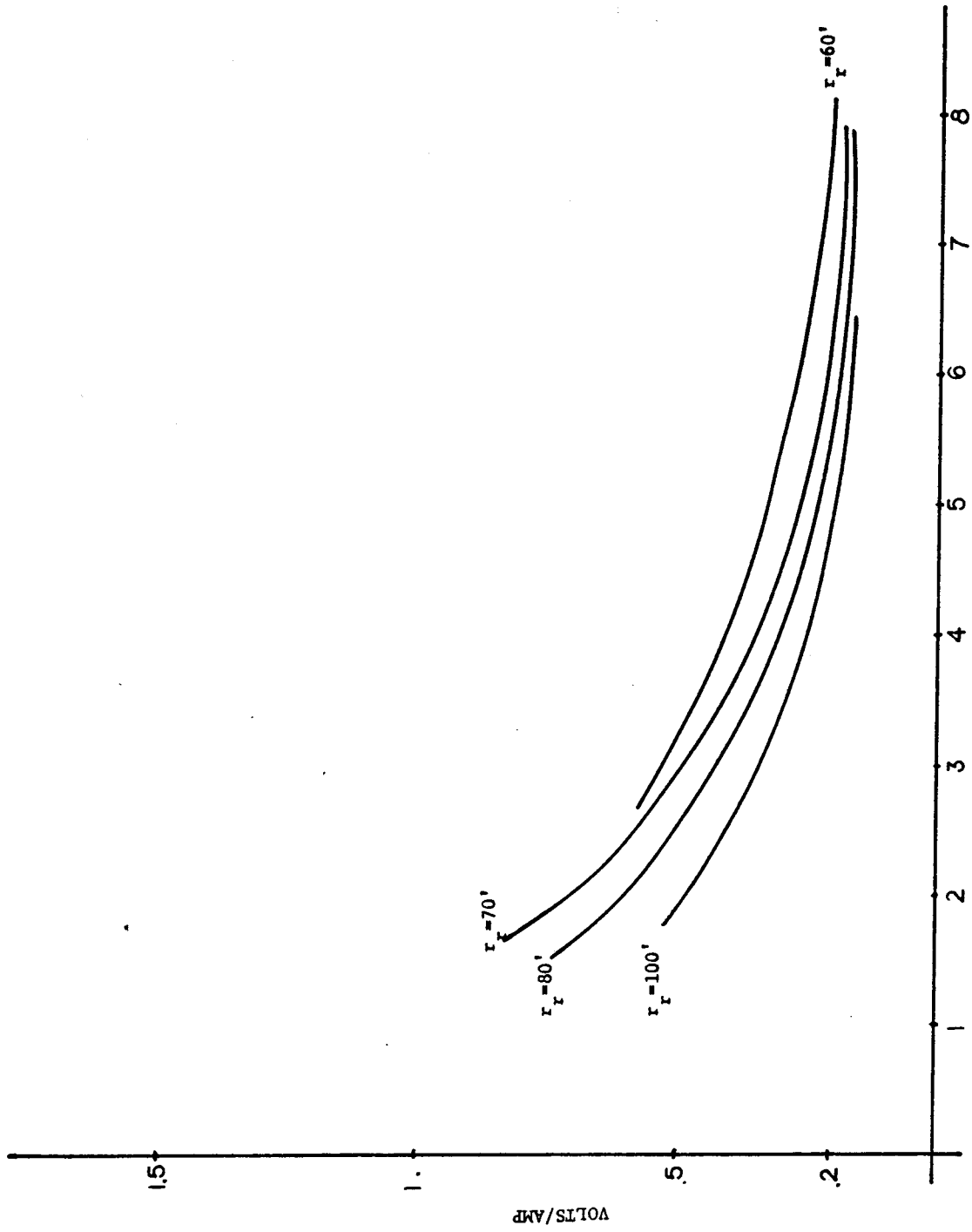

FIGURE 4.20. - Gradient over 2' from edge of fill as fill radius increases.

ρ= 1000 Ω-ft
rod length = 8'
rod radius .02'
81 rods
12.67' rod spacing

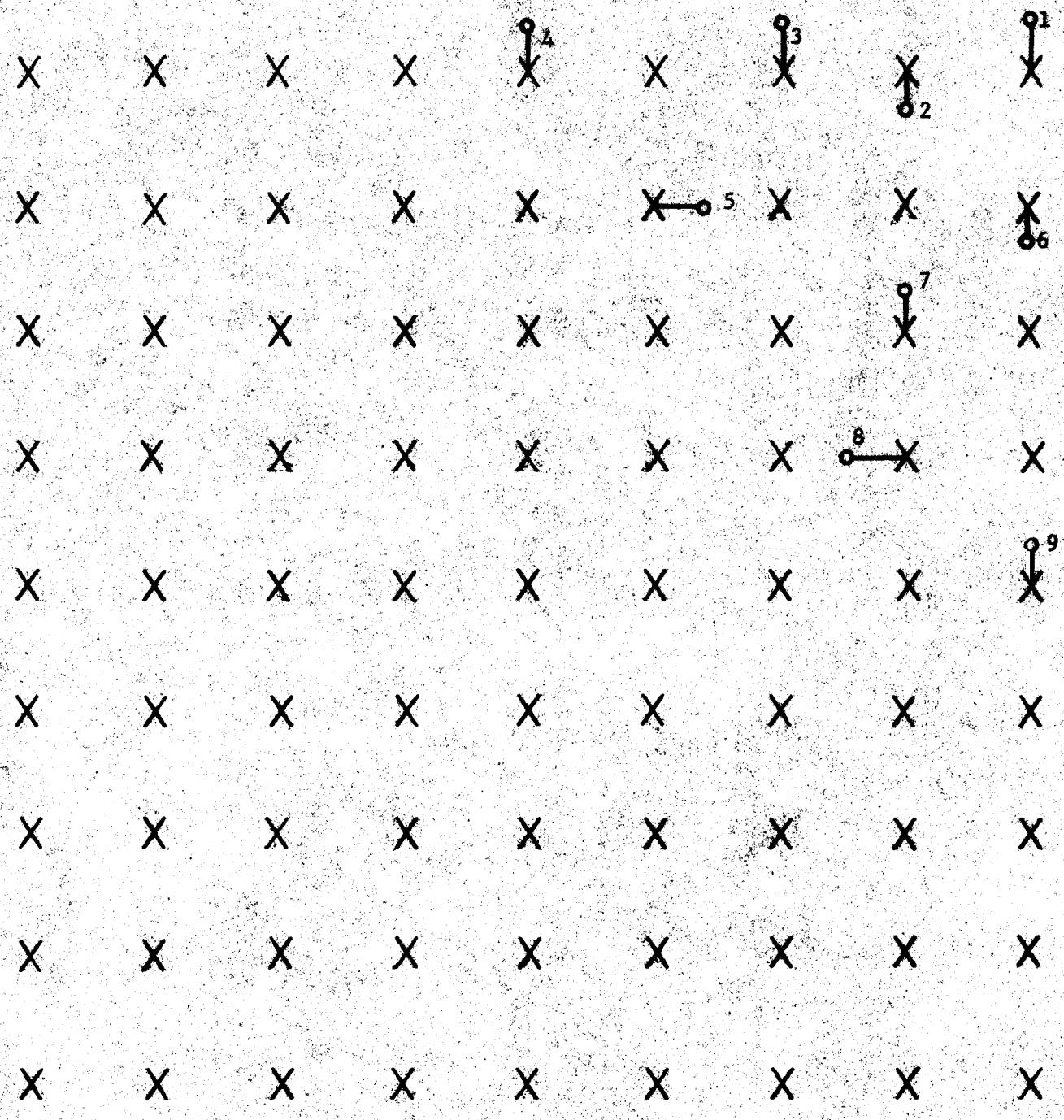

FIGURE 4.21. - Driven-rod ground bed.

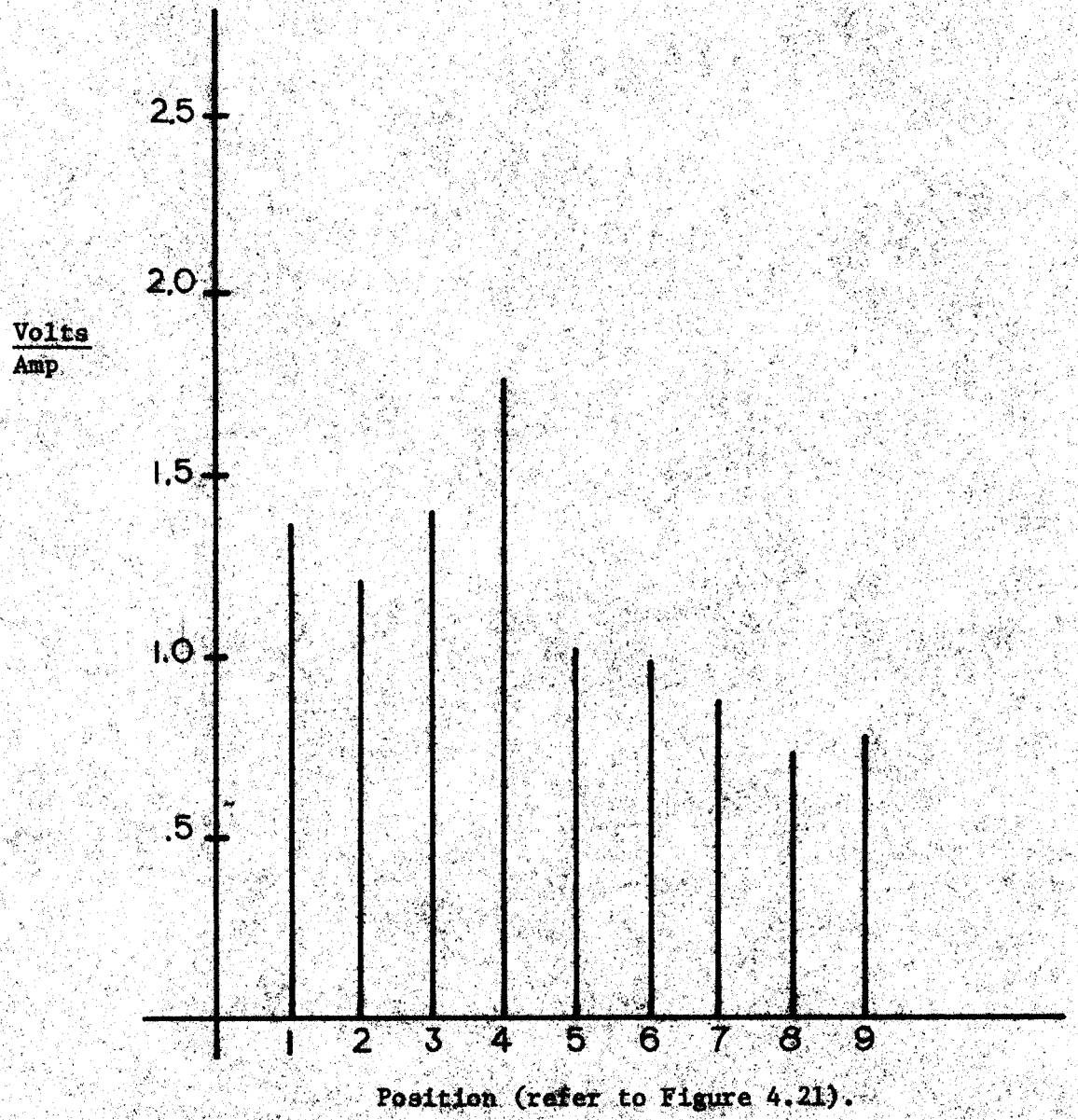

FIGURE 4.22. - Gradients for rod ground bed.

$$R = \frac{\rho}{\pi L}\left(\ln \frac{2L}{(2az)^{1/2}} + k_1 \frac{L}{(B)^{1/2}} - k_2\right), \quad [28]$$

where L = total length of buried conductor,

z = burial depth,

and B = area enclosed inside mesh perimeter.

The constants k_1 and k_2 depend upon the burial depth and the length-to-width ratio of the mesh. For a typical mesh where the length and width are similar and the burial depth is a few feet or less, $k_1 = 1.3$ and $k_2 = 6$.

Using equation 4.33 with z = 1' and a mesh as depicted in figure 4.23, the length x is found to be 103.5' for a 5-ohm ground bed. The spacing between adjacent wires is 25.9'. The total length of excavation is found to be 1035 feet. This again is much more than that required for the circular ring case, but it is comparable to that required for the driven rod case. However, to reduce the gradients of the mesh it is necessary to have the conductors closer together, and this entails an even greater cost.

4.7 CONCLUSIONS

A comparison of the circular ring composite ground bed, circular ring without fill, driven rod, and grounding mesh for 1000 ohm-foot soil can be seen in Table 4.1. By reviewing the table, it is noted that the composite circular ring ground bed requires more land than that required by the driven rod ground bed or the grounding mesh. This drawback, however, is offset by the fact that the composite circular ring ground bed can be constructed for a cost much less than that of the driven rod or grounding mesh.

TABLE 4.1 - Comparison of circular ring, composite circular ring, driven rod, and mesh ground beds

	Circular Ring	Composite Circular Ring	Driven Rod	Mesh	
Area required	46,225	14,440	10,404	10,712	
Cost in order	2	1	3	4	(Cheapest = 1)
gradients V/A	1.8	.77	1.78	Best	

The gradients associated with the composite ground bed area less than those associated with the driven rod. The grounding mesh, however, can be constructed so that its gradients are less than those of the composite ground bed. For many applications, ground faults occur so seldom and are so short-lived that the cost of construction would outweigh gradient considerations. For their type of application it would appear that a composite ground bed does have real-world applications.

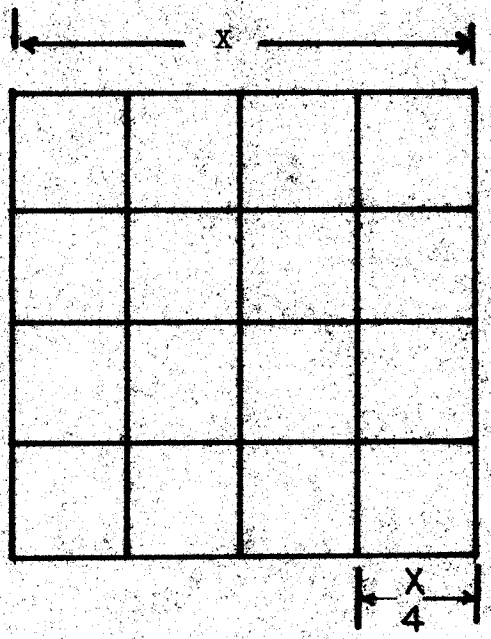

FIGURE 4.23. - Wire mesh ground bed.

For other applications, such as a substation ground, gradients are a very important consideration, and in most instances a combination of grounding mesh and driven rod ground bed is used. The addition of a grounding mesh to a driven rod ground bed can only reduce the resistance of the bed by about 15% [29] so that the size of the ground bed would not be significantly reduced. Therefore, the overall cost would be nearly the sum of the costs of each ground bed. Also, as discussed earlier, to lower the gradients associated with a mesh it may be necessary to have the conductors closer together then that given in the example. This would also entail a greater cost.

As mentioned in discussing the voltage gradients associated with the circular wire ring, lower gradients may be obtained by increasing the fill diameter (figure 4.20). If it is possible to obtain the fill at a reasonably low price, then a composite ground with acceptably low gradients could be constructed at a cost less than that of the driven rod and grounding mesh.

As a result of this investigation, the composite ground bed has been shown to have properties that are possibly suitable for use in safety ground beds and substation ground beds. To date, however, there have been no experimental results to verify the calculations set forth.

CHAPTER V

EVALUATION OF BOREHOLE SAFETY GROUND BEDS

5.1 INTRODUCTION

In arid regions of the far west, and even in the midwest, many mine operators have chosen to use boreholes as mine grounds. The hole is drilled deep enough to penetrate the coal seam, a large diameter bare conductor is threaded to the bottom, and the hole is backfilled to achieve contact between the conductor and the soil. Such grounds are quite popular for open pit mines, probably because they can be constructed relatively easily with available equipment and usually provide acceptably low resistance without using much real estate. The following analysis considers the effectiveness of a borehole as a safety ground bed. It considers also the desirability of having this borehole penetrate the coal seam.

5.2 RESISTANCE

Theoretically, there is no problem in obtaining 5 ohms or less with a borehole ground, even in soil of moderately high resistivity. For example, a 100-foot borehole casing should have a resistance under 5 ohms, even if soil resistivity exceeds 600 ohm-feet. This was borne out by the field measurements taken, where two different 75-foot boreholes had a resistance of 2 ohms or less, in soil of 180 ohm-feet resistivity.

Borehole grounds should more generally provide more stable resistance than more shallow ground beds, as the latter depend much more on the surface resistivity (which is subject to seasonal variation). The only foreseeable instance where a borehole ground might vary considerably with time is this: a borehole ground, driven far into the coal seam in an underground mine, would increase resistance considerably as the coal around the end of the borehole was taken.

The most simplistic analysis, assuming homogeneous earth, shows a slight advantage in having the borehole ground extend into the coal seam rather than terminate just above it. The increased length causes a decrease in resistance, as resistance is roughly inversely proportional to length; a 10% increase in length causes a 9% reduction in resistance. This alone hardly justifies having the coal-seam contact. However, a more practical model of the earth shows a much more significant difference. This is due to the anisotropic nature of earth conduction, the inhomogeneity of the earth resistivity, and the non-uniform distribution of leakage current along a cylindrical electrode such as the borehole casing. The consequences of these effects are, respectively, that current flows in horizontal directions more easily than in the vertical direction, that resistivity generally decreases with depth (over distances compatable to borehole lengths), and that the resistivity of lower layers is weighted more heavily in the resistance determination. Cumulatively, these three factors can make a much larger reduction in ground bed resistance than the 9% predicted for a 10% length increase.

The most extreme case is that of a borehole ground installed over a gobbed-out section of coal, with a basement resistivity an order of magnitude lower than the overburden resistivity. A borehole ground which extends into

the basement could have a resistance an order of magnitude lower than one which does not penetrate the mined-out area. Extensive voids between the coal seam and overburden would have much the same effect; a borehole ground not penetrating the coal seam could have 3-5 times the resistance of one that did penetrate.

Even if the resistance is satisfactory, a borehole ground is likely to have a significantly higher surge impedance than a driven-rod bed with the same resistance. When a lightning impulse impinges on a ground electrode, for instance, it has such a steep wavefront that the bed's reactive characteristics are often more important than its resistance. A long, thin earth electrode has a higher surge impedance than a distributed matrix of electrodes, and hence may develop much higher voltage in spite of having the same resistance. On the other hand, fields around earth electrodes become so high during lightning surges that the adjacent earth breaks down, significantly lowering the resistance.

Table 5-1 shows several theoretically calculated values of maximum surge impedance and dc resistance of boreholes in uniform soil. The analysis is quite complex, but can be found in the work of Erling D. Sunde [30]. The expression for the surge impedance of a borehole is approximately:

$$s(t) = \frac{(2\nu/K)^{1/2}}{4\Pi} e^{-\alpha v t} \{[1+ \frac{(\alpha v t)^2}{2} + \frac{1}{2} (\frac{\alpha y}{2})^2] [31]$$

$$\log \frac{tv + (t^2v^2 + y^2)^{1/2}}{y} - \frac{1}{2} (\frac{\alpha v t}{2})^2 (1+y^2/t^2v^2)^{1/2} \} \qquad (5.1)$$

where $\alpha = (2\nu/K)^{1/2} /4\rho$

y = radius of conductor

ρ = earth resistivity

K = capacitivity of earth

ν = inductivity of earth

v = velocity of propagation = $(2/\nu K)^{1/2}$ meters/sec.

The maximum value of the surge impedance varies approximately with the square root of resistivity, whereas resistance is directly proportional to resistivity.

TABLE 5.1. - Surge Impedance and Resistance of Borehole Grounds

radius = 5 mm, length = 50 m

Resistivity (Ωm)	Surge Impedance (max.) (Ω)	Resistance (Ω)
1000	82	32
300	45	9.5
100	26	3.2
30	14	1.0

This is a consequence of transient voltages decaying more rapidly in lower-resistivity soil. As a result, there is a greater disparity between surge impedance and resistance for low resistivity earth. It should be noted that this analysis does not include the effects of soil ionization; at high currents, the disparity will be even greater than that shown in Table 5.1.

5.3 MUTUAL RESISTANCE

Another significant difference between rod-bed grounds and borehole grounds may be the degree of coupling to the substation ground mat. Coupling is undesirable because it causes any potential which appears on the substation ground (due to lightning or a primary fault) to be partially transferred to the frames of the safety grounded equipment. Since borehole grounds are very different in shape from rod-bed grounds, it was expected that the coupling would be very different also. The amount of coupling is measured as the "mutual resistance", the voltage that appears on one bed due to a flow of current into the earth at the other.

The analysis of mutual resistance is similar to that for borehole ground bed resistance, in that simplistic analysis shows a slight advantage in having the borehole contact the coal seam, whereas a more detailed analysis reveals more substantial benefits. An important difference between (self-) resistances and mutual resistance evaluations is that a high mutual resistance is desirable whereas a low self resistance is sought.

An important distinction between surface and underground mines must be made. The mutual resistance between a borehole ground and the work area can be quite high for an underground mine, approaching the theoretical upper limit of the ground bed resistance. This is provided that the borehole ground extends into the coal seam, and even into the basement if the mine is at all developed. (This is in contrast to a nearly zero mutual resistance for shallow ground beds). For surface mines, the mutual resistance of a borehole ground with the work area into the coal seam may be an order of magnitude higher than the mutual resistance of other ground beds provided the ground bed extends into the basement if either the coal under the borehole has been mined extensively or if personnel to be protected are in contact with the exposed underburden.

Theory predicts, therefore, that a borehole ground will have a lower mutual resistance with nearby metallic structures than rod beds with the same

total resistance. Field measurements were made on two adjacent boreholes, each 75 feet long, separated by 83 feet. With the measured soil resistivity of 125 ohm-feet, theory predicts a mutual resistance between the two to be 0.26 ohms. The measured mutual resistance was 0.24 Ω, which is in excellent agreement. Two rod beds in the same location would have a mutual resistance of approximately 0.33 ohms. The rod beds would be much worse at shorter spacings (0.48 ohms for the borehole vs. 0.80 ohms for rod bed at the 25-foot regulatory minimum spacing).

5.3.1 Potential Difference within Earth Near Grounded Equipment

Under the most unfavorable circumstances, a safety ground bed can actually be the source of dangerous potentials for equipment connected to it. This is possible when the earth near the ground bed is at a significantly different potential than earth near the grounded equipment due to a high resistance path through the earth from the ground bed to the grounded equipment. This effect has been more difficult to analyze, but is very important to the behavior of borehole grounds in stratified earth: the anistropic resistivity of coal and coal-bearing strata. For flat-lying seams, conduction is facilitated in horizontal planes much more so than in vertical ones. Particularly in the presence of highly resistive layers of rock, or voids between layers, the mutual resistance between a shallow surface rod bed high above the coal and the coal seam may be much higher than predicted by homogeneous-earth theory.

This hazard produced by a low mutual resistance between the safety ground bed and the floor of the mine is prevented in an underground mine by having a borehole ground which extends near the location of underground equipment.

In surface mining, some of the same type of protection is achieved by having the borehole casing extend into the coal seam. Current flows through coal and coal-bearing strata in a highly anisotropic manner, with conduction in horizontal direction being easier than in the vertical direction for flat-lying strata. The theoretical prediction was confirmed by actual measurements on coal seams and nearby strata; the ratio in conductivity between the vertical direction and horizontal direction was 21.6 to 1. This enormous difference is attributable to the layered structure of coal and voids between strata.

For the borehole ground to fulfill its promise of minimal potential difference between it and the earth near grounded equipment, there must be an essentially horizontal path for current to flow between the end of the borehole casing and the equipment. Otherwise, if current must travel vertically, there is much greater probability that potential gradients will exist. The common practice of drilling the borehole into the coal seam does tend to accomplish the horizontal current flow. However, it would appear that an even higher degree of safety could be obtained by extending the borehole ground into the underburden beneath the coal. In such a case, a borehole ground would produce a much lower mutual resistance with the coal than a rod bed.

5.4 FIELD MEASUREMENTS

Extensive field measurements were made to confirm the theoretical analysis. The self-resistance calculations could be confirmed directly, whereas the mutual resistance calculations generally could not be. (An exception is the underground mutual resistance which is easily confirmed). Indirect evidence was collected which does appear to support the theoretical mutual resistance calculations for surface mines, but the large distances separating ground bed and equipment prevented any direct measurement. The data that was gathered generally supported the theoretical work undertaken.

CHAPTER VI

MINE SUBSTATION AND BONDING SHORT COURSE

6.1 INTRODUCTION

A short course was developed around the document entitled "Guide to Substation Grounding and Bonding for Coal-Mine Power Systems" which was submitted as part of the final report on Bureau of Mines Grant G0188087 to West Virginia University. This document was revised slightly by Roger L. King and published as a Bureau of Mines Information Ciruclar IC 8835, "Guide to Substation Grounding and Bonding for Mine Power Systems." It became available about October 1, 1980, and was used as the text for a Bureau of Mines Technology Transfer Workshop on Mine Substation Grounding and Bonding held four times at the Bruceton Research Center (Oct. 7, 8, 9, 10).

6.2 RUBBER SHEET ANALOG

The workshop was carried out as a series of illustrated lectures and demonstrations on a rubber sheet analog. Two rubber sheet analogs were fabricated for this purpose. These were constructed by rolling a 4-ft diameter "embroidery hoop" from light-weight steel channel. The open side of the channel faces outward so that a rubber sheet can be stretched over the edge of the hoop and held in place by a taut band of surgical rubber tubing placed in the open channel. Once the sheet has been supported on the hoop, it can be deformed by pushing or pulling it. Its deflection is analogous to the voltage profile which appears on the surface of the earth near a current-carrying earth electrode. The force required to cause the deflection is analogous to the magnitude of current flow. Many photographs were taken of this sheet to illustrate touch potentials, step potentials, 29° rule, effects of grid spacing, perimeter wires, potential ramps, ground-to-ground potentials, and other concepts being discussed in the lectures. These slides were used to illustrate the lectures. The rubber sheets were also used for live demonstrations during the class discussions.

6.3 FIELD PHOTOGRAPHS

Hundreds of photographs were taken of actual mine power system installations. A group of these was chosen to illustrate various aspects of electrical practice, both good and bad. These were used as a major component of the illustrated lectures.

6.4 OTHER AIDS

An electrolytic tank was constructed to provide a capability for making actual potential measurements on models of mine substation ground grids. The tank proved to be too bulky to transport to the site of the workshop, but photographs were taken to show its operation, and a field map that was generated using the tank was shown at the workshop. Instrumentation mentioned in the lecture was on display, as well as numerous publications related to the subject.

6.5 WORKSHOP SCHEDULE AND INSTRUCTOR

Three instructors shared the teaching duties at the workshop. They were

Roger L. King, Supervisory Electrical Engineer, Pittsburgh Research Center; Wils L. Cooley, Professor of Electrical Engineering, West Virginia University; and Herman W. Hill, Jr., Assistant Professor of Electrical Engineering, West Virginia University. Table 6.1 shows the schedule for the one-day workshop.

TABLE 6.1 - Workshop schedule and instructor

8:45 - 9:00	Opening Remarks
9:00 - 9:10	Separate Grounds Wils L. Cooley
9:10 - 10:00	Substation Ground Mat Wils L. Cooley
10:00 - 10:20	Surge Arresters Roger L. King
10:20 - 10:40	Break
10:40 - 11:00	Grounding Distribution Systems Arresters Roger L. King
11:00 - 12:00	Safety Ground Bed Herman W. Hill
PM 12:00 - 1:20	Lunch
1:20 - 2:15	Wiring of Ground Systems Roger L. King
2:15 - 2:30	Grounding the Borehole Casing Herman W. Hill
2:30 - 2:50	Break
2:50 - 3:25	Ground Check Monitoring Wils L. Cooley
3:25 - 3:40	Ground Bed Monitoring Wils L. Cooley
3:40 - 4:00	Wrap-up

6.6 Results

Course enrollment was limited to approximately 30 persons per day in order to maintain an atmosphere of open interchange with the audience. So many requests were received that the schedule was expanded from the original three days to four days, and it was still necessary to turn some persons away. Table 6.2 lists the attendees at the course. The persons represented a broad spectrum of the industry.

TABLE 6.2 - Attendees at Technology Transfer Workshop on Mine Substation Grounding and Bonding

TUESDAY - OCTOBER 7, 1980

1. Donald J. Beck - Hecla Mining Co.
2. Gary B. Rackliffe - Westinghouse Electric Corp.
3. C. R. McWilliams - West Virginia Inst. Tech.
4. E. M. desRochers, Jr. - United States Gypsum Company
5. David E. Murphy - Nemacolin Mines Corp.
6. Donald L. Sapp - Nemacolin Mine Corp., J & L Steel
7. Charles B. Vance - MSHA, Dept. Labor
8. Charles Odle - Olga Coal, J & L Steel
9. Victor L. Kitts - United States Steel Corp.
10. James L. Cotter, Jr. - Cotter Assoc.
11. Harry M. Thompson - U. S. Steel
12. Tod R. Stevens - Consolidation Coal Company
13. James Wood - White Pine Copper Div., Copper Range Co.
14. Daniel M. Clonch - W. Va. Institute of Technology
15. Richard L. Duncan - MSHA M/NM
16. John P. Halaburda - Dept. of Labor, Mine Safety and Health Administration
17. James R. Legro - Westinghouse Electric Corporation - AST
18. Robert C. Blanc - International Salt Co.
19. James S. Szczesniak - International Salt Co.
20. Bruce S. Tenney - West Virginia University
21. Adam Fishel - Field Service of Air Moving Equipment
22. David J. Podobinski - Consolidation Coal Co., Lee Engr. Div.
23. Donald G. Davies - Westinghouse Electric Corp.
24. Scott Ferg - Jones & Laughlin Steel (Vesta #5 Mine)
25. David M. Fortney - MSHA
26. Lemoyne M. Morris - MSHA
27. James A. Goble - The Ohio Brass Company
28. John R. Zamiela - Ohio Brass Co., Rectifier Div.
29. Victor H. Patterson - MSHA
30. Joseph M. Forte - Bethlehem Mines Corp.
31. Van Ivander Geest - Amax Company

WEDNESDAY - OCTOBER 8, 1980

1. Roger Sturgeon - Kerr-McGee Corp.
2. Paul Vancura - Bethlehem Mines Corp.
3. John A. Vandertoolen - Kennecott Minerals Corporation
4. Lloyd L. Seckman - Arch Mineral
5. Roy E. Jones - MSHA
6. Jesus Paniagua - Bethlehem Mines Corp.
7. Terry W. Bender - Bethlehem Mines Corp., Cambria Division
8. Don Perryman - Southwestern Ill. Coal Co. (Captain Mine)

TABLE 6-1 (continued)
Page 2

9. Mel Jarvis - Compton Electrical Equipment Corp.
10. Michael Anderson - PA Dept. of Environmental Resources
11. Charles Fenchok - PA Dept. of Environmental Resources
12. Harden Williams - Climax Molybdenum Co.
13. Steven F. Gaida - Bureau of Deep Mine Safety D.E.R.
14. K. L. Adams - Arch Mineral Corp.
15. Victor S. Kutay - Consol Coal
16. Neil Dorian - Consol Coal - Eastern Region
17. Raymond H. Holmes - Drummond Coal Co.
18. Robert E. Fleissher - U. S. Steel
19. Ron Flora - Barnes & Tucker
20. David Troutman - Carpentertown Coal & Coke
21. Ralph J. Long - Cemsco Inc.
22. George Crissman - Canterbury Coal Co.
23. Vernon Demich - Canterbury Coal Co.
24. W. B. Hopkins - Iron Ore Co. of Canada
25. Bob Brawley - Iron Ore Co. of Canada
26. Calvin H. Furfari - Westinghouse Electric Corp.
27. Gerald E. Brosius - Dept. Environmental Resources
28. Bruce H. Jones - MSHA
29. John Sheppard - Iron Ore Company of Canada
30. Richard Wood - Consolidation Coal Co.
31. Edward C. Cantwell - ECOS Electronics Corp.
32. John Peton - Penn State Univ. - Cont. Ed. - Univ. Park, PA

THURSDAY - OCTOBER 9, 1980

1. Jim Minor - Peabody Coal Company
2. Bart Bullock - Peabody Coal Co.
3. Dave Tennant - Eastern Coal
4. Kenneth A. Soroul - MSHA - Approval & Certification Center
5. Arup K. Mallik - West Virginia University
6. Paul S. Keroskin - J & L Steel Corp., Vesta #5 Mine
7. Jack Barli - J & L Steel
8. Daniel Lincaski - J & L Steel
9. Barbara Good - MSHA
10. Richard D. Carey - USDOL MSHA Metal & Non-Metal
11. Joe Uraco - MSHA, Approval & Certification Center
12. Bud Howard - West Virginia Elect. Corp.
13. Ward Tull - Stauffer Chem. Co. of Wyoming
14. E. C. Wade - Westinghouse Electric Corp.
15. Harry Buetz - Capitol Cement
16. Willis E. Cupp - MSHA Dept. of Labor
17. Wayne L. Carey - U. S. Dept. of Labor, Approval and Certification Center
18. Frank Peduti - Eastern Assoc. Coal Corp.
19. Kenneth P. Katen - Diamond Shamrock Coal Unit
20. Robert E. Conaway - Eastern Associated Coal Corp.
21. A. P. Barcellino - MSHA - Approval & Certification Center
22. John A. Evans - Amherst Coal Co.
23. M. D. Spencer - Armco Inc.

TABLE 6-1 (continued)
Page 3

24. Robert W. Hall - Westinghouse Engr. Service
25. William W. Kurczak - EMC Corp. Material Handling Systems Div.
26. William Rogers - West Virginia Electric Corp.
27. Ronald K. Pepper - Kerr-McGee Coal Corp.
28. Roger L. Hess - Consol Coal Co.
29. Zaglol Elrazaz - West Virginia University

FRIDAY - OCTOBER 10, 1980

1. George F. Stencer - Atlas Minerals - Mining Division
2. Charles Dickens - Rand Lake College
3. John W. Yates - Brown Elec. Equipment
4. W. R. Whitlatch - North American Coal Corp.
5. Kenneth L. Ellis, Jr. - Anker Mining & Development Company, Inc.
6. Terry G. Mullins - Westmoreland Coal Co.
7. Reginald O'Neal - Westmoreland Coal Co.
8. Tom Kohler - USBM
9. David J. Vaglia - Eastern Associated Coal Corp.
10. Larry Pechart - Florence Mining Co.
11. Charles W. Maus - Mine Safety Appliances
12. Martin H. Wahl - Mine Safety/Advanced Systems
13. Charles C. Dobbins - Helen Mining Co.
14. Basil Paschaledis - Salvucci Engineers Inc.
15. Robert B. Palmer, Jr. - Mountain Empire Community College
16. Gary Carroll - Westmoreland Coal Co.
17. David R. Rinehart - Westmoreland Coal Co.
18. Edward S. Gruca, Jr. - The North American Coal Co., Eastern Division
19. Philip Jaworski - North American Coal
20. Arne Larsen - Dravo Corp.
21. Edward L. Lehosky - Penn Allegh Coal Co.
22. Michael J. Corso - Salvucci Engrs. Inc.
23. Kenneth J. Stuthers - Salvucci Engineers Inc.
24. Gary W. Kiser - Mountain Empire Community College
25. Gary W. Ball - Westmoreland Coal Co.
26. Larry Ashby - Amax Coal
27. Joe Bedway - MSHA - A & CC

Attendees were asked to return a questionnaire concerning the usefulness of the course. Table 6.3 shows the results of some of the questions. It can be concluded that the course was very well received.

TABLE 6.3 - Course Survey Results
(118 respondents)

1. Did you find this workshop of value?
   Yes - 118 No - 0 No reply - 0

2. Was it of practical value to your company?
   Yes - 109 No - 5 No reply - 4

3. Were the work sheets (the text) useful?
   Yes - 98 NO - 4 No reply - 16

6.7 FUTURE PRESENTATIONS

MSHA requested that the workshop be condensed to two hours and be presented at the Mine Health and Safety Academy in Beckley, WV. This presentation was scheduled to be given to ten groups of mine electrical inspectors undergoing annual retraining. Because of the heavy time commitment required on the part of the course staff to conduct so many classes, it was proposed that a video tape be made. This was accomplished on Oct. 21, with Dr. Cooley delivering both hours of lecture for the condensed presentation.

CHAPTER 7

DIODE TESTING

7.1 INTRODUCTION

Several mining companies are using 2-conductor trailing cables for dc machinery. A diode must be used to partially isolate the machine frame from the ground-return wire. A discussion of this grounding method relative to other grounding methods is given in Chapter 3 of this report.

In order to be effective, the diode must remain in operating condition. Thus, it is required that the diode be tested on a periodic basis. There has been considerable difficulty encountered in this process. Some of the tests that are used generate safety problems under some conditions; others may damage the diode in the process of the test. In general, the test process is time-consuming and difficult. Testing methods will be discussed in this chapter and it will conclude with a proposed method of completely testing the diode automatically and safely.

7.2 THE GROUNDING DIODE CIRCUIT

A simplified circuit diagram of a dc shuttle car is shown in figure 7.1. This diagram is for a 250 V negative-grounded system. During normal operation, a dc voltage drop in the negative return would present a reverse bias on the diode which isolates the frame of the machine from the negative return. A person touching the machine frame would not be subjected to voltage or current.

A fault of the positive conductor to the machine frame will forward bias the diode and the frame will be connected to the negative return. A relay coil in series with the diode will then open a contactor in series with the positive conductor and shut the machine down.

If the diode fails open, it would not be noticed under normal conditions. A positive conductor to machine frame fault would, however, place the positive potential on the machine frame. This is a completely unacceptable situation. Fortunately, very few open diodes have ever been found, but enough have been found that the situation must be considered when testing.

A shorted diode presents another problem. The machine frame is effectively connected to the negative return. Thus, any voltage appearing on the negative wire also appears on the frame. Anyone touching the frame would then feel some shock as the machine is operated. This situation is the same as a short from the machine frame to the negative conductor except that the ground relay will still operate with a shorted diode in the event of a positive conductor to machine frame fault.

A diode is considered to fail short if the reverse leakage current exceeds some threshold value. A typical threshold value is 15 mA, although no specific value is required.

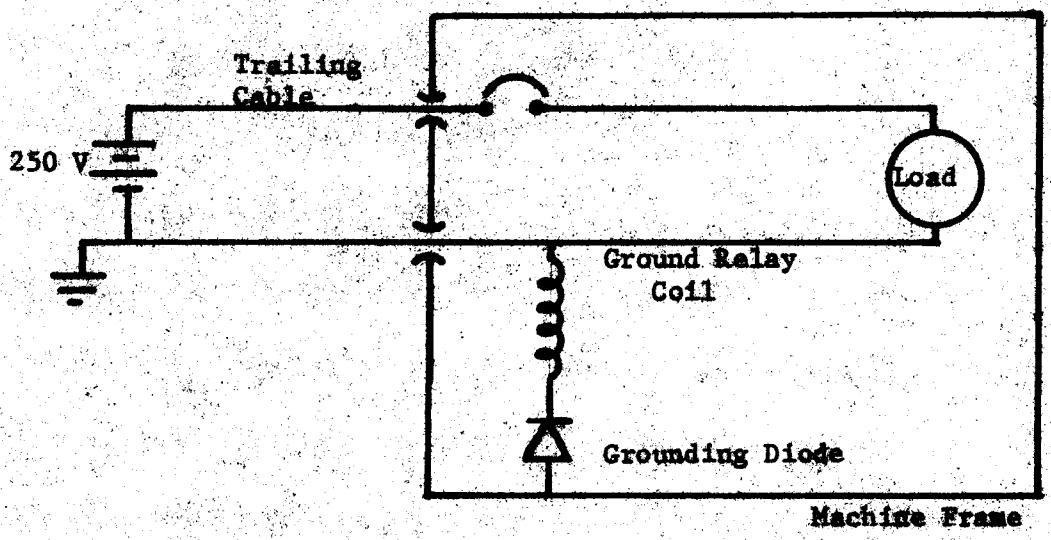

FIGURE 7.1. - Simplified circuit diagram of a DC shuttle car.

A particular problem is a short of the positive conductor to the machine frame out by the contactor. This usually occurs on the cable reel. In this case, the contactor will not remove the fault. The diode must carry the fault current which may or may not be interrupted at the power center. As a result, some voltage may appear on the machine frame due to the voltage drop in the negative conductor for the duration of the fault.

Because a short from the positive conductor to the frame on the source side of the contactor, such as on the cable reel, cannot be opened by the contactor, the diode must be able to withstand continuous short circuit current. This current is limited only by the conductor impedance, the fault impedance, and the short circuit protection at the source. Such a large diode is quite rugged and would seem unlikely to fail. However, a fairly large number of failures has been observed.

As shown in Chapter 3, the reverse voltage appearing on the diode can be several hundred volts. Thus it is important to choose a diode with a high reverse voltage rating. A reverse breakdown will often destroy the diode.

7.3 TESTING THE DIODE

The diode can be simply tested by passing a current through it in the forward direction and checking that the diode does not pass current in the reverse direction. These tests can be performed in a number of ways. In general, the current is measured when both forward and reverse voltages are applied.

A typical forward conduction test is shown in figure 7.2. A resistor is connected between the positive conductor and the frame. If the diode conducts, the machine frame will rise only a few tenths of a volt above the negative return conductor. If the diode is open, the machine frame voltage will rise to the positive supply. Thus, this test could be dangerous and the machine frame voltage should be measured. The diode current can be increased until the ground relay trips at the contactor. In some cases, this latter procedure is used without monitoring the frame voltage. This method cannot discriminate between an open diode and a frame to negative wire short. A voltage measurement would improve the diagnostic value and greatly improve the safety of the test. In some cases, the diode current has not been sufficiently limited and the diode has been damaged.

Several reverse leakage tests are in use. In one case, shown in figure 7.3, the supply voltage to the machine is reversed. A resistance is connected between the frame and negative wire and the voltage across the resistance is measured. Ohms Law then tells the value of the leakage current. If the internal resistance of the meter is in the proper range, it may be used in place of the external resistor. A shorted diode or a short between the frame and positive conductor will place the supply voltage on the machine frame. Again, extreme caution must be used. This test cannot distinguish between a shorted diode and a fault.

Another reverse leakage test utilizes a Hall-effect current sensor to measure diode leakage current, as shown in figure 7.4. The induced voltage

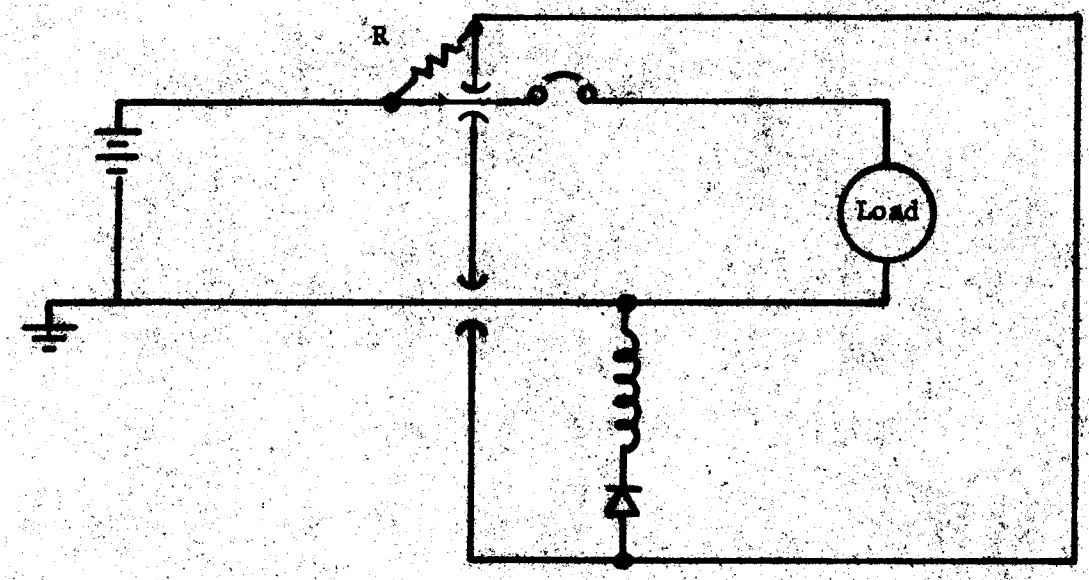

FIGURE 7.2. - Forward conduction test.

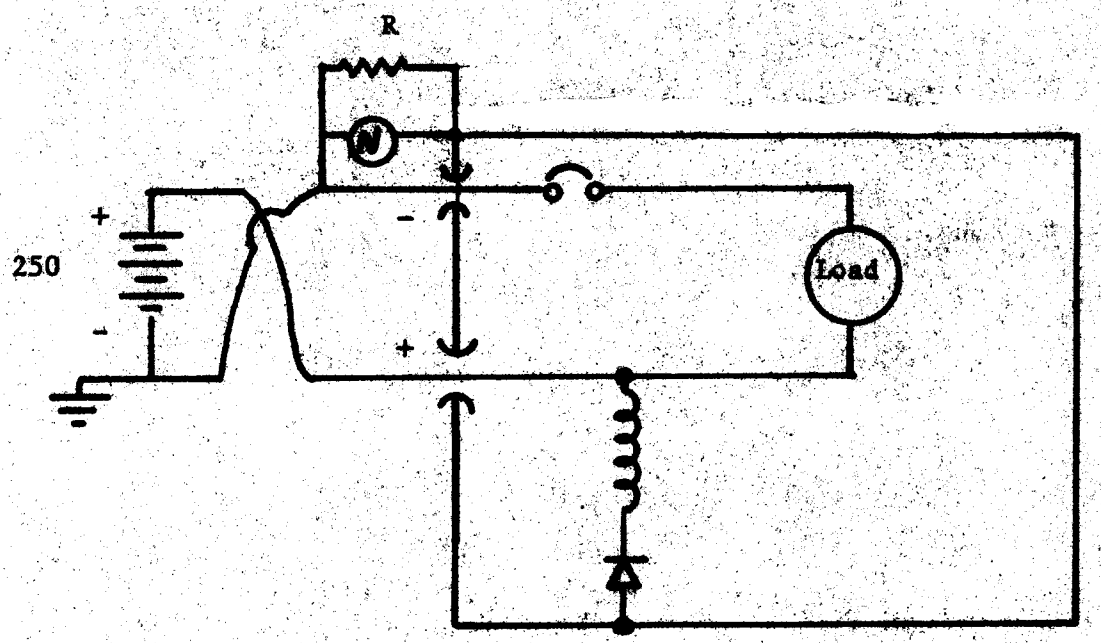

FIGURE 7.3. - A reverse voltage test for diode reverse leakage.

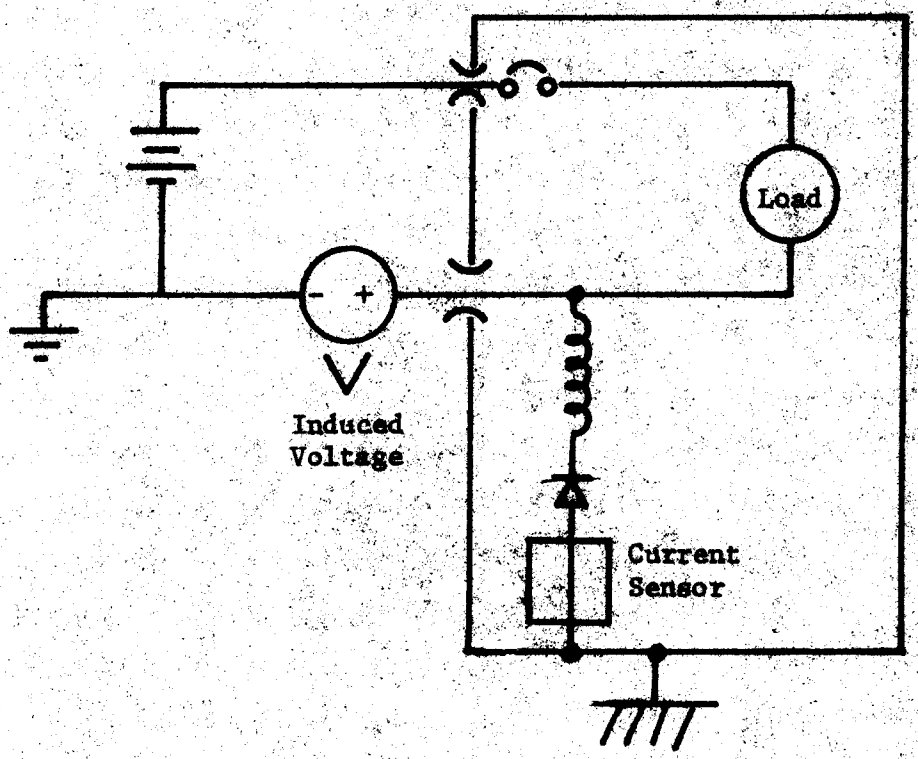

FIGURE 7.4. – A reverse leakage test utilizing the induced voltage in the negative return conductor.

in the negative return conductor supplies the reverse potential across the diode. The machine frame must be grounded in order for this test to work. Prototype models of this system were built by Bendix [32].

Another method of testing diodes has been used in a forward and reverse ohmmeter test. The diodes must be removed from service for this test. This procedure is almost fool-proof but is very time-consuming. Hence, this test is not popular.

For a complete test, a combination of the above tests may be made. It is necessary to check diode forward conduction and reverse leakage, and it is also a good idea to make sure that the ground relay trips out the contactor.

7.4 TEST CIRCUITS

Two circuits have been built in the WVU Laboratories to test reverse leakage of the diodes. Both use the Hall-effect sensor to measure the current and both rely on the voltage drop in the trailing cable to provide the reverse voltage across the diode. The circuits are shown in figures 7.5 a and b. The voltage output of Hall-effect sensor is 0.1 V/mA up to 50 mA. In the circuit of figure 7.5a), the current threshold is set by the double base-emitter turn-on voltages of the Darlington pair. This threshold is between 10 and 15 mA (1.0-1.5 V).

In circuit 7.5b), a voltage comparator allows an adjustable threshold, which is determined by the setting of the potentiometer. Otherwise, the two circuits are identical in operation.

If the leakage current exceeds the threshold value the SCR is turned on which in turn closes a relay which removes power to the control circuit and turns on a light to indicate the cause of the shutdown. The circuit must be reset to restore normal operation.

The diode forward conduction and ground relay are to be tested by connecting a resistor between the positive conductor and the machine frame as discussed in the previous section. It should be noted that there is no way of distinguishing between a good diode and an open diode with the above tests. Therefore, extreme caution should be used when making the forward conduction tests.

7.5 IMPROVED TESTS

The tests described earlier are not completely satisfactory. The reverse leakage tests rely upon a chance coincidence of a grounded frame and a voltage drop in the negative conductor, while the forward conduction test is potentially hazardous and could result in injury.

The problems and shortcomings of these tests arise from the fact that controlled sources are not used. If limited voltages and currents are applied on demand, these limitations can be overcome. Because of the possibility of hazardous potentials on the machine frame, it is a good idea to limit the voltage available at least until it is determined that the hazardous potentials will not exist. One method of doing this is to use a voltage divider network

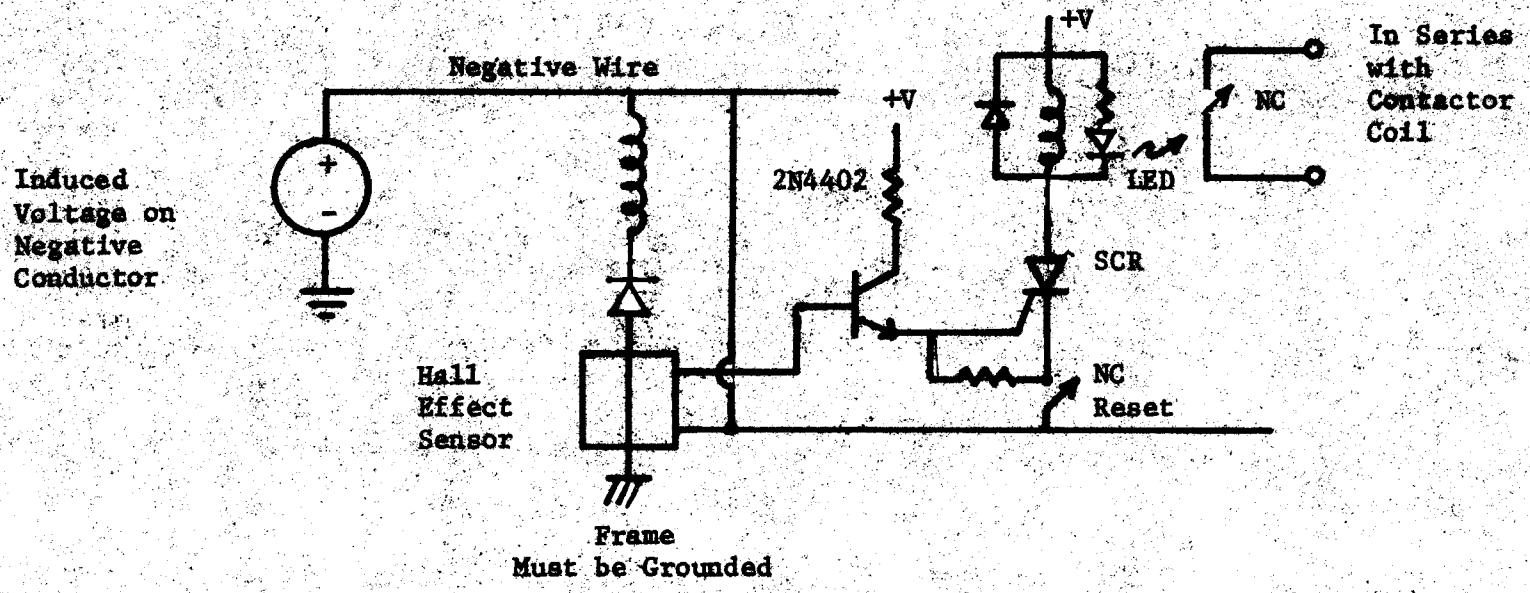

FIGURE 3.5a. - Reverse leakage tester with fixed threshold.

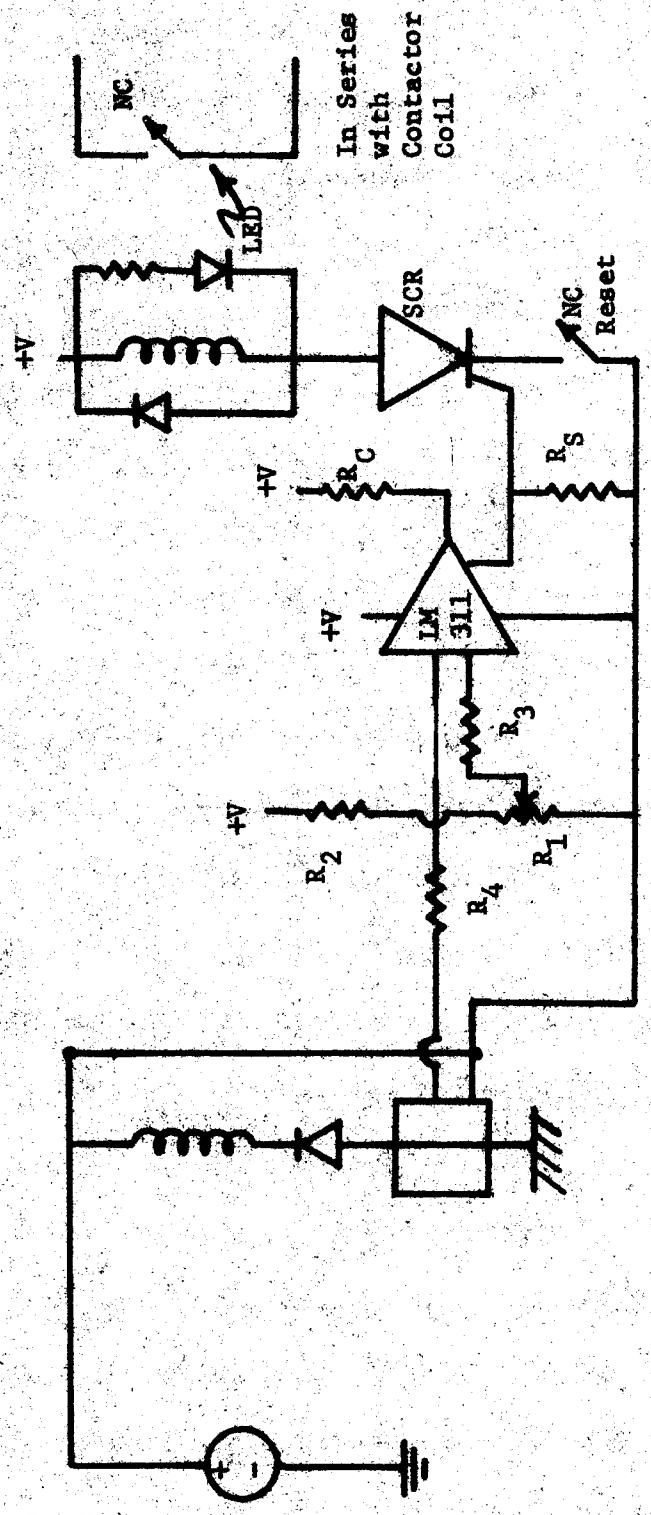

FIGURE 7.5b. - Reverse leakage tester with adjustable threshold.

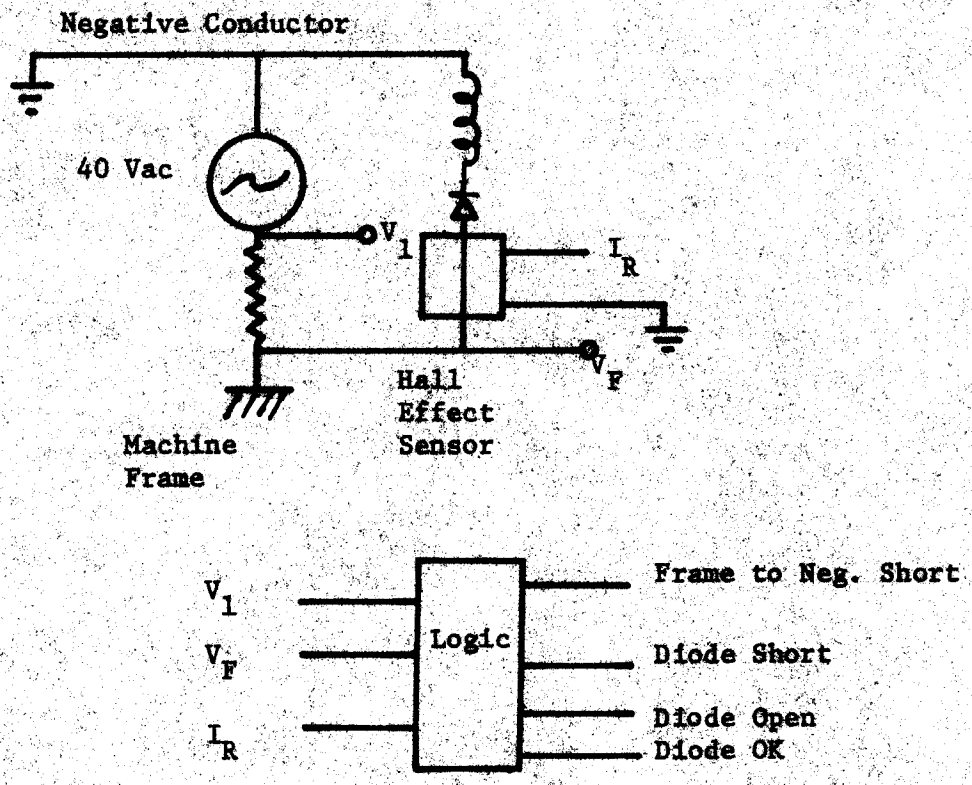

FIGURE 7.6. - Improved diode tester.

as shown in figure 7.6. If R_1 is variable, it can be reduced to a low value so that the ground relay can be checked. A similar arrangement can be used for the reverse voltage test.

Another method is to use inherently safe voltages. For example, an ac voltage of less than 40 volts with limited current capacitv could be used to make all the necessary diode tests and thus be completely safe. An example is shown in figure 7.7. In this case, the frame to negative conductor voltage is measured and the reverse diode current is measured. When these measurements are logically compared to expected values during each half cycle of the test supply, it can be determined if the frame is grounded and if the diode is good. Once this test is made, the ground relay trip can be safely checked with a resistive connection to the positive supply. There are many ways in which this type of testing system can be implemented.

One method of implementing an inherently safe system is shown in figure 7.8. The ac voltage is derived from the ripple voltage on the dc source. This voltage is calculated to be approximately 6 volts at 360 Hz. Thus transformers are necessary to provide the correct voltages. The 30 volts (RMS) is connected between the machine frame and the negative return conductor through a resistor. A switch is used to connect the test signal and presumably would be used at the beginning of each shift or before the contactor is closed as desired. The tests are broken into two parts; when the source is positive (PS) and when it is negative (NS). Appropriate comparisons are made during the positive and negative cycles.

During the positive cycle, two tests are made. The first is a check that the forward voltage drop across the diode is less than approximately 1.5 volts: i.e. an open circuit test (POC). The second test is for a short circuit test (PSC) to make sure the voltage across the diode is at least 0.3 volts.

During the negative cycle, another two tests are made. Again a short circuit test is made (NSC). Secondly the diode current is measured with the Hall-effect sensor and compared to 5 mA (IDL5).

If any of the four measurements indicate a problem, a latch corresponding to the problem is set and a light turned on. These latches are reset with a switch. If no problems are found, two signals POK and NOK indicate positive and negative measurements are adequate. The six outputs can be used by the operator or maintenance personnel for diagnoistics, and may also be used to lock-out the operation of the machine.

Many variations of this system are possible. The system may be used automatically or may be manually initiated. The ac signal may be derived from an oscillator instead of the dc ripple. The system may be machine installed or used externally for periodic inspection.

7.6 CONCLUSION

While the presently used tests on the diodes do adequately test the diode, they are difficult and/or dangerous to perform. It is possible to provide

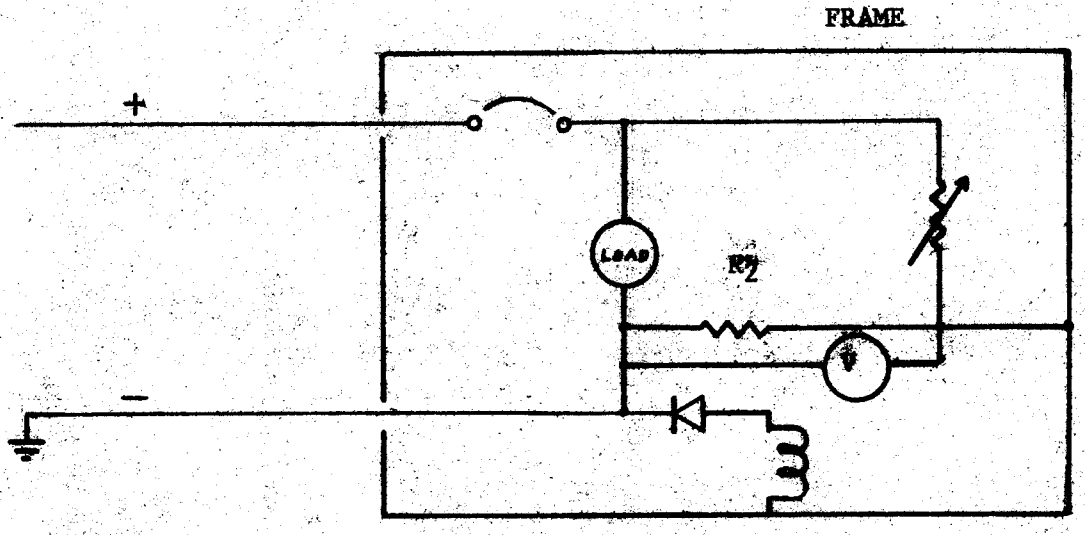

FIGURE 7.7. - A method of safely testing the diode for forward conduction. Initially, the frame voltage would be limited to 40 volts if the diode were open. This voltage would be read on the voltmeter or another indicator.

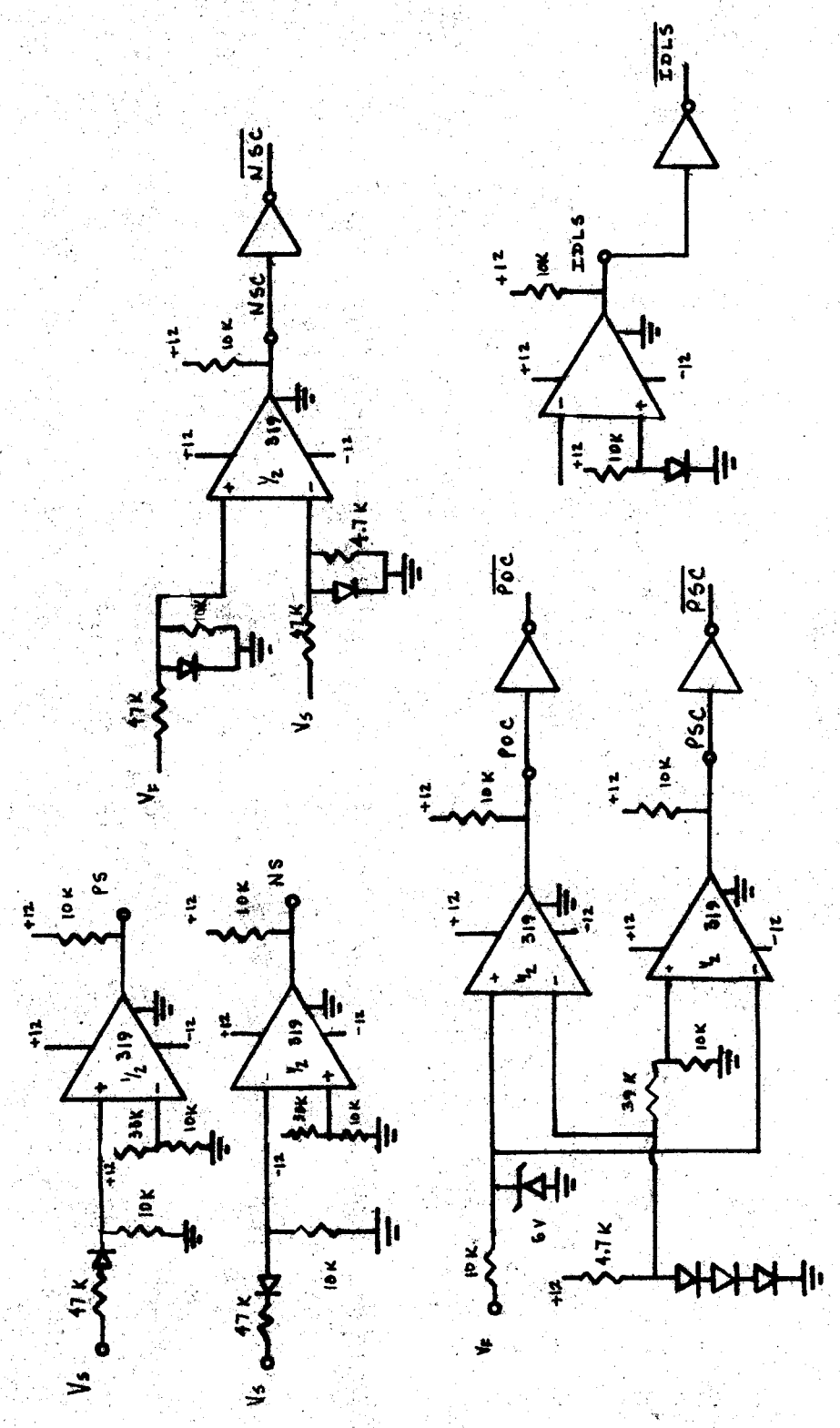

FIGURE 7.8a. Detector circuitry for diode testing.

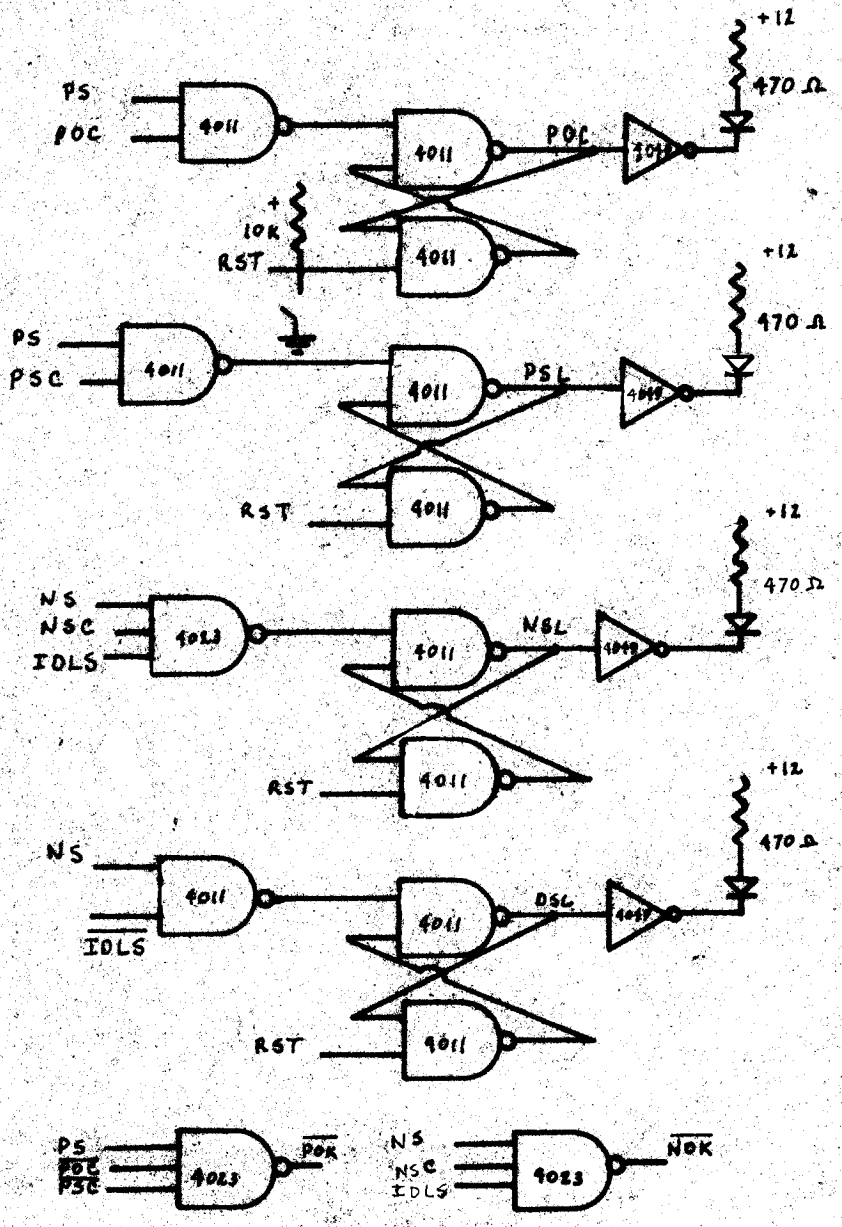

FIGURE 7.8b.- Logic for diode testing.

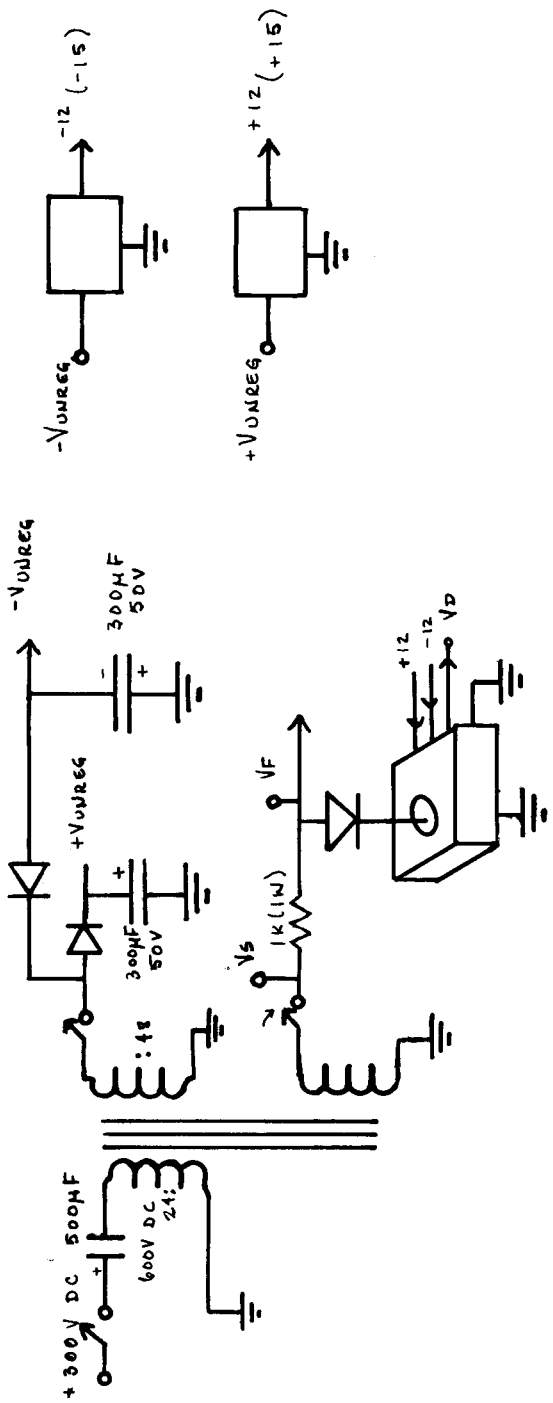

FIGURE 7.8c. - Power source and signal generator for diode testing.

circuitry which will adequately test the diodes safely and conveniently. Such circuitry needs only to be developed and thus the benefits of two-conductor cable can be safely retained.

REFERENCES

1. Cooley, W. L. "Mine Grounding Systems: Evaluation of Ground Beds and Ground Bed Monitors and Evaluation of Modular Ground Wire Monitor" from 1975-76 Annual Report of Research,(USBM Grant #G0144138),Chapter IV., pp. 151-167.

2. Powell, G. L. The Safety Grounded System, West Virginia University, 1972.

3. Smith, H. D. Chief Engineer, PEMCO Corporation, Bluefield, WV.

4. Johnson, D. E. and J. L. Hilburn. Rapid Practical Design of Active Filters, John Wiley and Sons Inc., New York, 1975, pp. 101-163.

5. Jung, W. G. I. C. Op Amp Cookbook, Howard W. Sams and Co., Indianapolis, Indiana, 1977, pp. 191-194.

6. Garza, P. P. Jr. "Getting Power and Gain out of the "741-Type Op Amp", from Circuits for Electronics Engineers, Weber, S., Ed., McGraw-Hill Co., New York, 1977, p. 7.

7. Coal Age. "About Silicon Diodes and DC Frame Grounds", Aug. 1974, p. 98.

8. Coal Age. "Consol Power Systems . . . Deep and Strip", Oct. 1964, p. 171.

9. Smith, H. P. "Present U. S. Practice on AC and DC Ground Fault Protection for Underground Coal Mine Face Equipment", from the 1978 WVU Coal Mine Electrotechnology Conference.

10. Coal Age. "Electronic Monitor Guards Machines, Cables", Aug. 1971, p. 70.

11. Joy Manufacturing Co. "Joy P.C. Lectronic Sentry-Training Program".

12. Coal Age. "Power For Low Cost Operation", July 1961.

13. IBM Corporation. 1620 Electronic Circuit Analysis Program (ECAP) User's Manual.

14. Jones, D. R. "Frame Grounding DC Mining Machines with Silicon Diodes", from Mining Congress Journal, May 1965, p. 58.

15. Heller, S. "Understanding and Maintaining Mine-Type Rectifiers", from Mining Congress Journal, May 1968, p. 69.

16. Joy Manufacturing Co. "Direct Current Mining Machinery", Franklin, PA, 1972.

17. Manufacturer's Literature. "Xit-Rod Grounding Devices", P. O. Box 1314, Covina California 91722.

18. Ibid.

19. Ibid.

20. A. G. Leach and Co., Limited. Marconite for Electrically Conductive Concrete", Colchester, England, 1976.

21. Tagg, G. F. Earth Resistances, Pitman Publishing Corp., London, 1964.

22. Hill, H. W. "Design and Measurement of Driven Rod Ground Beds", MSEE Thesis, 1977.

23. Weber, E. Electromagnetic Theory, Dover Publications, New York, 1965.

24. Ibid.

25. Sunde, E. D. Earth Conduction Effects in Transmission Systems, Dover Publications, New York, 1968.

26. Ibid.

27. King, R. L., H. W. Hill, R. R. Bafana and W. L. Cooley. Guide for the Construction of Driven-Rod Ground Beds, U. S. Department of the Interior, Bureau of Mines Information Circular, IC 8767, 1968.

28. Bellaschi, P. L., R. E. Armington, and A. E. Snowden. "Impulse and 60 Cycle Characteristics of Driven Rods - II", AIEE Transactions, 1942.

29. Sunde, E. D. Earth Conduction Effects in Transmission Systems, Dover Publications, New York, 1968.

30. Ibid.

31. Ibid.

32. Bendix Corporation. Feasibility Study of Electric Shock Prevention, Phase III Report. (U. S. Department of the Interior Contract No. J0357115) Sept. 1976.

Appendix A

Ground Check Monitor Calculations

A.1 MATHEMATICAL MONITOR DESCRIPTION

This appendix summarizes the design of the overall monitor in mathematical detail and is divided into five separate subsections:

1) The bridge

2) Detector front end

3) Detector rear end

4) Power supplies

5) Support circuitry

A.1.1 The Bridge

The bridge is shown in figures 1.4 and 1.5 and its function has been described in section 1.1. Its configuration is that of the standard resistive Wheatstone bridge and is balanced at nodes 1 and 2 when R_{SW} (the unbalancing resistor) is shorted. The bridge is designed such that the voltage difference between the nodes when R_{SW} is in the circuit is $\approx$ 1.0 V_{PP}. This is approximately one-tenth the value of the 60 Hz noise expected to be present at the inputs. The 60 Hz noise is attenuated by the biquad active filters.

The sizes of the bridge resistors are selected as follows: The nominal ground wire resistance (R_{WE}) is assumed to be 2 Ω. During a line-to-frame fault on 4160 V L-G a grounding resistor of 173 Ω will limit the fault current to 24 A. A pilot-to-frame resistor (R_P) of 2 Ω is used to allow detection of pilot-to-ground wire shorts. These resistors make up Z_3 (R_G=173 Ω) and Z_4 (R_P+R_{WE}) legs of the bridge (figures 1.4 and 1.5). Since the Z_1 and Z_2 legs must conduct some fault current, it is desired they be as large as possible and still allow a 1.0 V_{PP} unbalance. The bridge driving voltage is 12.8 V rms (36 V_{PP}) and a current of $\simeq$ 0.21 A is required across a 2 Ω R_{SW} to create a (1.0 V_{PP}) change in bridge voltage. The equation is $\frac{12.8 \text{ V rms}}{RA_2 + R_P + R_{WE}} = 0.21$;

56 Ω = RA_2. Thus RA_2 = 56 Ω at balance $Z_1 Z_4 = Z_2 Z_3$.

$$Z_1 \ (4\ \Omega) = (56)\ (173)$$

$$Z_1 = 2.4\ K\Omega = RA_1$$

Note that R_{SW} is shorted when the bridge is balanced.

The power rating for these resistors is calculated under fault conditions. Referring to figure A.1.1 which shows the bridge under a line-to-frame fault, fault current flowing through R_P, R_{SW}, RA_1 and RA_2 is given by:

$(4160\ V)/(2460\ \Omega) = 1.7\ A$

The grounding resistor and ground wire resistance limit the frame voltage to a maximum of 40 V with respect to ground, and this presents no personnel hazard.

The 60 Hz voltage appearing on the oscillator output during a fault is not serious since it is about 50 V with respect to ground (this voltage varies with different resistance levels, but will not become large enough to harm the driver). It is prevented from feeding further into the driver, because it is blocked by a capacitor that appears as a very high impedance at 60 Hz (500 kΩ) and also by a 56 kΩ resistor. The voltage also appears at the collector of two high-voltage transistors which are rated to withstand it.

For node 1, however, the situation is different, as here the neutral of the transformer shifts to produce a large potential with respect to ground.

This potential is 1.7 A (2400 Ω) ≃ 173 Ω (24 A) = 4 kV. The power in the 2.4 kΩ resistor is $(1.7\ A)^2$ 2400 Ω = 7 kW. Since this is a continuous rating and the fault voltage appears only momentarily, the resistor rating was reduced by a factor of 15. The wattages for the other resistors are not nearly as large. The calculated wattage ratings are shown in Table A.1.1. R_P was sized to withstand a line-to-pilot fault.

The final bridge is shown in figure A.1.2. The balance voltage at nodes 1 and 2 is (12.8 V rms)(4 Ω)/(60 Ω) = 0.85 V rms, and when R_{SW} is switched in the circuit the node 2 voltage rises to (12.8 V)(6 Ω)/(62 Ω) = 1.24 V rms. This results in a ≈ 0.35 V rms (1 V_{PP}) voltage difference due to R_{SW}.

A.1.2 Detector Front End

The actual circuitry referred to here is all of the detection circuitry up to and including the balance relay. The high voltage detectors are also included here. The "rear end" which coordinates the detection is discussed in the subsequent section.

This section is broken into six parts. They are:

a) HV suppression

b) buffer

c) filters and rectifier

d) difference amplifier and comparator

e) relay driver and relay

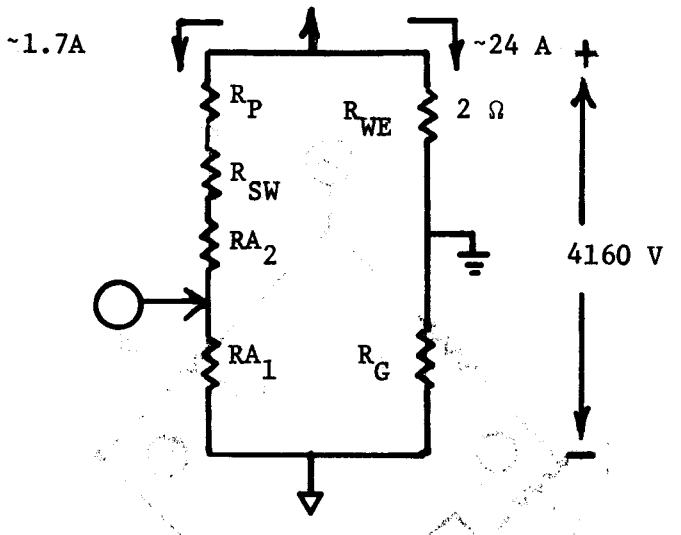

FIGURE A.1.1. - Bridge under fault.

TABLE A.1.1. - Bridge resistor power ratings

Resistor	Value	Continuous Power Rating	Power Rating Used
RA_1	2.4 k	6.9 kW	225 W
RA_2	56 Ω	162 W	100 W
R_{SW}	2 Ω	6 W	50 W
R_P	2 Ω		50 W

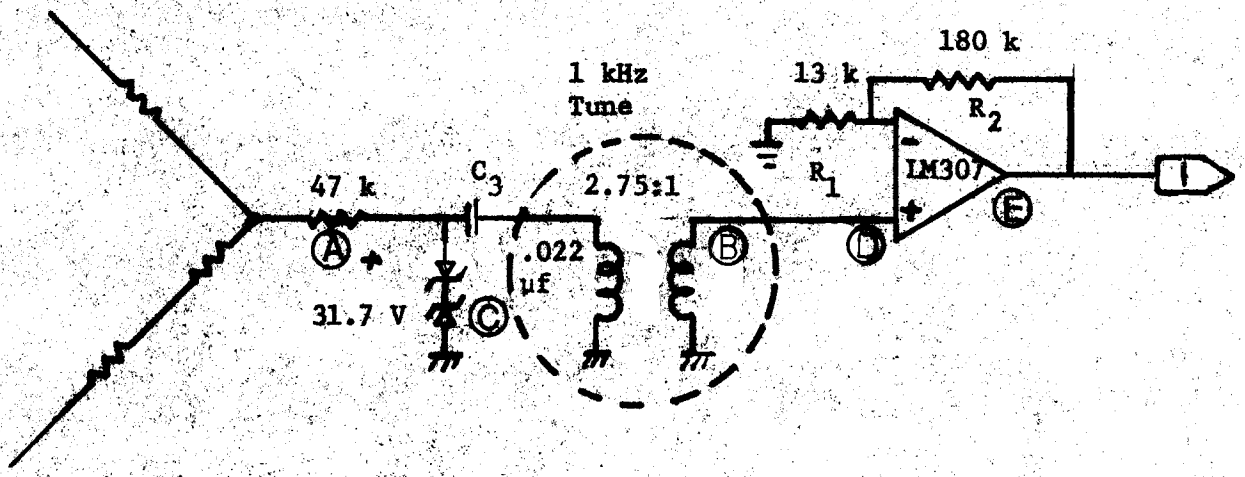

FIGURE **A.1.3a. - Inital detector stage + high voltage suppression circuitry (Nodes 1 + 2 identical).**

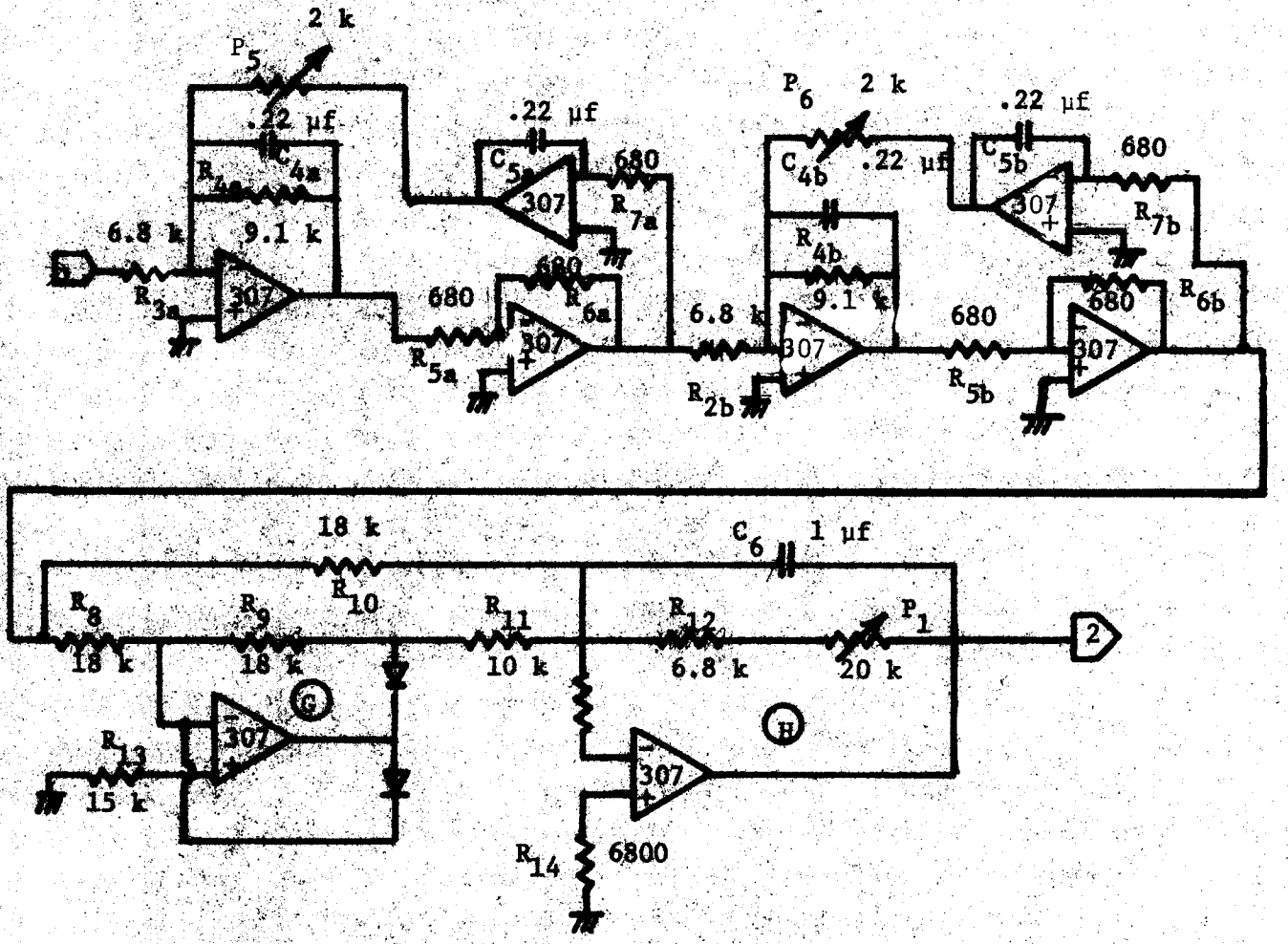

FIGURE A.1.3b. - Filters and rectifier.

f) HV detectors.

Note in figures A.2.2 through A.2.9 that some resistors are identically numbered. This is because the balance detectors are equivalent up to the difference amplifier. The HV detectors are also largely identical.

A.1.2.1 High Voltage Suppression

The first few stages of the detector and HV protection circuitry are shown in figure A.1.3a). The only difference between the HV suppression at nodes 1 and 2 is the wattage rating of the 47 kΩ resistors (A figure A.1.3a)) at the input. At node 2 this resistor is 1/2 W, as the voltage at this point will only rise to 40 V with respect to ground. At node 1 a rating of 100 W was selected since $(4160\ V)^2/(47\ k\Omega) = 370\ W$. This wattage was selected since the fault voltage will persist for only a short time.

This 47 kΩ resistor is in series with a capacitor inductor tuned circuit (B figure 1.11a)). The 33 V zener diodes at C are used to protect this input-tuned circuit. The tuned circuit filter reduces the 60 Hz voltage by approximately 30 db. The signal appearing at pt D figure A.1.3a) has an amplitude of 0.12 V_{PP}, having been reduced by a factor of $\tilde{-}$ 20 by the voltage suppression circuitry and the transformer.

A.1.2.2 Buffer

This circuit is at E in figure A.1.3a). The gain in this stage is set to produce a 1.8 V_{PP} voltage at its output when the bridge is balanced at nodes 1 and 2. Using the 0.12 V_{PP} voltage at D, the desired gain here is 15.

The signal output of the node 1 buffer is therefore a 1 kHz waveform with an amplitude of 1.8 V_{PP}. The signal from the node 2 buffer is also a 1 kHz sine wave, but its amplitude varies from 1.8 V_{PP} ← 2.4 V_{PP} at a 10 Hz rate.

A.1.2.3 Bandpass Filters and Rectifiers

The purpose of the bandpass filters is to pass the 1 kHz bridge signal and to reject all others, thus eliminating the remainder of the 60 Hz noise in the circuit. The filters in this case are of the biquad Butterworth (flat passband) type consisting of two cascaded 2-pole filters [3]. The schematic of these filters along with the rectifiers is shown in figure A.1.3b).

The 0.22 μF capacitors C_{4a}, C_{4b}, C_{5a} and C_{5b} were empirically selected such that they were small enough to let the filters respond to the 10 Hz amplitude change. A Q of 10 was selected, because larger Q's are too slow for the 10 Hz switch frequency. Also a 2 kΩ pot was inserted to tune the filters to the 1 kHz center frequency. The gain was chosen as 1, so that the signal level at F figure A.1.3b) is identical to the input.

The 1 kHz signals are rectified to eliminate phase shift effects and to obtain dc signals to pass into the difference amplifier. The gain of the rectifiers is about one, but this value is made variable for calibration. The basic rectifier circuit was taken from reference 5, but adjustments to the gain and filter were made to optimize it for this circuit. Stage 1 at G functions as a full wave rectifier and stage 2 at H is a low-pass filter. The RC time constant is set by C_6 = 1 μF; this allows some ripple but provides satisfactory speed of response. The output of the rectifiers is approximately equal to the RMS value of the input waveform. Therefore, at the node 1 rectifier output there is $\frac{1.8\ V_{PP}}{2\sqrt{2}}$ = 0.7 V DC, and the waveform coming from the other rectifier varies between ≈ 0.7 V and ≈ 1.0 V at a 10 Hz rate.

A.1.2.4 Difference Amplifier and Comparator

The difference amplifier takes the difference between the two rectifier outputs. A voltage is generated which indicates that the bridge is unbalanced. The circuit and its following window comparator is shown in figure A.1.3c). The gain is set so that the difference of the nodes 1 and 2 voltages when R_{SW} is unbalancing the bridge is 0.7 V. Therefore, the amplifier output varies between zero (when the bridge is balanced), and 0.7 V (when unbalanced) at a 10 Hz rate. Due to the low-pass response of the previous circuitry, the actual output waveform appears as a 10 Hz sawtooth.

The amplifier is designed with a gain of 2.5 so that the output voltage change at point I in figure A.1.3c) is 1 V.

Following this difference amplifier is a gain-of-two buffer, shown at J figure A.1.3c). The purpose of this amplifier is to boost the difference voltage by a factor of two for improved tuning accuracy.

Next is a window comparator, and it is here that the allowed ground wire impedance change is set. The comparator is shown in figure A.1.3c) (pt J is the input) and is constructed with an LM 319 dual comparator chip with both comparator outputs tied together through diodes. Thus, either output may go high independently of the other, resulting in a "window effect". The comparator functions so that as long as the sawtooth input is within the limits set at pins 4 and 10 (figure A.1.3c)), the comparator output is high (+15 V). If the input goes out of this range, the output goes low (0 V). The positive input excursion voltage is set at pin 10 and the negative at pin 9. Under normal operation the sawtooth varies in and out of this window, switching the comparators at a 10 Hz rate.

At the difference amplifier input, V_1 corresponds to the voltage at node 1 and V_2, node 2. Therefore, the actual difference when R_{SW} is switched in is 0.4 V, and the amplitude of the sawtooth will vary from 0 to -1.4 volts (the buffer yields a gain of two). Note that the ground wire impedance (R_G) variances do not change this amplitude so much as they change the

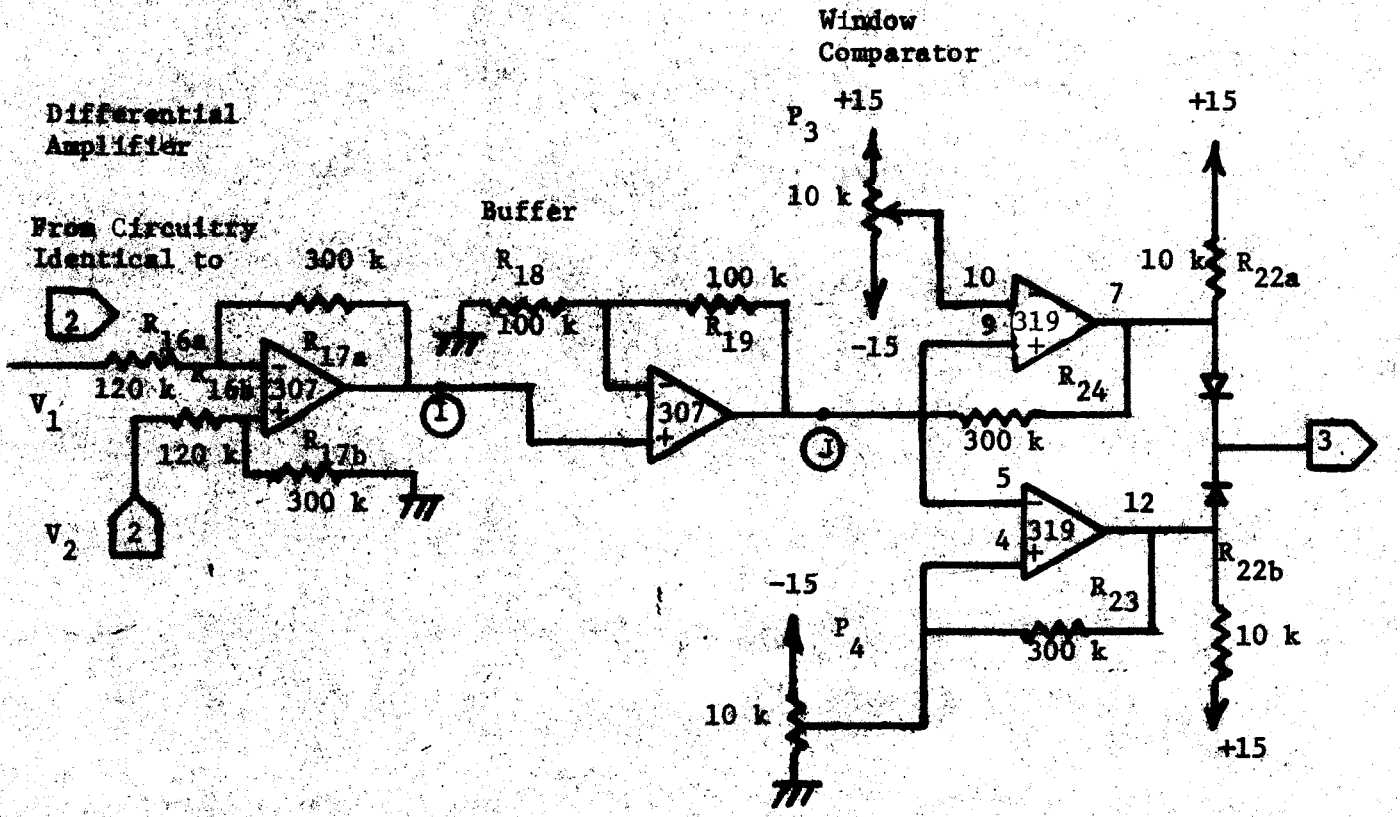

FIGURE A.1.3c. - Difference amplifier and comparator.

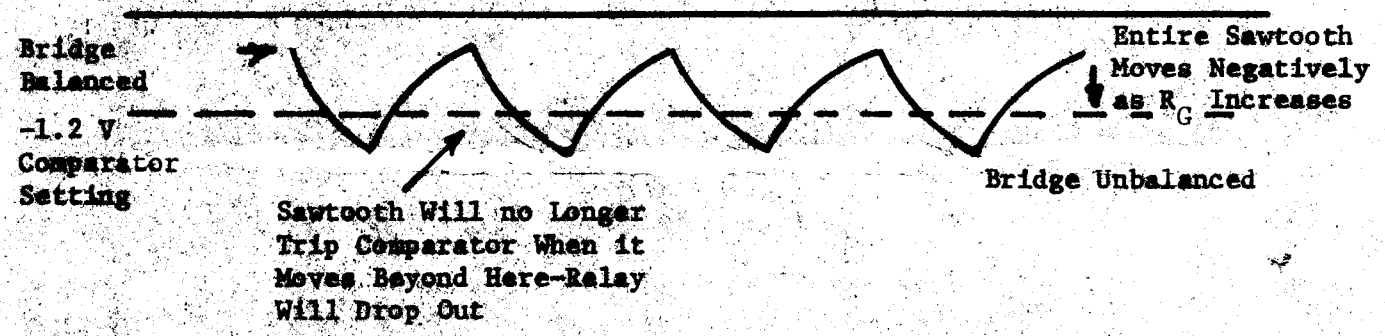

FIGURE A.1.3d. - Sawtooth output of difference amplifier (X2) by buffer.

sawtooth position relative to zero (i.e. as R_G increases the entire 1.4 V sawtooth moves negatively as shown in figure A.1.3d). This is expected since the voltage drop across R_{SW} should remain fairly constant, because changes of 2 Ω or slightly more in R_G will not significantly affect the bridge current.

Because a 2 Ω change in R_G results in a 1.4 V change out of the buffer, one can set the voltage at pin 4 on the comparator (figure 1.11c)) at -1.3 V. This will result in the sawtooth tripping the comparator as long as the ground wire impedance is between 2 and 4 ohms. This is done by adjusting P_4, a 10 kΩ potentiometer. If R_G becomes less than 2 Ω, then the sawtooth will move positively, and the voltage set by the P_3 10 kΩ potentiometer at pin 10 (figure A.1.3c)) will allow the comparator to trip repeatedly until the sawtooth moves about ≈ - 0.4 V. This would indicate a pilot-to-ground short. R_{22} a and b are used as pull-up resistors at the comparator outputs. Feedback resistors R_{23} and R_{24} provide hysteresis to eliminate comparator oscillation due to threshold voltages.

With this type of design, the monitor is very versatile since virtually any ground wire impedance value may be allowed. The calibration and use section (Appendix A.2) describes setting the comparators.

A.1.2.5 Relays

The comparator output is a 10 Hz square wave. This voltage is used to drive the charge pump circuit that holds in the relay as long as the voltage switches. The circuit is shown in figure A.1.3e). A Darlington pair at K is alternately cutoff and saturated by the comparator voltage, which drives a capacitor-diode circuit that provides current to hold in the relay. If the sawtooth goes out of the comparator range due to an R_G increase or pilot-to-ground short the comparator will cease to switch. C_2 then discharges through the relay which has an impedance of 500 Ω.

A.1.2.6 The High Voltage Detectors

Located at nodes 1 and 2 in figures 1.4 and 1.5 are the high voltage detectors, which are to detect fault voltages and trip the relay. In all cases except double line-to-ground faults this circuitry is redundant, and in this case, the node 1 detector is redundant with the balance detector. This will be described later.

The high voltage (HV) detector circuits for nodes 1 and 2 are similar except for voltage suppression and gain. The node 1 circuitry is described first, referring to figure A.1.4.

The input at (a) is protected by a 300 K (R_{65}) resistor in series with an 8:1 transformer. Most of the fault voltage is dropped across the 300 K resistor, with the remainder being transformed down to the input of the

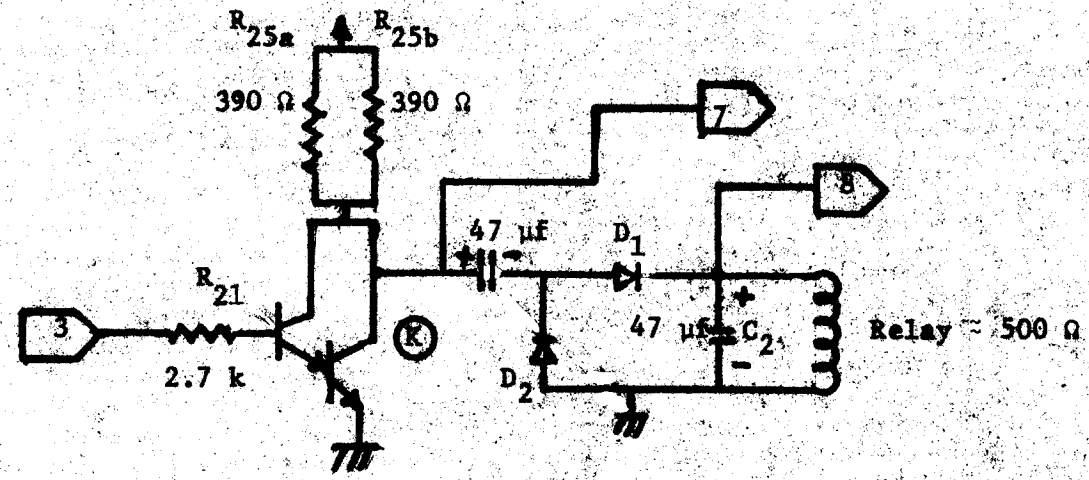

FIGURE A.1.3e. - Relay circuit.

60 Hz bandpass filters at (b). The filter gain is set at 11. A fault voltage of 4160 V will appear as 10 V rms at the filter output.

Following the filter and a diode rectifier and filter capacitor (point (c) figure A.1.4) feeding into the comparator. The detector response time is set with this capacitor (C_{10}) and the input impedance of the comparator (taken as 1 M Ω). This gives an RC time constant of (.1 μf)(1 M Ω) = 0.1 sec. The rectified signal then goes into a comparator (LM 311). The value of the rectified 60 Hz fault voltage is 10 V. In order to detect this, the comparator trip voltage used is 9 V. The comparator is normally low and goes high with the fault and the neutral voltage shifts 3500 V. This voltage is adjustable as described in Appendix A.2.

The detector at node 2 is identical to that at node 7 except for the filter gain and input resistor. The 8:1 transformer is tied directly to the input node 2 of this detector. P_{11} is set to detect at 32 V fault on the machine frame. More details are given in Appendix A.2.

A.1.3 Detector Rear End

A.1.3.1 TTL and Interfacing

The next circuitry is to interface the two high voltage detectors to their relays. LED indicators are used to show whether both detectors received and processed the fault. A display is also given if a detector fails to see the fault.

A two-stage transistor interfacing circuit is shown in figure A.1.5. The transistors are used to interface the 15 V comparator signal to the 5 V TTL logic. The logic is used to show which HV comparator has gone high and to trip the relay if either goes high. Then the output of the detectors is latched, protecting mine personnel by preventing power from being re-applied until the monitor is deliberately reset.

Referring to figure A.1.6 when either detector goes high (indicating a fault condition) it is latched by a 7475 latch (pt. L). This high is then taken to an exclusive or (XOR) circuit (7486) (point M) where it is compared with the other HV detector output. If only one detector sees the fault the XOR output will go high, turning on the red LED. In addition, the green LED of the detector receiving the fault will light. When both detectors detect the fault, both green lights come on and the red LED will be off. If either or both detectors receive the fault a 7402 nor gate (point N) drives a transistor to drop out the relay. The transistor is designed like the TTL interface transistor. Pushing the RESET button resets both detectors and latches which allows the relay to be picked up.

The other relay involved here is that of the balance detector. This relay is not latched, being free to pull in and out depending on the bridge balance. This presents no problem, as the main breaker must be reset whenever the relay drops out and may not be pulled back in unless the bridge is balanced. The HV detectors latch when they trip, which requires the monitor to be reset after a fault has tripped the relay. This feature

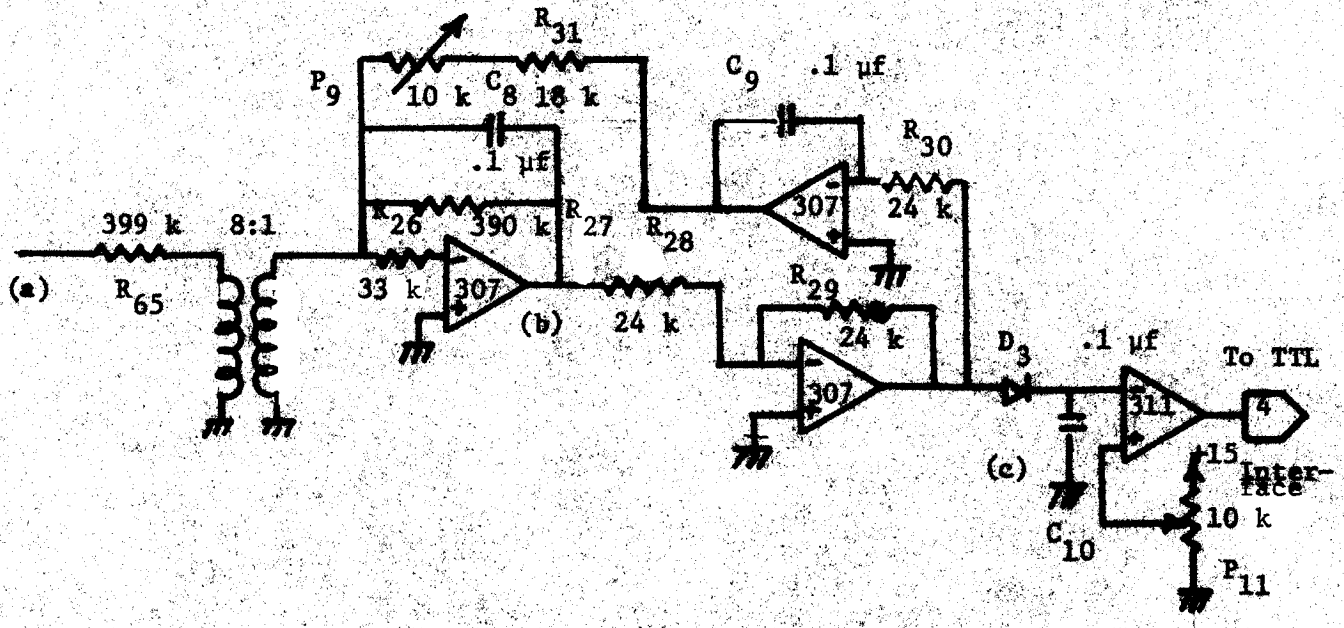

FIGURE A.1.4. - High voltage detectors.

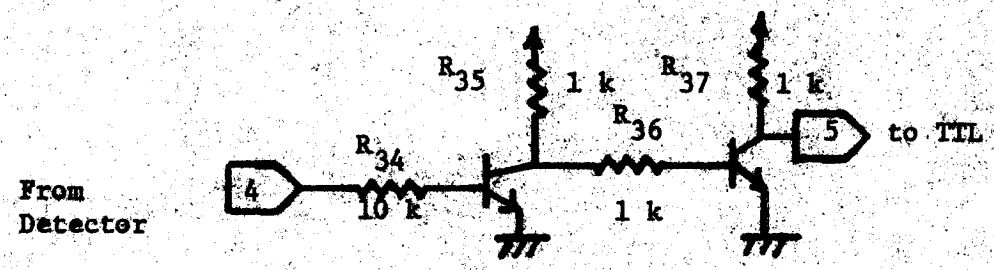

FIGURE A.1.5. - Interface-HV detectors to TTL logic.

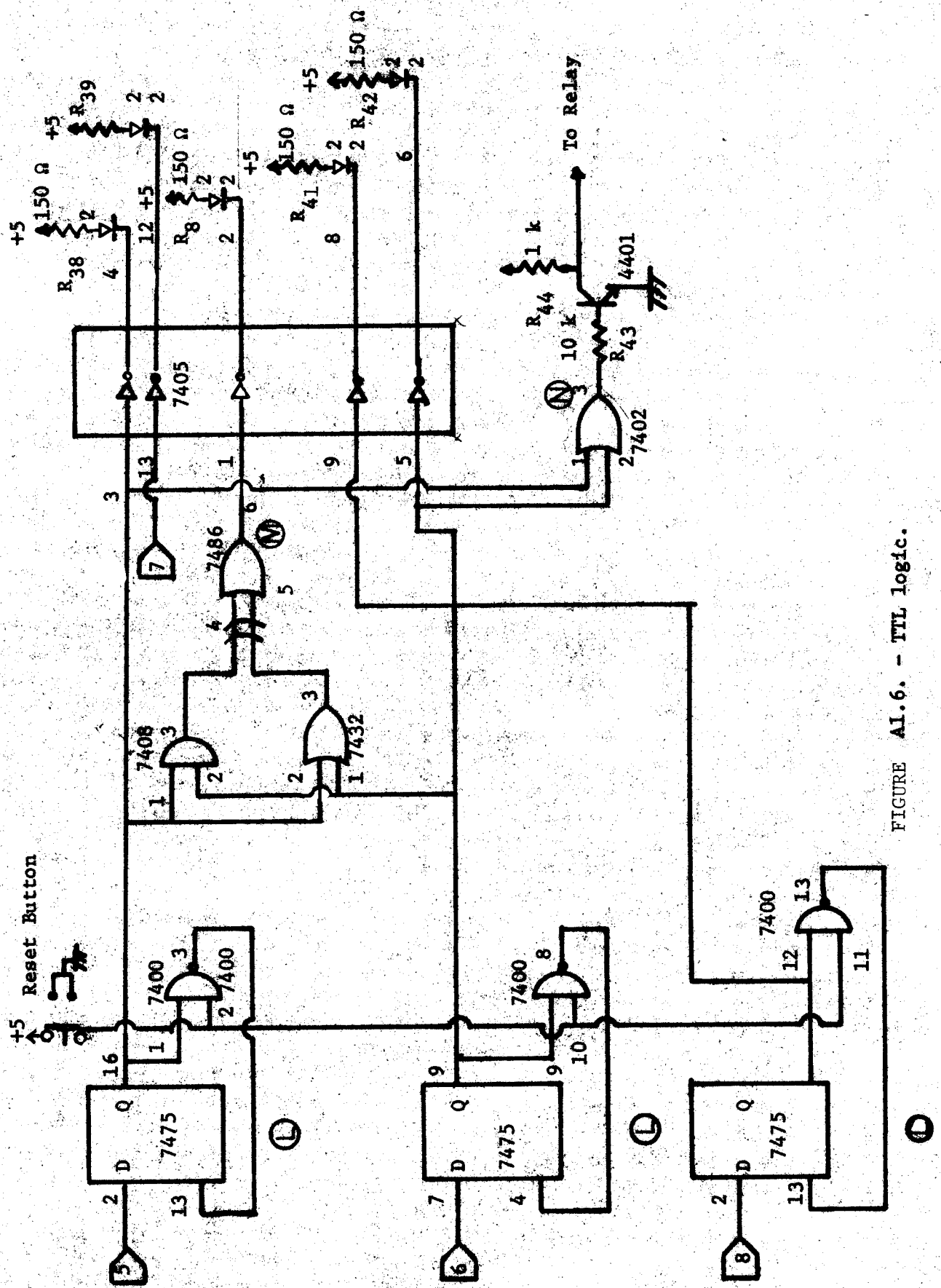

FIGURE A1.6. - TTL logic.

was included for additional safety.

The balance detector is interfaced into the TTL such that when the relay drops out a latched LED comes on that indicates to the person resetting the breaker that the relay tripped. This is necessary since this relay could trip due to a transient imbalance, and then pick back up. This indicator informs personnel that the trip was indeed valid. The reset button described before resets this LED. In addition to this latched LED, there is another tied to the collector of the Darlington relay driver. This LED blinks at a 10 Hz rate when the relay is in and stays on or off when the relay is out. The condition of this LED gives clues as to what causes the relay to come out, and is described in the calibration and use section (Appendix A.2).

All of these LED's are operated by an open collector 7405 inverter chip and are connected as per figure A.1.6.

A.1.3.2 Power Supplies

These have already been described in some detail. Figures A.1.7a), A.1.7b), and A.1.7c) show the ±70 V, ±15 V, and +5 V schematics, respectively.

A.1.3.3 Support Circuitry

This consists of the oscillator and amplifier that drives the bridge, (Fig. A.1.8) and the switching circuitry that switches the balance resistor (R_{SW}) in and out of the bridge (Fig. A.1.9).

An 8038 waveform generator is used to generate a sine wave, which is buffered and amplified by the 3 W amplifier that drives the bridge. Figure A.1.8 shows the schematics. The output signal of the sine wave generator is buffered by the LM 307 op. amp. circuit with a gain of -1.

The final amplifier stage (T figure A.1.8) was designed with the aid of reference 6. The overall amplifier gain is 6.15 to give an output voltage of 36 V_{PP} and 3 W power to the bridge.

The other portion of the support circuitry is "the switch". The relay is placed across the resistor in the ground wire leg (see figures 1.4 and 1.5). It is used to balance and unbalance the bridge by switching R_{SW} in and out of the bridge. This relay is driven by a switching transistor, which is in turn driven by an 8038 generator set up to generate a 10 Hz square wave.

This chip provides a 3 V_P square wave to the 2N4401 switching transistor, which drives the relay in and out 10 times per second, providing the varying node voltage for the bridge detector. Complete schematics of the detector are provided in Appendix A.3.

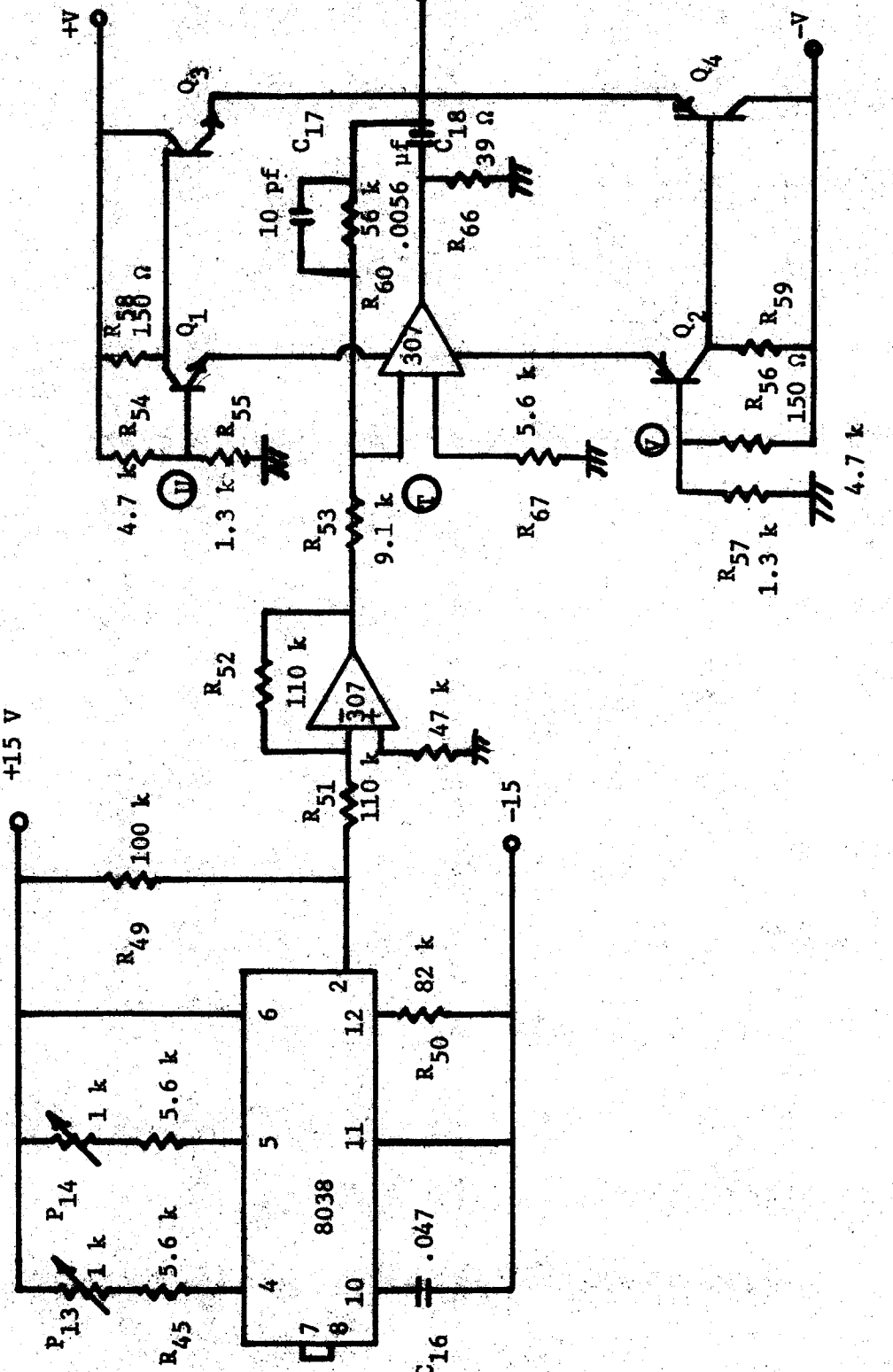

FIGURE A1.8. - Bridge driver circuitry.

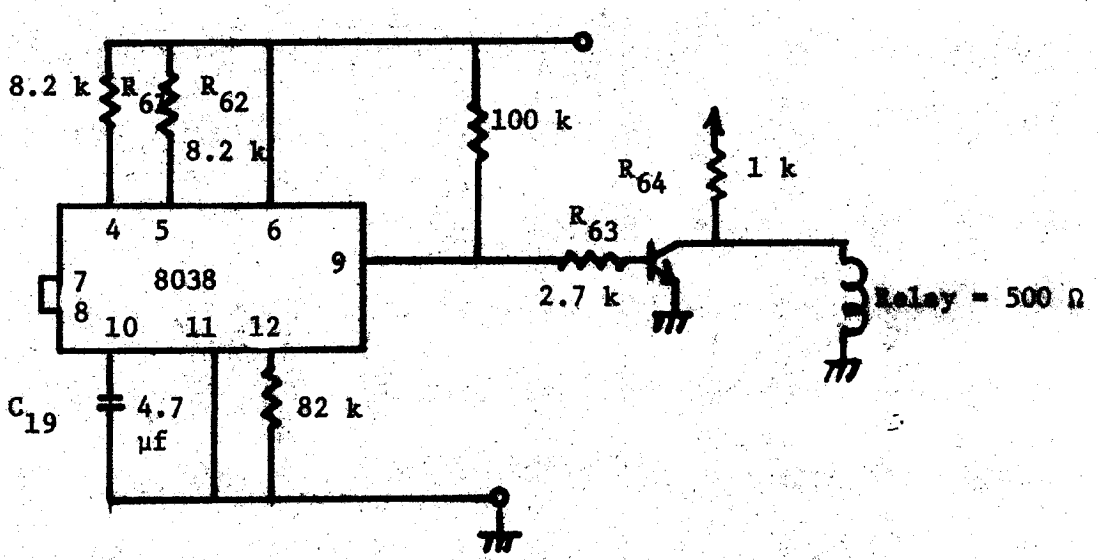

FIGURE A1.9. - The bridge switch.

A.2 CALIBRATION AND USE

A.2.1 Balance Selection

The bridge is designed for a 7200 V_{LL} (4160 V_{LN}) substation system with a resistance-grounded neutral and a grounding resistor value of approximately 170 Ω. The system can be easily adapted to any other sized circuit, however, by changing the bridge resistors. The bridge balance voltage may be set at any value $\leq$ 4 V_{PP}. Larger voltages will cause clipping in the filters. Caution should also be taken to assure that all resistors used in the bridge have an adequate power rating.

For ordinary calibration it is necessary only to perform section A.2.2. If a readjustment of the bridge is necessary, refer first to sections A.2.1 and A.2.3. Should there be a problem with frequency or filtering, perform first section A.2.5 and then A.2.4 followed by A.2.2.

The sections A.2.1, A.2.2 etc. are arranged so as to cover first the bridge and impedance tolerances, second the potentiometers, and thirdly the LED indicators. Finally, the fault voltage tolerance is described.

A.2.2 Zero Calibration

Once the bridge is set up, it is calibrated as follows: The switch marked "Switched Resistor" on the outside of the box should be off. Potentiometers P_1 and P_2 (figure A.2.6) are set so that the dc voltage at pt Z is zero. This is done by adjusting them such that the voltage at pts X and Y = 0.7 V.

A.2.3 Impedance Levels

The next step is to set the allowed ground wire impedance. For the system to detect a change of 2 Ω in a 2 Ω ground wire and be immune to parallel paths, a setting of -0.4 on P_3 and -1.2 V on P_4 (figure A.2.6) is suggested. Custom-made circuits can be designed here by noting that a change of balance of 0.4 Vrms at the bridge looks like 1.4 V_{PP} into the comparators. An example is given below. This example is the actual detector set-up used. Example: Given: a 2 Ω ground wire and R_{SW} = 2 Ω. Desired: Trip if the ground wire impedance (R_G) exceeds 4 Ω or becomes less than 0.5 Ω. Note that a 0.4 V difference in node voltages at the bridge results in a 1.4 V_{PP} difference at the comparator.

Referring to figure A.2.1, assume node 1 remains balanced and the voltage drop across it is 1.1 V_P. Node 2 will balance this if the current through $R_P + R_G$ = 2 Ω + 2 Ω is equal to $\simeq$ .21 A. (.21 (2+2) = 1.1 V_P). When R_{SW} is switched in the circuit, the voltage at node 2 rises to 0.21 A ($R_P+R_G+R_{SW}$) = 0.21 A (6 Ω) = 1.8 V_P. (The addition of R_{SW} = 2 Ω does not

significantly alter the bridge current as this R_{SW} is a small value compared to the overall resistance). Thus the sawtooth input to the comparator will have its amplitude given by 2 (Node 1 V - node 2 V) = 2 (1.1 V_P-1.1 V_P) = 0 V and (1.1 V_P-1.8 V_P) = -1.4 V. This is shown in A, figure A.2.1.

If R_G rises to 4 Ω, the voltages are .21 (R_P+R_G) = .21 (6) = 1.8 V_P (R_{SW} out) and .21 (R_P+R_G+R_{SW}) = .21 (8) = 2.4 V_P and the sawtooth will be 2 (1.1 V_P-1.8 V_P) = -1.4 V and 2 (1.1-2.4) = -2.6 V shown in B figure A.2.1. Potentiometer P_4 should then be set at -1.2 V, C figure A.2.1 as here the waveform when R_G = 4 Ω never trips the comparator. This is because the difference voltage has moved out of the comparator range. The relay comes out because the capacitor will not be charged if the comparator is not triggered.

For the 0.5 Ω case, the node voltages will be 0.21 (R_P+R_G) = 0.21 = (2.5) = 0.75 V_P and 0.21 (R_P+R_{SW}+R_G) = 0.21 (4.5 V) = 1.34 V_P and the sawtooth is 2 (1.1-.75) = 0.7 V and 2 (1.1-1.35) = -0.5 V. P_3 should then be set at ≃ -0.4 V because for R_G < 0.5 Ω the sawtooth will fail to trip the comparators, which trips the relay.

A.2.4 Filter Adjustment

There are ten other potentiometers in the circuit. These are all used to set the center frequencies of the 1 kHz and 60 Hz bandpass filters and to adjust the 1 kHz sine generator. These potentiometers should not ordinarily need adjustement, but are provided in case of long term circuit component changes. To check these filters, read the following and refer to figure A.2.5. There are two identical boards.

First, P_5, P_6, P_7 and P_8 are checked. P_7 and P_8 are not shown here as the two filter boards are identical, the monitor should be on and "switching resistor" switched to off. Point 1, figure A.2.5 is first observed with an oscilloscope and P_5 is adjusted until the 1 kHz waveform at this point is a maximum. This is repeated for P_6, P_7 and P_8 in that order. In figure A.2.5, P_5 corresponds to P_7 and P_6 to P_8. P_5 must always be tuned before P_6, as P_5 is the first stage of the filter. Similarly, tune P_7 before P_8.

Four more potentiometers P_9, P_{10}, P_{11} and P_{12} are located in figure A.2.7. Two of these, P_9 and P_{10} are used to set the 60 Hz bandpass filters. In order to adjust these filters, a 60 Hz waveform at the inputs (marked with I's) and P_9 and P_{10} are turned until their respective filter outputs are maximum. The P_9 output is at point (1) and the P_{10} output is at point 2 in figure A.2.7.

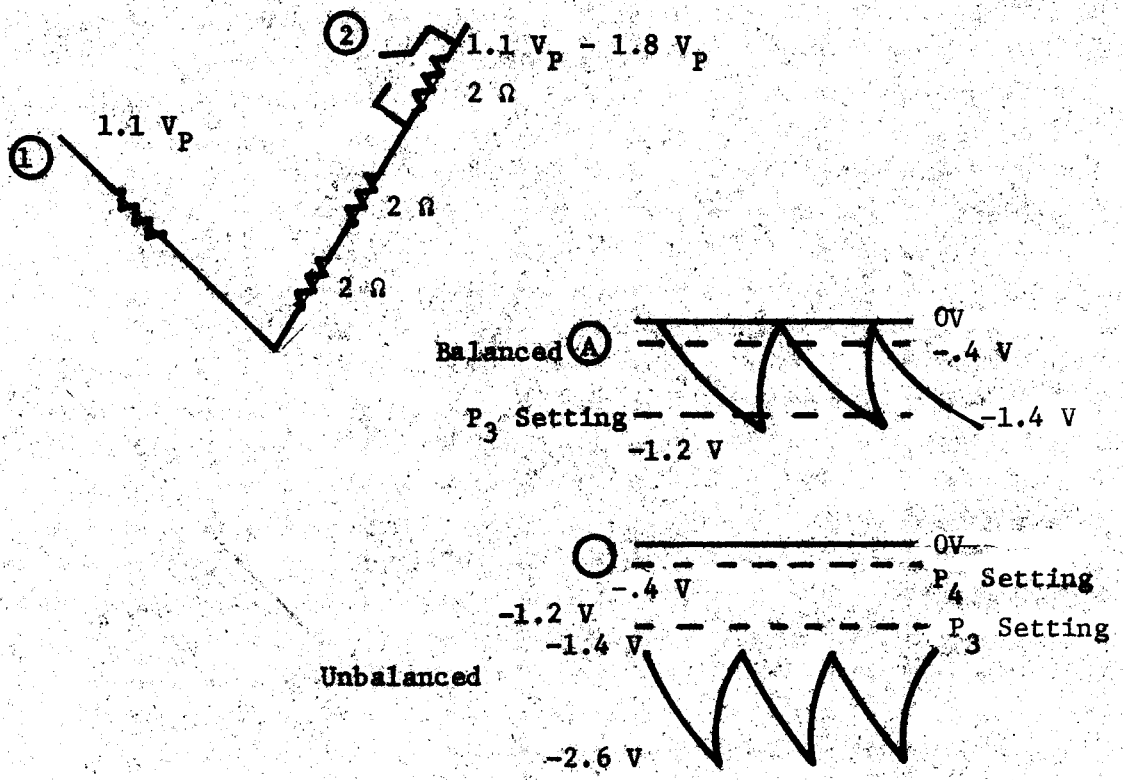

FIGURE **A.2.1. - Balanced and unbalanced sawtooth voltage inputs to comparator.**

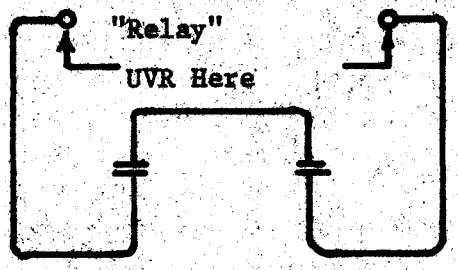

FIGURE **A.2.10. - Relay schematic.**

P_{11} and P_{12} are used to set the comparators for the trip voltages for the HV detectors. The voltages settings are described later, but for detection of 24 A ground wire current and 32 V frame voltages, P_{11} is set at 4 V at pt 3 and P_{12} at V at point 4.

A.2.5 Oscillator Adjustment

The other two potentiometers, located in figure A.2.4 change the symmetry of the 1 kHz oscillator and should not be adjusted unless the 1 kHz waveform is badly unsymmetrical. One can tell which direction and which potentiometer to turn from the waveform at pt 1. Here, potentiometers P_{13} and P_{14} adjust the 1 kHz sine wave. In making these adjustments one must be careful to keep the frequency constant as adjusting P_{13} and P_{14} also changes the frequency.

A.2.6 Indicator Lights

There are five indicator lights that protrude from the monitor when the lid is closed. The function of these lights is to indicate the status of the monitor relay. There are two green LED's marked "neutral" and "frame", a red one marked "single detection", a yellow one marked "balance relay tripped" and a clear one with a red light marked "balance relay". The red button marked "reset" resets the lights, in the case of the HV detectors, it resets the relays. The clear red light marked "balance relay" is tied to the collector of the Darlington through a 7405 open collector inverter and will oscillate as long as the transistor pumps the relay and keeps it pulled in. Whenever this light is oscillating, the relay is pulled in. Should an unbalance occur that allows the relay to trip, this light will cease to blink and the "balance relay tripped" light will latch on until reset. The light (and consequently the UVR) cannot be reset until the "balance relay" light once again is blinking, indicating that the bridge is balanced and the relay is pulled in.

The function of the "balance relay tripped" LED is merely to inform personnel that the relay has tripped due to an imbalance.

The green and red LED's are concerned with the high voltage detectors. If the HV detector at the prescribed node detects a fault, then the corresponding LED comes on, indicating that the breaker was tripped due to a high voltage detected at that node. If only one detector sees a fault, the red LED comes on, indicating that a detector failed to detect a fault. One can easily ascertain which detector it is by reading which green LED is off. If the red LED lights and the "frame" LED failed to see the fault, a possibility is that a line-to-line fault has occurred and therefore there is not voltage present on the frame to be detected. Otherwise, the detector which didn't see the fault, should be checked.

A.2.7 Fault Voltage Settings

P_{11} and P_{12} potentiometers (figure A.2.7) adjust the amount of voltage tolerate at the machine frame and neutral grounding resistor. A good

setting for the node 2 relay which must detect the 40 V faults is a 4 V at pt 3 potentiometer 11 setting which will trip if an excess of 32 V appears on the frame. For P_{12} at the neutral of the transformer a setting of 9 V at pt.4 will detect 4160 V, or 24 A in the ground wire. A general rule-of-thinking to use for these two potentiometer settings is: for P_{11} (the frame voltage potentiometer setting) the voltage at point 3 is equal to 1/8 the tolerated frame voltage. P_{12} (the neutral detect potentiometer) is set using the formula:

$$\frac{[\text{Voltage at pt 4}] \times [300\ \text{k}\Omega]}{700\ \Omega\ (60\ \text{Hz reactance of transformer})} = \text{neutral voltage}$$

$$\therefore\ [\text{Voltage at pt 4}] \times [430] = \text{neutral voltage}$$

This may also be used to set the allowed ground wire current as the neutral voltage divided by the grounding resistor is equal to the ground wire current.

A.2.8 MA Boards

There are three sets of plug-ins used for the PC boards. These are MA I, MA II, and MA III. MA I feeds the 60 Hz detectors, oscillators, both 1 kHz filters and the rectifiers and comparator. MA II feeds the ±70 V supply, the ±15 V and 5 volt supplies and the high voltage detectors, MA III handles the relays and the oscillator-drivers.

The plug-in for each board is plainly marked and is color coded so that each board may be put in with the correct orientation. To insert them just line up the paint markers. The colors correspond to the MA board that the board plugs into and the boards and plugs are numbered. MA I is black, MA II is red, and MA III is blue.

A.2.9 Interface to Mine Circuitry

The monitor is interfaced to the mines as follows. There are four places to interface. One is labeled "neutral" which is connected to the top of the grounding resistor, "ground" is connected to the substation ground that the grounding resistor is grounded to, "pilot" where the pilot wire ties in and "relay" for the UVR. It is required that a 2 Ω frame-to-pilot resistor be installed between the frame and the pilot wire.

The UVR is tied into the "relay" connections, which is a set of three relays in series (as shown in figure A.2.10). These may be connected with either polarity, since they are essentially a set of open or closed circuits. A 240 UVR would be adequate here.

A.2.10 Testing

The circuitry has been thoroughly tested in all areas except very high voltage faults. In construction and subsequent use, many faults, both

accidental and planned have been placed on the circuitry. These include a ±70 V rms voltage being accidentally fed into the power supply busses (and hence the detector circuitry) during oscillator testing and a 282 V_{PP} fault placed on the HV detectors, both with no effect other than the tripping of the relays.

The monitor has no problems detecting ground wire impedance or component changes on the bridge and is very accurate at its set trip points. During testing, nearly every conceivable failure and fault was applied to the bridge, all with the expected results.

Appendix B

Programs Used in Comparison of DC Grounding Systems

The basic ECAP programs are included on the following pages. The explanations are provided for clarification only; they are not part of the actual programs. The JCL (Job Control Language) statements have not been included because they pertain only to the computing services at West Virginia University. Also, the output intervals and the start and finish times varied between programs and, thus, are not given.

Program 1 is for the Diode Grounding System when the shuttle car motor is started under normal conditions. The control circuit is explained in Section 2.4, and an illustration of the ECAP equivalent circuit is shown in figure 2.9.

Programs 2 through 5 are for the Diode Grounding System, the Basic Ground-Wire System, the Resistance-Derived Neutral System, and the Transformer-Derived Neutral System, respectively, with a positive-to-machine frame fault. To avoid redundancy, the other fault programs mentioned in Section 2.4 are not included, because most of these changes involved one or two branches only.

There are several modifications in the control circuit program (see Program 1) to make it suitable for the introduction of faults once steady state operation has been reached. These are given below:

1. Initial conditions have been added for all inductors using steady-state operation values.

2. Normally-open switches that close during starting have been modified to show this.

3. The one-second time delays for the M1 and 1A contactor closings have been deleted.

4. The current level test circuits have been modified to prevent switch reclosing (see section 2.4).

For specific details on the programming techniques, refer to the ECAP User's Manual (13).

PROGRAM 1

Diode Grounding System When the
Motor is Started

TRANSIENT ANALYSIS

```
B1   N(1,2)R=(.1,1E7)                    Overcurrent relay switch
B2   N(2,3),R=(1E7,.1)                   Tram switch
B3   N(3,4),R=(1E7,.1)                   M1 switch (1 second delay)
B4   N(4,5),R=(1E7,.1)                   1A switch (1 second delay)
B5   N(2,6),R=(1E7,1),E=(0,-.7)
B6   N(2,6),R=1E7                        Control diode
B7   N(6,7),R=100
B8   N(3,8),R=100                        Contactor
B9   N(4,9),R=100                        Coil resistances
B10  N(5,10),R=100
B11  N(7,16),L=1E-3
B12  N(8,16),L=1E-3                      Contactor
B13  N(9,16),L=1E-3                      Coil inductances
B14  N(10,16),L=1E-3
B15  N(1,11),R=(1E7,.1)                  M1 switch
B16  N(11,12),R=1.025                    Starting resistors
B17  N(12,13),R=.67
B18  N(11,12),R=(1E7,.1)                 1A switch
B19  N(11,13),R=1E7,.1)                  2A switch
B20  N(11,14),R=124                      Shunt field impedance
B21  N(14,15),L=1E-4
B22  N(13,15),R=.01                      Armature resistance
B23  N(15,16),R=(1E7,.1)                 M2 switch                    Control
B24  N(17,0),R=1E3,I=-.1                                              Circuit
B25  N(17,0),R=1E3
B26  N(17,0),R=1E3
B27  N(18,0),R=1E3,I=-.1                 Contactor
B28  N(18,0),R=1E3                       current
B29  N(18,0),R=1E3                       level
B30  N(19,0),R=1E3,I=-.1                 tests
B31  N(19,0),R=1E3
B32  N(19,0),R=1E3
B33  N(20,0),R=1E3,I=-.1
B34  N(20,0),R=1E3
B35  N(20,0),R=1E3
B36  N(0,21),R=10,E=(0.10)
B37  N(21,0),L=4.343
B38  N(22,0),R=1E3,I=-.9                 M1 1 second delay
B39  N(22,0),R=1E3
B40  N(22,0),R=1E3
B41  N(0,23),R=10,E=(0,10)
B42  N(23,0),L=4.343
B43  N(24,0),R=1E3.I=-.9                 1A 1 second delay
B44  N(24,0),R=1E3
B45  N(24,0),R=1E3
B46  N(25,0),R=1E3,I=-.75E-7             Control diode current
B47  N(25,0),R=1E3                       level test
B48  N(25,0),R=1E3
```

PROGRAM 1

(continued)

```
B49  N(0,26),R=.02,E=250                    Source
B50  N(26,27),R=.07
B51  N(27,1),L=10E-3                        Cable
B52  N(16,28),L=10E-3                       Impedance
B53  N(28,0),R=.07
B54  N(16,29),R=(1E7,1),E=(0,.7)            Grounding Diode
B55  N(16,29),R=1E7
B56  N(30,0),R=1E3,I=.75E-7                 Grounding diode current
B57  N(30,0),R=1E3                          level test
B58  N(30,0)R=1E3
B59  N(0,29),R=1E7
S1   B=25,(2,23),OFF                        Reference to ground
S2   B=28,(15,36),OFF
S3   B=31,(18,41),OFF
S4   B=34,(19),OFF                          Switches
S5   B=39,(3),OFF
S6   B=44,(4),OFF
S7   B=47,(5),OFF
S8   B=57,(54),ON
T1   B(21,22),BETA=-12400
T2   B(11,26),BETA=-1
T3   B(12,29),BETA=-1
T4   B(13,32),BETA=-1                       Dependent
T5   B(14,35),BETA=-1                       current
T6   B(37,40),BETA=-1                       sources
T7   B(42,45),BETA=-1
T8   B(54,58),BETA=-1
T9   B(5,48),BETA=-1
```

PROGRAM 2

Diode Grounding System With a
Positive-to-Machine Frame Fault

```
      TRANSIENT ANALYSIS

B1    N(1,2),R=(.1,1E7)
B2    N(2,3),R=(.1,1E7)
B3    N(3,4),R=(.1,1E7)
B4    N(4,5),R=(.1,1E7)
B5    N(2,6),R=(1,1E7),E=(-.7,0)
B6    N(2,6),R=1E7
B7    N(6,7),R=100
B8    N(3,8),R=100
B9    N(4,9),R=100
B10   N(5,10),R=100
B11   N(7,16),L=1E-3,IO=2.4398737
B12   N(8,16),L=1E-3.IO=2.463893
B13   N(9,16),L=1E-3,IO=2.4589775
B14   N(10,16),L=1E-3,IO=2.456521
B15   N(1,11),R=(.1,1E7)
B16   N(11,12),R=1.025                    Revised
B17   N(12,13),R=.67                      control
B18   N(11,12),R=(.1,1E7)                 circuit
B19   N(11,13),R=(.1,1E7)
B20   N(11,13),R=(.1,1E7)
B21   N(14,15),L=1E-4,IO=1,997658
B22   N(13,15),R=.01
B23   N(15,16),R=.1,1E7)
B24   N(17,0),R=1E3,I=(-.1,-5)
B25   N(17,0,R=1E3
B26   N(17,0),R=1E3
B27   N(18,0),R=1E3,I=(-.1,-5)
B28   N(18,0),R=1E3
B29   N(18,0),R=1E3
B30   N(19,0),R=1E3,I=(-.1,-5)
B31   N(19,0),R=1E3
B32   N(19,0),R=1E3
B33   N(20,0),R=1E3,I=(-.1,-5)
B34   N(20,0),R=1E3
B35   N(20,0),R=1E3
B36   N(21,0),R=1E3,I=(-.75E-7,-1E4)
B37   N(21,0),R=1E3
B38   N(21,0),R=1E3
B39   N(0,22)R=.02,E=250                  Source
B40   N(22,23),R=(.07,1E3)
B41   N(23,1)L=10E-3,IO=11.817382         Cable
B42   N(16,24),L=10E-3,IO=11.817382       impedance
B43   N(24,0),R=.07
B44   N(16,25),R=(1E7,1),E=(0,.7)
B45   N(16,25),R=1E7                      Grounding
B46   N(26,0),R=1E3,I=(.75E-7,-1E4)       diode
B47   N(26,0),R=1E3
B48   N(26,0),R=1E3
```

PROGRAM 2

(Continued)

```
B49   N(27,0),R=1E3,I=(100,-1E4)          Overcurrent relay
B50   N(27,0),R=1E3                       of diode
B51   N(27,0),R=1E3
B52   N(28,0),R=1E3,I=(-20,1E4)
B53   N(28,0),R=1E3                       Overcurrent relay
B54   N(28,0),R=1E3                       at power center
B55   N(0,25),R=1E7
B56   N(1,25),R=(1E10,.1)
B57   N(0,29),R=10,E=10                   Positive-to-
B58   N(29,0),L=.0434                     machine frame
B59   N(30,0),R=1E3,I=-.9                 fault with
B60   N(30,0),R=1E3                       .01 sec delay
B61   N(30,0),R=1E3
S1    B=25,(2,23,24),ON
S2    B=28,(3,15,27),ON
S3    B=31,(4,18,30),ON
S4    B=34,(19,33),ON                     Switches
S5    B=37,(5,36),ON
S6    B=47,(44,46),ON
S7    B=50,(1,49),ON
S8    B=53,(40,52),OFF
S9    B=60,(56),OFF
T1    B(21,22),BETA=-12400
T2    B(11,26),BETA=-1
T3    B(12,29),BETA=-1
T4    B(13,32),BETA=-1                    Dependent
T5    B(14,35),BETA=-1                    Current
T6    B(40,54),BETA=-1                    Sources
T7    B(44,48),BETA=-1
T8    B(44,51),BETA=-1
T9    B(58,61),BETA=-1
T10   B(5,38),BETA=-1
```

PROGRAM 3

Basic Ground-Wire System with
Positive-to-Machine Frame Fault

B1 through B38: Same as revised control circuit in Program 2

B39	N(0,22),R=.02,E=250	Source
B40	N(22,23),R=(.07,1E3)	
B41	N(23,1),L=10E-3,I0=11.817385	Cable
B42	N(16,24),L=10E-3,I0=11.817382	impedance
B43	N(24,0),R=.07	
B44	N(25,26),L=10E-3,I0=.24892743E-5	Ground-wire
B45	N(26,0),R=.14	impedance
B46	N(27,0),R=1E3,I=(-20,1E4)	
B47	N(27,0),R=1E3	Main overcurrent
B48	N(27,0),R=1E3	Relay
B49	N(1,25),R=(1E10,.1)	
B50	N(0,28),R=10,E=10	Positive-to-
B51	N(28,0),L=.0434	machine frame
B52	N(29,0),R=1E3,I=-.9	fault with .01 sec
B53	N(29,0),R=1E3	delay
B54	N(29,0),R=1E3	
S1	B=25,(1,2,23,24),ON	
S2	B=28,(3,15,27),ON	
S3	B=31,(4,18,30),ON	
S4	B=34,(19,33),ON	Switches
S5	B=37,(5,36),ON	
S6	B=47,(40,46),OFF	
S7	B=53,(49),OFF	
T1	B(21,22),BETA=-12400	
T2	B(11,26),BETA=-1	
T3	B(12,29),BETA=-1	Dependent
T4	B(13,32),BETA=-1	current
T5	B(14,35),BETA=-1	sources
T6	B(40,58),BETA=-1	
T7	B(51,54),BETA=-1	
T8	B(5,38),BETA=-1	

PROGRAM 4

Resistance-Derived Neutral System with
Positive-to-Machine Frame Fault

B1 through B38: Same as revised control circuit in Program 2

```
B39  N(22,23),R=.02,E=250
B40  N(23,23),R=(.07,1E3)                    Cable
B41  N(24,1),L=10E-3,I0=11.817266            Impedance
B42  N(16,25),L=10E-3,I0=11.817264
B43  N(25,22),R=.07,1E3)
B44  N(23,0),R=1E3                           Voltage relays
B45  N(0,22),R=1E3
B46  N(27,26),L=10E-3,I0=.12404375E-5        Ground-wire
B47  N(26,0),R=.14                           impedance
B48  N(28,0),R=1E3,I=(-.175,1E4)
B49  N(28,0),R=1E3
B50  N(28,0),R=1E3                           Voltage
B51  N(29,0),R=1E3,I=(-.175,1E4)             relays
B52  N(29,0),R=1E3
B53  N(29,0),R=1E3
B54  N(30,0),R=1E3,I=(-20,1E4)               Main
B55  N(30,0),R=1E3                           overcurrent
B56  N(30,0),R=1E3                           relays
B57  N(31,0),R=1E3,I=(-20,1E4)
B58  N(31,0),R=1E3
B59  N(31,0),R=1E3
B60  N(1,37),R=(1E10,.1)
B61  N(0,32),R=10,E=10                       Positive-to-
B62  N(32,0),L=.0434                         machine frame
B63  N(33,0),R=1E3,I=-.9                     fault with .01 sec
B64  N(33,0),R=1E3                           delay
B65  N(33,0),R=1E3
S1   B=25,(1,2,23,24),ON
S2   B=28,(3,15,27),ON
S3   B=31,(4,18,30),ON
S4   B=34,(19,33),ON
S5   B=37,(5,36),ON                          Switches
S6   B=49,(40,43,48),OFF
S7   B=52,(40,43,51),OFF
S8   B=55,(40,43,54),OFF
S9   B=58,(40,43,57),OFF
S10  B=64,(60),OFF
T1   B(21,22),BETA=-12400
T2   B(11,26),BETA=-1
T3   B(12,29),BETA=-1                        Dependent
T4   B(13,32),BETA=-1                        current
T5   B(14,35),BETA=-1                        sources
T6   B(40,56),BETA=-1
T7   B(43,59),BETA=-1
T8   B(44,50),BETA=-1
T9   B(45,53),BETA=-1
T10  B(62,65),BETA=-1
T11  B(5,38),BETA=-1
```

PROGRAM 5

Transformer-Derived Neutral System with Positive-to-Machine Frame Fault

B1 through B38: Same as revised control circuit in Program 2

```
B39  N(23,22),R=.01,E=125
B40  N(24,23),R=.01,E=125                    Source
B41  N(23,0),R=10                            Grounding resistor
B42  N(22,25),R=(.07,1E3)
B43  N(25,1)L=10E-3,I0=11.817384             Cable
B44  N(16,26),L=10E-3,I0=11.817382           impedance
B45  N(26,24),R=(.07,1E3)
B46  N(27,28),L=10E-3,I0=.1240456E-5         Ground-wire
B47  N(28,0),R=.14                           impedance
B48  N(29,0),R=1E3,I=(-20,1E4)
B49  N(29,0),R=1E3                           Main
B50  N(29,0),R=1E3                           overcurrent
B51  N(30,0),R=1E3,I=(-20,1E4)               relays
B52  N(30,0),R=1E3
B53  N(30,0),R=1E3
B54  N(1,27),R=(1E10,.1)
B55  N(0,31),R=10,E=10                       Positive-to-
B56  N(31,0),L=.0434                         machine Frame
B57  N(32,0),R=1E3,I=-.9                     fault with .01 sec
B58  N(32,0),R=1E3,                          delay
B59  N(32,0),R=1E3
S1   B=25,(1,2,23,24),ON
S2   B=28,(3,15,27),ON
S3   B=31,(4,18,30),ON
S4   B=34,(19,33),ON                         Switches
S5   B=37,(5,36),ON
S6   B=49,(42,45,48),OFF
S7   B=52,(42,45,51),OFF
S8   B=58,(54),OFF
T1   B(21,22),BETA=-12400
T2   B(11,26),BETA=-1
T3   B(12,29),BETA=-1
T4   B(13,32),BETA=-1                        Dependent
T5   B(14,35),BETA=-1                        current
T6   B(42,50),BETA=-1                        sources
T7   B(45,53),BETA=-1
T8   B(56,59),BETA=-1
T9   B(5,38),BETA=-1
```